MORTAR CONSTITUENT OF CONCRETE UNDER CYCLIC COMPRESSION

by
Ataullah Maher
David Darwin

A Report on Research Sponsored by
THE NATIONAL SCIENCE FOUNDATION
Research Grants
ENG 76-09444
CME 79-18414

UNIVERSITY OF KANSAS
LAWRENCE, KANSAS
October 1980

50272-101

REPORT DOCUMENTATION PAGE	1. REPORT NO. NSF/RA-800322	2.	3. Recipient's Accession No.

4. Title and Subtitle
MORTAR CONSTITUENT OF CONCRETE UNDER CYCLIC COMPRESSION

5. Report Date
October 1980

6.

7. Author(s)
Ataullah Maher and David Darwin

8. Performing Organization Rept. No.
SM Report No. 5

9. Performing Organization Name and Address
University of Kansas Center for Research, Inc.
2291 Irving Hill Drive, Campus West
Lawrence, Kansas 66045

10. Project/Task/Work Unit No.

11. Contract(C) or Grant(G) No.
(C) NSF ENG 76-09444
(G) NSF CME 79-18414

12. Sponsoring Organization Name and Address
National Science Foundation
Washington, D.C. 20550

13. Type of Report & Period Covered

14.

15. Supplementary Notes

16. Abstract (Limit: 200 words)

The behavior of the mortar constituent of concrete under cyclic compression was studied and a simple analytical model was developed to represent its cyclic behavior. The experimental work consisted of monotonic and cyclic compressive loading of mortar. Two mixes were used, with proportions corresponding to concretes with water-cement ratios of 0.5 and 0.6. Forty-four groups of specimens were tested at ages ranging from 5 to 70 days. Complete monotonic and cyclic stress-strain envelopes were obtained. A number of loading regimes were investigated, including cycles to a constant maximum strain. Major emphasis was placed on tests using relatively high stress cycles. The degradation was shown to be a continuous process and a function of both total strain and load history. No stability limit (fatigue limit) was indicated. The nature of damage in concrete and mortar may dominate the behavior of concrete.

17. Document Analysis a. Descriptors
cement paste, compression, compressive strength, concrete, cracking (fracturing), cyclic loading, degradation, failure, fatigue, load history, microcracking, modulus of elasticity, model, mortar, Poisson ratio, strain gages, strains, stresses, testing techniques

b. Identifiers/Open-Ended Terms

c. COSATI Field/Group

18. Availability Statement	19. Security Class (This Report)	21. No. of Pages
Release Unlimited	Unclassified	
	20. Security Class (This Page) Unclassified	22. Price

ACKNOWLEDGMENTS

This report is based on a thesis submitted by Ataullah Maher in partial fulfillment of the requirements for the Ph.D. degree.

This research was supported by the National Science Foundation under NSF Grant Numbers ENG 76-09444 and CME 79-18414.

Additional support was provided by University of Kansas General Research Allocation #3408-X0-0038.

TABLE OF CONTENTS

TABLE OF CONTENTS (continued)

LIST OF TABLES

LIST OF TABLES (continued)

LIST OF FIGURES

LIST OF FIGURES (continued)

LIST OF FIGURES (continued)

LIST OF FIGURES (continued)

LIST OF FIGURES (continued)

CHAPTER 1

INTRODUCTION

1.1 General

Concrete is a nonlinear inelastic composite material. The behavior of concrete is dependent upon its load history. Under cyclic compressive loading concrete degrades in both stiffness and strength (11,12,22).

Microcracks exist in concrete prior to loading and propagate with load (7,9). It has been observed that microcracking is related with, not only the short term behavior of concrete (7,9), but also with its behavior under long term and cyclic loading (17,18,22). Recent studies (15,24-26), however, have demonstrated that the nonlinearity of concrete under compressive loading is highly dependent upon the nonlinearity of its cement paste and mortar constituents. Cement paste and mortar are not elastic and brittle materials as supposed in the past (23), but rather nonlinear materials that are damaged continuously under load (5,26). The process of damage in concrete is, also, continuous and begins at very low strains. The degree of damage is greater than for paste (27). These recent studies not only seem to downgrade the importance of microcracking (1), but also strongly indicate that the relationships between the behavior of concrete and its constituents and the factors that control the behavior of concrete under general types of loading need further study.

Concrete is used in structures subjected to cyclic and dynamic loads. The experimental characteristics of concrete and its constituent materials under cyclic loads must be investigated. Analytical models to simulate and, therefore, better understand the response of the material need to be developed.

The present study endeavors to evaluate the experimental characteristics of the mortar constituent of concrete under cyclic load and develops an analytical model based on the observed behavior.

1.2 Previous Work

Using a light microscope at 40X magnification, Hsu, Slate, Sturman and Winter (10) studied the formation and propagation of microcracks in concrete subjected to uniaxial compressive load. They found that bond cracks (microcracks at the mortar-aggregate interface) exist prior to loading. With the application of load, these initial bond cracks begin to propagate at 30 to 40 percent of the compressive strength of concrete, f'_c. The stress-strain curve deviates from linearity at this point, and there is an increase in the lateral expansion of the concrete. Mortar cracks (microcracks in the mortar) begin to form at extensions of the bond cracks at about 70 to 90 percent of f'_c. Mortar cracking continues at an accelerated rate until the material ultimately fails. Typical cracking maps are shown in Fig. 1.1.

Derucher (7) obtained a somewhat different picture of the microscopic behavior of concrete, using the scanning electron microscope (SEM). He subjected concrete specimens to eccentric compressive loading to facilitate the use of the SEM, without having to unload the specimens, as did Hsu, et al. (10). For optimum utilization of SEM, the specimens had to be dried. Using an optical microscope, Derucher determined that the drying did not cause additional microcracking. He observed that microcracks existing prior to loading are in the form of bond cracks, with extensions into the surrounding mortar at right angles to the bond cracks. Under increasing compression, the bond cracks do not propagate at all but merely

widen. The mortar cracks begin to widen and propagate at a stress as low as 15 percent of the ultimate strength. Under increasing load, they begin to bridge between the bond cracks, and at 45 percent of f'_c, the bridging is about complete. At 75 percent of the ultimate strength, the mortar cracks start to join one another and continue to do so until failure.

The interfacial bond between mortar and coarse aggregate has been studied experimentally. The strength of the interface can be represented using the Mohr-Coulomb failure envelope (Fig. 1.2) (9,23,28).

Aggregate used in normal weight concrete is essentially linear and elastic (8). The ultimate strength of most aggregate is much higher than that of mortar in ordinary strength concrete, and therefore, aggregate does not fracture during the loading of concrete to failure. In high strength concretes, on the other hand, aggregate failure does accompany concrete failure (4).

Experimental work indicates that both cement paste (24) and mortar (2,15) are nonlinear materials, contrary to the previous belief that they are elastic, brittle materials (23).

To measure the effect of load on the degree of damage in concrete, Spooner and Dougill (25) developed highly sensitive techniques, which utilize a cyclic sequence of loading, unloading and reloading of the specimen. The energy dissipated in damage is measured, based on the behavior of an ideal material, and the initial modulus of elasticity is measured as the initial slope of the reloading curve. Spooner and Dougill indicate that the energy dissipated in damage correlates closely with changes in the modulus of elasticity and report that both of these indicators of damage show the effects of load at strains as low as 0.0004 (a strain at which Hsu, et al. (10) did not detect an increase in microcracking).

Spooner, et al. (25,26) demonstrate that the process of damage in cement paste and concrete in uniaxial compression is continuous. The degree of damage which occurs for a given applied strain, however, is linked to the aggregate concentration (27). The damage is more severe, the higher the aggregate concentration.

Cook and Chindaprasirt (5) indicate that the damage in concrete is also governed by the strength of the cement paste. For low strains, the damage is less for a higher strength paste (hence concrete) than for a weaker one.

The shape of the stress-strain curve under compression correlates with the degree of damage (27). Concretes which are damaged more at lower strains have a flatter descending branch of the stress-strain curve. The stronger the concrete and the lower the volume of aggregate, the steeper descending branch of the stress-strain curve (4,27).

Quite a few experimental studies have been conducted to investigate the characteristics of concrete under uniaxial compressive cycles of load (5,12,18,21,22,25,29). These works agree that, in general, for a maximum stress below 60 to 70 percent of the short-term compressive strength, the primary effect of a cyclic stress is inelastic deformation, while for a higher maximum stress, the effect is progressive microcracking and eventual failure (12,18,23).

Karsan and Jirsa (12), and Spooner and Dougill (25) indicate that the envelope drawn around cyclic stress-strain curves is equivalent to the monotonic stress-strain curve. They further note that the initial modulus of elasticity decreases and permanent deformation accumulates after each loading cycle in which the maximum strain increases.

Spooner, Pomeroy, and Dougill found that the higher the aggregate

volume, the larger the changes in the initial modulus of elasticity which occur with each cycle (27), and that the decrease in the initial modulus of cement paste, for a given increase in strain, is independent of age and water-cement ratio (26).

Spooner and Dougill (25) suggest that during successive cycles to the same maximum strain, significant damage occurs only during the first loading. Karsan and Jirsa, show that stability is obtained after several cycles, and the minimum stress obtained represents the fatigue limit. However, these cycles to stability used both a decreasing maximum stress and a decreasing maximum strain and cannot be directly compared with the work of Spooner and Dougill.

Conflicting views exist on the changes in the properties of concrete produced by cycles of load below the fatigue limit.

Whaley and Neville (29) indicate that such cycles accelerate the process of creep. Neville and Hirst (18) state that limited microcracking, probably at the mortar-aggregate interface, contributes to the accelerating effect of cyclic load on the process of creep. Neville, et al., feel that the influence of the cyclic loading and the resulting limited microcracking is not detrimental to the strength or stiffness of concrete.

On the other hand, Cook and Chindaprasirt (5) showed that cyclic loading decreases the initial modulus of elasticity and strength of concrete upon reloading. This contradicts a key conclusion of Neville, et al. (18,29). Since creep specimens tend to show both increased strength and stiffness, the structural changes due to cyclic loading appear to be of a different nature than those due to creep. Cook and Chindaprasirt further note that the decrease in the modulus of elasticity is influenced by the material heterogeneity, the decrease being greatest in concrete, followed

in turn by mortar and paste. They observed no reduction in the strength of paste or mortar as the result of previous cyclic loading history. They conjecture that the damage which occurs in the cyclically loaded specimens is due to limited microcracking.

Studies of the multiaxial monotonic compressive behavior of mortar (2,15) have demonstrated that different strengths of mortar are observed under different combinations of load and that the effects of biaxial loading are similar to those in concrete.

Andenaes, Gerstle and Ko (2) studied the behavior of mortar under uniaxial and biaxial compressive loads. They report that both uniaxial and biaxial strength is affected by the degree of restraint provided by the loading surfaces. In these tests, the maximum strength increase for biaxial compression is 38 and 25 percent, using steel platens and fluid cushions, respectively. The maximum strength occurs at a biaxial stress ratio of about 0.67. Andenaes, et al., compare the biaxial strength envelope obtained from the fluid cushion tests with those of Kupfer, Hilsdorf and Rusch (14) for concrete and Liu (15) for concrete and mortar. Both Kupfer, et al., and Liu employed brush bearing platens, but of slightly different shape. The shape of Andenaes mortar and Kupfer's and Liu's concrete envelopes have the same general shape. However, the biaxial strength envelope of mortar obtained by Liu, shows a considerably smaller strength increase (maximum approximately equal to 15 percent), as shown in Fig. 1.3 (2,14,15).

Jeragh (11) studied the behavior of concrete under biaxial cyclic load. He used platens made of high strength steel, along with friction reducing pads. The strength corresponding to a biaxial stress ratio of 0.5 obtained with this type of loading head was approximately 1.38 f'_c, compared with 1.27 f'_c obtained with brush bearing platens by Kupfer, et al.

The stress-strain characteristics under uniaxial compressive cycles of load obtained by Jeragh exhibit a general trend similar to the results obtained by Karsan and Jirsa (12) for uniaxial cyclic loading. However, the loading portion of the cyclic curves becomes concave to the left as early as in the second cycle, a phenomenon which is generally not observed until after the maximum strain has exceeded the strain at the peak of the envelope (12). Jeragh defined "failure" as occurring when the value of strain exceeded the measurement capacity of his instruments. He indicates that the factors that control the cyclic behavior of concrete are similar to those that affect its static strength. His results show a substantial improvement in the cyclic life of the specimens in biaxial tests over uniaxial tests, a property similar to the improvement in strength under biaxial compression, as compared to uniaxial compression. In addition, the beneficial effect of biaxial cyclic loading is dependent on the ratio of the biaxial stresses in a pattern similar to the static biaxial strength envelope. The initial modulus of elasticity decreases with an increasing number of cycles under biaxial compressive cycles of load, as it does under uniaxial cycles.

Physical and analytical models have been proposed to simulate the behavior of concrete under load (3,16,23). The models incorporate the basic equivalent structure of concrete and consist of either a single cylindrical disc of aggregate (23) or a number of cylindrical discs of aggregate (3) in a mortar block. The analytical models of Shah and Winter (23) and Buyukozturk (3), neglect the nonlinear behavior of mortar and are unable to duplicate the nonlinear behavior of concrete. Shah and Winter (23) were able to obtain a nonlinear stress-strain curve for concrete by invoking a statistical variation in the strength of their model.

Maher and Darwin (16) incorporate a nonlinear representation

of mortar. Their work indicates that the nonlinear behavior of concrete is controlled by the nonlinearity of mortar, as illustrated in Fig. 1.4. Their work also seems to confirm the experimental results of Darwin and Slate (6), and Perry and Gillot (19), which indicates that the effect of interfacial bond strength on the uniaxial strength of concrete is small. No work has been done to model the cyclic behavior of concrete as a heterogeneous material.

No data exists on the characteristics of the cyclic behavior of mortar, or the influence of cyclic load on the characteristics of the interface between mortar and aggregate.

Cement paste and mortar appear to play an important role in controlling the behavior of concrete under both monotonic and cyclic compressive loading; however, considerable effort will be needed before a complete picture of the behavior of concrete is obtained.

1.3 Object and Scope

The purpose of this research is to study the behavior of the mortar constituent of concrete under cyclic uniaxial compressive load and develop an analytical model to represent its cyclic behavior.

Experimental tests to investigate the cyclic behavior of mortar were conducted utilizing procedures similar to those used by Karsan and Jirsa (12) in their study of concrete. Mortar mixes, with proportions comparable with the mortar constituent of concrete, were used. Mixes with water-cement ratios of 0.5 and 0.6 were tested at ages from 5 to 70 days. Complete stress-strain curves were obtained for monotonic and cyclic loading. The characteristics of degradation under cycles of load were studied using a number of load regimes. Major emphasis was placed on tests using

relatively high stress cycles.

The observations made in this study are compared with those obtained in studies of the cyclic behavior of cement paste and concrete. The similarities and differences in the behavior are evaluated, within the scope of this investigation.

An analytical model is developed to represent the experimental characteristics of mortar under cyclic load and is compared with the test results obtained in this study.

CHAPTER 2

EXPERIMENTAL WORK

2.1 General

The purpose of the experimental phase of this research was to determine the behavior of the mortar constituent of concrete under monotonic and cyclic compressive uniaxial loading. The basic procedures closely paralleled those used by Karsan and Jirsa (12), in their study of concrete.

Two mortar mixes were used. The proportions corresponded to concretes with water-cement ratios (W/C) of 0.5 and 0.6. The mix employing W/C = 0.6 was used in all phases of the experimental work. The mix with W/C = 0.5 was used to supplement the information obtained using the first mix.

Specimens were loaded in compression using a closed-loop, electro-hydraulic testing machine. The closed-loop system of the testing machine was modified to allow the direction of the loading to be reversed at specified stress and/or strain limits.

To establish the stress-strain envelope, complete stress-strain curves for monotonic compressive loading were obtained, including the descending branch. For this purpose, strain control was used. To determine the degree of softening and loss of strength produced by cyclic loading, a number of loading regimes were investigated.

Average axial strain was obtained using a compressometer. Strain-gages were installed on a few specimens to determine the variation of the total and incremental "Poisson's ratio" with load history.

The results of the tests are analyzed to better understand the behavior of concrete and its mortar constituent under general types of load (Chapter 3) and used to develop an analytical representation of mortar

under monotonic and cyclic loading (Chapter 4).

2.2 Materials

Cement: Type I Portland Cement, Ashgrove Brand

Fine aggregate: consists mainly of quartz, with 10 to 15 percent chert, larger particles contain some limestone and dolomite. Fineness Modulus = 2.9. Bulk Specific Gravity (Saturated Surface Dry) = 2.62. Absorption = 0.5 percent. Source: Kansas River, Lawrence, Kansas.

The sand was passed through a #4 sieve and washed before use.

Coarse aggregate: 1/2 inch nominal size, crushed limestone. Bulk Specific Gravity (SSD) = 2.52. Absorption = 3.5 percent. Unit weight = 90 pcf. Source: Hamm's Quarry, Perry, Kansas.

The coarse aggregate was passed through a 1/2 inch sieve and washed before use.

Two mixes of mortar were used, corresponding to the proportions that occur in concretes with water-cement ratios of 0.5 and 0.6. Concrete mixes were designed in order to obtain the proportions of the corresponding mortar constituents. The mix designs, relative proportions and the slumps for the concrete and the constituent mortar are given in Table 2.1.

The mortar was very fluid. It was, therefore, susceptable to an excessive amount of bleeding, which required special handling as explained in Section 2.3.1.

2.3 Apparatus and Procedure

2.3.1 Test Specimen

The test specimen is shown in Fig. 2.1. It is fourteen inches high with flared ends. The middle six inch portion of the specimen is prismatic and has a uniform two inch square cross-section. A finite

element analysis, simulating the state of fixed ends, showed that the prismatic portion of the specimen was subject to an approximately uniform state of uniaxial compression.

The specimens were batched in the following manner. The sand was sprinkled with water and then thoroughly mixed. The amount of water in excess of the saturated surface dry state of the sand was determined. The mixing water was correspondingly reduced in amount during batching. Sand and cement were hand mixed and then mix water was added. The mixture was thoroughly blended. Batching was performed at a room temperature of 68° to 84°F. Two or three specimens were prepared from each batch. The steel molds (see Fig. 2.2) were greased and sealed with modelling clay. During casting, the steel molds remained vertical. Each mold was filled in three layers (lower flared portion, middle prismatic portion, and upper flared portion). Each layer was rodded twenty-five times using a three-eighths inch diameter rod. The molds were stored in a curing room in a horizontal position, while the mortar was still plastic.

During the initial phase of the study, the specimens were stored vertically. Extensive bleeding in the fluid mortar produced decreasing strength through the height of the specimens. When loaded, failure occurred at the upper intersection of the prismatic and flared portions. To correct this problem, the storage procedure was changed. When the specimens were stored horizontally, the bleeding was negligible, and uniform strength was obtained throughout the prismatic portion of the specimen. Due to uniform strength throughout the prismatic portion, the failure occurred inside the prismatic portion of the specimen. This was confirmed by the occurrence of vertical cracking through the length and width of the prismatic portion (see Fig. 2.3).

After twenty-four hours, the specimens were removed from the molds and again stored in the curing room.

The specimens to be strain-gaged (details in Section 2.3.2) were taken out of the curing room three days before the test. The rest of the specimens were taken out, approximately, two hours before the test. All specimens were ground, immediately after taking them out of the curing room, to insure a uniform cross-section.

Specimen preparation and testing required three to eight hours, depending on the type of the test. The specimens were allowed to dry during this period. Two or three specimens per batch were tested at the same age. Specimens were tested 7, 14 or 28 days after casting. In a few cases, the number of specimens to be tested and the time required per test did not permit all of the specimens from a batch to be tested on the same day. In such cases, testing of a single batch was completed in two days. Hence, some specimens were tested 6, 8, 13, 15, 29 or 30 days after casting. A small number of specimens were tested at ages in excess of 30 days.

Alignment of the specimens in the testing machine was obtained using the following procedure. A one-eighth inch layer of high strength gypsum cement paste (Hydrostone) was spread on the greased surface of the lower platen of the testing machine. The specimen was firmly placed on this layer, making sure that the marked centroidal axes of the bottom of the specimen coincided with those of the platen. The specimen axis was made perpendicular to the surface of the platen. The cement was allowed to harden. Approximately thirty minutes later, another thin layer of the cement was spread on the top of the specimen. By raising the lower platen, the specimen was slowly brought into contact with the greased surface of the top platen. Fifty to one-hundred pounds of load were applied. The

cement spread uniformly, and good alignment of the specimen with the top platen was obtained. The cement hardened in approximately thirty minutes, and then, the load was released.

During the early tests, it was discovered that the sharp edges of the set screws on the legs of the compressometer (description of the compressometer in Section 2.3.4) acted as wedges driven into the specimen. They split the specimen, as the specimen expanded laterally during the test. In addition, slipping of one or more of the legs of the compressometer introduced an apparent strain, resulting in either premature failure or unloading of the specimen. To correct these problems, small strips of wood (about 1/16-inch thick and 1/4-inch wide) were glued to the test specimen. They provided a compressible material to attach the compressometer to. The set screws of the compressometer were lightly tightened into the wood strips. The wood strips acted as reliable supports for the legs of the compressometer throughout the test.

2.3.2 Strain Gages

SR-4, A-9-5 and A-12 strain-gages, with the corresponding gage lengths of three and a half inches and one inch, were used. The strain-gages were installed both longitudinally and laterally. At large strains, the strain gages became ineffective due to extensive cracking of the specimens, and strains measured by the strain-gages became unrealistically high. In some cases the gages failed. The strain-gages were primarily used to determine the variation of the total and incremental "Poisson's ratios" with load history. Strain-gage readings were obtained with a six-channel automatic strain recorder (Visicorder). A change in strain altered the position of the galvanometer of the corresponding channel. This change was recorded on light-sensitive paper.

2.3.3 MTS Testing Machine

A 50,000 pound capacity closed loop electro-hydraulic, MTS testing machine (System No. 905.84) was used. The load was transmitted through flat rigid platens.

It was important to ensure that the displacement imposed by the testing machine was, as nearly as possible, the same at all points across the width of the specimens. This was especially important for specimens on the descending branch of the stress-strain curve. Thus, it was necessary to ensure good alignment of the testing machine platens with the ends of the specimens and also to prevent significant platen rotation during the test (23).

Rigid, flat, non-rotating platens ensured that the displacement imposed was the same at all points across the width of the specimens. During the preparation of the specimens for the test, good alignment of the platens with the ends of the specimen was obtained using thin layers of Hydrostone, high strength gypsum cement (Section 2.3.1), at both ends of the specimen.

The testing machine allowed the test to be controlled by either load or strain. To obtain complete records of the descending portion of the stress-strain curve, a constant strain rate (strain-control-ramp) was used throughout each test. For cyclic loading, the load limit detectors of the testing machine were modified to allow a reversal in the direction of load at the specified maximum and minimum stress limits, while using the strain-control-ramp. This capability was very useful, since the load could be cycled between fixed load limits at a constant rate of strain increase or decrease. When the load failed to reach the upper load limit during the loading portion of a cycle, the system continued to increase the

strain at the constant specified rate and a complete record of the remaining portion of the descending branch of the stress-strain curve was obtained.

2.3.4 Compressometer

To measure the average axial strain, a variable gage length compressometer was designed and used in all tests (see Figs.2.3 and 2.4). The compressometer was attached to wood strips on the test specimens using set-screws. Preliminary studies showed that a satisfactory measurement of the deformation, caused by sliding of the material in the extensively cracked prismatic portion of the specimen, was obtained by employing a three-inch gage length of the compressometer. The three-inch gage length was used for all tests.

2.3.5 Extensometer

An MTS extensometer, Model 632.11 B-20, was installed on the compressometer to measure the strain and to provide closed-loop control for the testing machine. The gage length of the extensometer was one inch, and the range of displacement was $\pm$ 0.150 inches. Since the displacement was measured over the three-inch gage length of the compressometer, the "strain" readings were magnified three times. This magnification improved the sensitivity of the closed-loop control. Strain rate control was selected to obtain the desired rate of actual strain increase. The output (i.e., load vs average strain) was plotted using an x-y recorder.

2.4 Results

2.4.1 General

The results of the experimental work are grouped based on loading regime. Each group represents a specific loading regime. The data is examined to study the behavior of mortar subjected to different load

histories.

Forty-four batches of mortar were tested. The specimens were subjected to various loading regimes for each batch.

The following groupings are used:

(i) Monotonic loading;

(ii) Cyclic loading to the envelope;

(iii) Cyclic loading with a constant strain increment between successive cycles;

(iv) Cyclic loading between fixed maximum and minimum stresses;

(v) Cyclic loading to a constant maximum strain; and

(vi) Cyclic loading to common points.

The variation of the total and incremental "Poisson's ratio" with load is also studied.

2.4.2 Monotonic Loading to Failure

This group of tests was designed to study the monotonic stress-strain behavior, investigate the existence of an envelope curve, and provide data to compare the behavior of mortar under monotonic and cyclic loading.

A complete stress-strain curve consists of a nonlinear ascending branch, which attains zero slope at its peak, and a nonlinear descending branch which has decreasing stress capacity with increasing strain.

Fig. 2.5a shows a typical stress-strain curve. As load increases, the material softens, indicated by the decreasing tangent modulus of elasticity of the stress-strain curve. Hairline cracks begin to appear in the specimen, slightly after crossing the peak of the stress-strain curve. As strain increases further, the size and length of these cracks increase. The cracks begin to pass through the length and width of the

prismatic portion of the specimen. At larger strains, sliding of the material in the cracked zone is observed. The deflection due to sliding may be the major strain component in the descending branch of the stress-strain curve. Quick unloading and premature failure occurs (Fig. 2.5b) when the major portion of cracking exists outside the range (gage length) of the compressometer. The resulting descending branch of the stress-strain curve is not representative of the material as a whole. The compressometer (Section 2.3.4) used a three-inch gage length for the six-inch-long prismatic portion, reducing the possibility of obtaining an unrealistic descending branch. To be on the safe side, only those tests yielding strains in the descending branch of the stress-strain curve, at least twice as large as the strain at the peak stress, were considered to yield realistically "complete" records of stress-strain behavior of mortar. Table 2.2 shows the results for the monotonic loading tests. The specimens are identified by batch and specimen number (2-1), type of test (M), age of test in days (28) and W/C (0.6). The key to specimen identification is provided in Appendix A.

Sixty-one specimens were tested under monotonic loading. Thirty-eight specimens yielded "complete" records of the stress-strain curve. For water-cement ratio = 0.6, thirty-six specimens were tested at the age of 28, 29 or 30 days, seven specimens at the age of 14 or 15 days, and five specimens at the age of 5 to 8 days. For W/C = 0.5, eleven specimens were tested at the age of 28, 29, or 30 days, and two specimens of the same batch at 50 and 52 days.

The average time to reach the peak stress varied from seven to fifteen minutes.

The results of the monotonic loading tests are compared for the

same batch, different batches, different ages, and different W/C ratios. The variations in the value of the initial modulus of elasticity, E_i, peak stress, σ_m, and corresponding strain, ε_m, and the stresses at twice and three times the strain at the peak, $\sigma_{2\varepsilon_m}$ and $\sigma_{3\varepsilon_m}$, respectively, are studied. The effect of the rate of loading on these properties is also investigated.

Specimens from the Same Batch: The monotonic loading test results for the specimens of the same batch at the same rate of loading are compared in Table 2.3. The scatter in the values of the different properties is consistently small for the specimens within a batch. Fig. 2.6 illustrates that the scatter is larger in the descending branch.

Specimens from Different Batches: The average values of the experimental results of mortar for several batches are also shown in Table 2.3. For the same rate of loading, W/C ratio and age at test, the various properties of mortar have comparable values for different batches.

Specimens of Different Ages: Table 2.4 shows the average values of the properties of mortar for the ages of 7, 14, and 28 days with the W/C = 0.6. Due to the significant scatter and the relatively small number of test results, only the trend of the behavior may be suggested. The initial modulus of elasticity tends to increase with increasing age. The peak stress and the corresponding strain increase with age. The descending branch of the stress-strain curve becomes steeper with increasing age. These results are similar to the behavior of concrete, which becomes stiffer, stronger, has an increasing strain corresponding to the peak stress, and a steeper descending branch with increasing age.

Specimens with Different W/C Ratios: Table 2.4 shows the average values of the properties of mortar for W/C = 0.6 and 0.5. The average initial modulus of elasticity is slightly higher and the average peak stress

and strain are larger for the specimens with the lower W/C. For specimens with W/C = 0.5, the loading was stopped when the material reached a strain of about twice the strain at the peak of the stress-strain curve. The ratio of stress at twice the strain at the peak stress to the peak stress is slightly lower for the lower W/C ratio (higher strength mortar). This result is similar to the behavior of concrete, which yields a steeper descending branch with increasing strength.

Effect of Rate of Loading: For monotonic loading, the peak stress was reached between seven and fifteen minutes. For cyclic loading, the peak stress was reached between one-half and two hours. To study the effect of this time difference on the stress-strain behavior, monotonic loading tests were conducted in which the time needed to reach the peak stress was equal to approximately one hour. Table 2.5 shows the comparison of the normal and slow test results of monotonic loading. No significant differences in the behavior of mortar are observed at the two different rates of loading. This similarity in the behavior is not totally unexpected, since the loading rates are within one order of magnitude of each other (25).

2.4.3 Cyclic Loading

The purpose of these tests was to study the degradation of mortar with cycles of load and to examine the shape of the envelope curve for cyclic loading. The cyclic loading regimes are subdivided into a number of groups, depending on the specific details of the loading procedure. These groups are described specifically in later sections.

To understand the basic characteristics of the stress-strain response of mortar under cyclic loading, an example is shown in Fig. 2.7. This cyclic loading response of mortar, illustrates the basic characteristics

of the degradation of mortar upon which the foundations of further groups of tests are laid:

(i) When the material is unloaded to zero stress, the strain does not return to zero. Instead, at the end of every cycle, additional permanent or residual strain is accumulated.

(ii) Upon reloading, the stress-strain curve passes below the point at which it was previously unloaded. The decrease in the reloading stress to the previous unloading strain is termed the "stress-drop per cycle." The point of intersection of the unloading and loading curves is called a "common point" (12).

(iii) The initial modulus of elasticity of each successive loading cycle is less than that of the previous cycle. The decreasing slope is an indication of a softening or degradation of the mortar.

(iv) A smooth curve passing through the upper portions of the cycles represents the envelope curve (Fig. 2.7).

(v) To reach the same value of stress upon reloading as that corresponding to the point of previous unloading, the material undergoes a larger value of strain in the ascending branch. In the descending branch the same stress is never achieved.

(vi) Both the loading and unloading components of a cycle are nonlinear.

The tests described in the following sections were conducted to study the effect of loading history on (i) the shape of the envelope curve, (ii) the accumulation of residual strain as a function of the maximum strain per cycle, (iii) the changes in the initial modulus of elasticity,

(iv) the stress drop per cycle, and (v) the existence of a stability limit below which no further damage occurs.

2.4.4 Cyclic Loading to the Envelope

These tests were designed to study the shape of the envelope curve, the changes in the shapes of the loading and unloading components of the cycles during cyclic loading to the envelope, and to investigate the inter-relationships between the strains at reloading and unloading, the residual strain, and the initial modulus of elasticity.

Each cycle of load was carried to the envelope, during loading and, to zero stress, during unloading.

The tests for this group are described in Table 2.6. Twelve specimens were tested. A typical test result is shown in Fig. 2.7, and the characteristics of the behavior of mortar under cycles to the envelope are described in Section 2.4.3. In addition, for cycles beginning at low values of strain, the shape of the loading component of the cycles is convex to the left. For intermediate values of strain, the shape becomes essentially linear, and ultimately at very large strains, the shape of the curve is concave to the left.

The continuously decreasing slope of the loading component of the cycles beginning at small strains indicates that damage continuously occurs throughout the range of strain traversed during loading of the specimens for such cycles. The loading component of the cycles beginning at medium strains is essentially linear until it approaches the previous unloading strains, where it becomes very curvilinear. This indicates that extensive damage for such cycles begins when the curve approaches the previous unloading strain. At large strains, the material has developed large cracks passing through the length and the width of the specimen.

As reloading is begun, the deformation consists mainly of sliding within the cracked region, and the resistance is constituted primarily by friction between the sliding surfaces of the material. As the stress nears the peak of the cycle, further damage and extension of cracking occurs. Hence, in the lower portion of the curve,the material offers lower resistance, but the resistance increases in the upper portion. This is shown by the concavity of the loading component.

Table 2.7 compares the test results for monotonic loading and cyclic loading to the envelope. It is observed that the initial modulus, peak stress, and corresponding strain have comparable values for both monotonic loading and cyclic loading to the envelope. The stresses at twice and three times the strain at the peak are higher for cyclic loading. The approximate time to reach the same strain is larger for cyclic loading. These results indicate that the descending branch of the envelope is higher for cyclic loading. The factors contributing to the higher cyclic envelope are discussed in Chapter 3.

2.4.5 Cyclic Loading with a Constant Strain Increment Between Successive Cycles

The general purpose of these tests was the same as the tests described in the previous section. In addition, the effect of the magnitude of the strain increment on the behavior of mortar was investigated.

Table 2.8 describes the tests conducted in this group. Eleven specimens were tested with varing strain increments. A typical test result is shown in Fig. 2.8. The general observations are similar to those made in Sections 2.4.3 and 2.4.4.

Unloading in this type of cyclic loading was begun when the difference between the current maximum strain and the previous maximum

strain equaled the specified strain increment. When the strain increment was small enough, it yielded a maximum strain during reloading lower than that required to reach the envelope. This phenomenon usually occurred in the intermediate strain region of the descending branch of the envelope. Hence, unloading in such case began at a value of stress below the corresponding point on the envelope.

Table 2.9 compares the test results for monotonic loading and cyclic loading with a constant strain increment between successive cycles. The stresses at twice and three times the strain at the peak do not show any specific trend. This may be explained by the fact that the curves did not reach the true envelope.

2.4.6 Cyclic Loading Between Fixed Maximum and Minimum Stresses

The purpose of these tests was to investigate the effect of cycling between fixed stresses on the degradation and failure of mortar. The effect of this type of cyclic loading on the shape of the envelope curve was also investigated.

The load was cycled between fixed maximum and minimum stress limits. "Failure" was indicated when the specified maximum stress could not be reached and the stress-strain relation entered the descending branch of the envelope. In a few tests, the cyclic loading was terminated before failure, and the specimen was loaded monotonically to study the shape of the envelope curve.

The tests in this group are summarized in Table 2.10. Out of twenty-two specimens tested, seven had a non-zero minimum stress limit. Seven specimens were used to investigate the effect of cyclic loading on the shape of the envelope.

A typical test result is shown in Fig. 2.9. It is observed

that the maximum strain (i.e., the strain to reach the upper stress limit) increases with each cycle. For cycles with a zero minimum stress level, the residual strain accumulates with each cycle. The softening of the material also continues, which is indicated by the decreasing slope of the loading components of the cyclces. The size of the increment in maximum strain first decreases and then continues to increase as the material approaches failure. This fact is discussed at greater length in Chapter 3. For the same maximum stress, the accumulation of strain is faster and, therefore, degradation is greater, in the specimens subject to zero minimum stress than in specimens subject to a non-zero minimum stress. This is shown by tests 1 and 2 of batch 41 ((15) and (16) in Table 2.10) in Fig. 2.10. The maximum stress is approximately the same for the two specimens. The specimen with a minimum stress level equal to approximately half the maximum stress failed after sixteen cycles. The specimen with zero minimum stress level failed after eight cycles. Two specimens of batch 13 (tests (8) and (9) in Table 2.10) were cycled to the same maximum stress level (Fig. 2.11). Both specimens were cycled 12 times. The specimen with a minimum stress level equal to about half of the maximum stress, had a total maximum strain accumulation equal to 83 percent of that for the specimen with the zero minimum stress limit. As expected, the higher the maximum stress level, the faster the degradation of the material. This is, also, illustrated by the two specimens of batch 42 (tests (17) and (18) in Table 2.10). The specimen with the 3800 psi maximum stress limit failed after eight cycles, while the specimen with 3700 psi maximum stress limit failed after 15 cycles.

Table 2.11 compares test results for monotonic loading with results for cyclic loading between maximum and minimum stresses. The

first pair of tests compares the particulars of the envelope when the cyclic loading was continued until failure. The other two pairs compare the results when the cyclic loading was terminated before failure and loading was then continued monotonically. For the first pair, the stresses at twice and three times the strain at the peak stress are higher for cyclic loading. For the second and third pairs, the results are comparable. These limited comparisons indicate that the descending branch of the envelope curve is higher when cyclic loading is continued up to failure, otherwise, the shape is little changed from the monotonic loading curve.

2.4.7 Cyclic Loading to a Constant Maximum Strain

The purpose of these tests was to investigate the degradation of mortar when cycled to constant values of maximum strain. The shape of the envelope curve was also studied for this type of cyclic loading.

For a given value of maximum strain, the testing machine automatically cycled load between zero stress and the specified strain. Each cycle produced a stress drop (i.e., the value of reloading stress at the maximum strain decreased for each cycle). The softening (change in the slope of the loading curve) mainly occurred when it approached the maximum strain. The unloading curves were nonlinear and residual strain accumulated with each cycle. As cycling continued, the stress drop became smaller. The accumulation of residual strain also decreased, correspondingly. The decreasing rates of stress drop and residual strain accumulation suggested the possibility of ultimate stability (i.e., no further damage). In the present study, stability was not achieved up through a maximum of 42 cycles.

When the stress drop and residual strain accumulation became sufficiently small, the specimen was subjected to a new (larger) value of

maximum strain, and cycling was restarted. In this way, degradation was studied at a number of strains for the same specimen.

Table 2.12 describes the specimens tested using this type of loading. Table 2.13 gives the values of peak stress for successive cycles to the same value of maximum strain for each specimen tested. Fig. 2.12 shows a typical example of this type of loading.

Table 2.14 compares the test results for monotonic loading and cyclic loading to a constant maximum strain. The properties of the ascending branch are approximately the same for this type of cyclic loading as they are for monotonic loading. However, for the descending branch, the stress at twice the strain at the peak stress is considerably higher for the cyclic loading.

2.4.8 Cyclic Loading to the Common Points

The purpose of these tests was to investigate the existence of a stability stress level (minimum stress level), below which cyclic loading produces no additional strain and the stress-strain curve forms a closed hysteresis loop. The effect of this type of cyclic loading on the shape of the envelope curve was also studied.

After completing one cycle of load, reloading for the next cycle was continued until the reloading curve intersected the previous unloading curve. The point of intersection is the "common point." Unloading was begun at the common point. For each of the next cycles of load, unloading was begun at the common point of the current loading curve and the initial unloading curve. This type of cycling was first conducted by Karsan and Jirsa (12). Successive common points occurred at lower values of stress and strain, indicating a drop in stress for each cycle. Residual strain also accumulated with each cycle. The rate of stress drop

and residual strain accumulation decreased as they did for the tests to a maximum strain, but at a faster rate. After just a few (five to ten) cycles, it became increasingly difficult to locate the next common point exactly. At this stage, upon reloading, the next cycle was carried to a larger value of strain on the envelope, and then unloading was started again. The new set of common points corresponded to the intersections of the loading curves with the first unloading curve from the envelope. The cycling was, again, conducted for a number of cycles. In this manner, the common points, showing dropping stress for successive cycles, were obtained at several locations in stress-strain space.

These tests were conducted early in the research program. It was later realized that this method may not be a realistic way to obtain the stability limit. The material experiences a large strain initially and then successively smaller strains. It initially undergoes an extent of damage which corresponds to the larger value of strain. Cycling to smaller values of strain may indicate converging stress-strain curves, but the results may be misleading. This observation was confirmed when the specimens were subjected to cyclic loading to a specified value of maximum strain (Section 2.4.6). Those tests showed dropping values of peak stress, but convergence to a stability limit was never achieved.

Table 2.15 gives a description of the specimens tested for this type of loading. Fig. 2.13 shows a typical stress-strain curve.

Table 2.16 compares the test results for monotonic loading and cyclic loading to the common points. The stresses at twice and three times the strain at the peak are generally higher for the specimens tested under cyclic loading than for specimens subjected to monotonic loading. This continues the trend observed for the other cyclic tests.

2.4.9 Envelope Curves for Various Load Regimes

Table 2.17 compares the values of the initial modulus, peak stress and corresponding strain, and stresses at twice and three times the strain at peak stress for various load regimes. The stresses at twice and three times the strain at the peak stress are generally higher for the cyclic loading tests. It seems that the shape of the ascending branch of the envelope curve is the same for all types of loading, but the descending branch is flatter and higher for cyclic loading than for monotonic loading.

2.4.10 Tests to Measure Poisson's Ratio

The incremental "Poisson's ratio" is defined as the ratio of a small increment in lateral strain with the corresponding increment in longitudinal strain. The incremental Poisson's ratio at a given stress, σ, is calculated by measuring the changes in longitudinal and lateral strains corresponding to a stress range of $\sigma \pm 300$ psi. The total "Poisson's ratio" relates the total lateral strain with the corresponding longitudinal strain.

Table 2.18 describes the tests conducted to study the variation of total and incremental Poisson's ratios with load. Only two specimens were tested under monotonic loading, and only one of the two gave a complete stress-strain record. Only one specimen was tested under cyclic loading.

Monotonic Loading: Fig. 2.14 shows the stress-strain curves for test 9-1/M/29/0.6. Figs. 2.15 and 2.16 show the changes in total and incremental Poisson's ratios, respectively, with stress changes. It is observed that the Poisson's ratios increase with increasing stress and continue to increase past the peak of the stress-strain curve. The plot of the Poisson's ratios versus strain (Fig. 2.17) shows that the incremental

as well as the total Poisson's ratio seems to be a curvilinear function of the strain. The strain at the peak of the stress-strain curve does not bear any significance in this relationship. This result is similar to the observations of other investigators (27) who observed that the peak of the stress-strain curve is not significant in the continuous process of degradation of cement paste and concrete. The observed increase in Poisson's ratio exceeds 0.5 indicating that an increase in the volume of the mortar has taken place.

Cyclic Loading: Fig. 2.18 shows the stress-strain plot and Table 2.19 shows the variation of the incremental and total Poisson's ratios during cycles of load for test 9-3/CEN/28/0.6. In each cycle the Poisson's ratio increases as the stress increases in the loading component of the cycle and decreases with decreasing stress in the unloading component. The exception occurs at stresses at the beginning of unloading, where the incremental Poisson's ratio suddenly becomes very small, then comes back to the larger value at a slightly lower stress, and then continues to decrease with decreasing stress. It is, also, observed for cyclic loading that the incremental and total Poisson's ratios do not exceed a value of 0.3, up to strains as large as about one-and-a-half times the strain at the peak of the envelope. However, in the absence of any verification of this data, it may be premature to make any sweeping statements about the variation of Poisson's ratio during cycles of load.

CHAPTER 3

ANALYSIS AND DISCUSSION OF TEST RESULTS

3.1 General

Damage is defined as the reduction in strength or useable strain capacity of a material. During cyclic loading of mortar, a number of indications of damage are observed. Indicators of damage are the initial modulus of elasticity for successive cycles, the residual strain upon completion of a cycle, the increase in maximum strain for cycles between fixed stress limits, and the stress drop for cycles to a specified strain.

The indicators of damage provide a consistent assessment of degradation and, therefore, will be studied in detail as quantitative measures of damage for different types of cyclic loading. From the study of the sensitivity of the indicators of damage to the degradation caused by different types of loading regimes, the best indicators will be selected. Ths various forms of damage that may occur within mortar and their relationships with the indicators of damage will be discussed. The factors that control the degradation of mortar will, also, be discussed.

Finally, the observations made in the present investigation about the behavior of mortar will be compared with the observations made by other investigators about concrete, mortar and cement paste.

3.2 Residual Strain as a Function of Unloading Strain

During cyclic loading, the accumulation of residual strain, ε_r, occurs for all types of loading regimes. The rate of accumulation of residual strain, however, depends on the specific type of loading.

The residual strain at the completion of a cycle is plotted against the strain prior to unloading or unloading strain, ε_u, for each cycle.

The points thus obtained are joined to obtain a curve, which shows the general relationship between the residual strain and the unloading strain. The relationship of residual strain to unloading strain is described for the various loading regimes utilized.

3.2.1 Cycles to the Envelope

For this type of cyclic loading, the unloading strain represents the envelope strain and is, therefore, termed unloading envelope strain, ε_{eu}. Plots for three tests are shown in Fig. 3.1. For small strains, the accumulation of residual strain is very low. The rate of residual strain accumulation initially increases with increasing ε_{eu}. At large strains, the curves become linear, with a slope of one. At this stage, the increase in unloading envelope strain causes approximately the same increase in the accumulated residual strain. The relationships for the three tests are similar.

3.2.2 Cycles with Constant Strain Increment

For this type of cyclic loading, the stress corresponding to the unloading strain may be below the envelope. Residual strain versus unloading strain curves are shown in Figs. 3.2a and b for five tests. These curves initially have the same shape as those for cycles to the envelope. At about twice the strain at the peak of the envelope or higher, the slope of the curves exceeds one. This indicates that the increase in residual strain becomes larger than the strain increment. As unloading strain increases further, the slope of the curves begins to decrease. Finally, the slope of the curves becomes less than one.

Coinciding with the point at which the slope of these curves exceeds one, the stress at the point of unloading is lower and remains lower than the stress at the envelope. The increase in ε_r is higher than

obtained for cycles to the envelope (Fig. 3.1). As the stress at the peak of a cycle stays lower than the envelope, the residual strain-unloading strain curve begins to rise. For larger strains, the peaks of the cycles again begin to approach the envelope. As the peak stress prior to unloading approaches the envelope stress, the ε_r-ε_u relationship begins to drop. The fact that its slope becomes less than one indicates that the curve will join the ε_r-ε_{eu} curve at sufficiently large strains.

3.2.3 Cycles between Fixed Stresses

In this type of cyclic loading, the unloading strain does not represent the envelope strain except for the first and final cycles, when unloading occurs from the ascending and descending branches of the envelope.

When mortar is cycled between fixed stresses with a zero minimum stress limit, the strain increases with each cycle. The plots of residual strain versus unloading strain (ε_r-ε_u) for these tests are approximately straight lines. Table 3.1 gives the slopes of these lines and comments on the location of these lines compared with ε_r-ε_{eu} curve. The results indicate that the ε_r-ε_u line generally bridges ε_r-ε_{eu} curve, beginning and ending at the strains on the ascending and the descending branches of the envelope, respectively, corresponding to the maximum stress limit. This observation is illustrated by a typical example in Fig. 3.3.

Fig. 3.3 also illustrates the fact that cycles to a lower maximum stress tend to accumulate more residual strain for a given value of ε_u.

The data in Table 3.1 indicate that the slope of the ε_r-ε_u line generally decreases with an increasing ratio of the maximum stress limit to the average strength of the mortar, f'_m. Fig. 3.3 also illustrates this

fact. This is compatible with the previous observations. For a given increase in the maximum stress - f'_m ratio, the corresponding increase in ascending branch strain is less than the accompanying decrease in the descending branch strain, due to the greater steepness of the ascending branch. Hence, the ε_r-ε_u line (for the higher stress) has a lower slope.

3.2.4 Cycles to a Constant Maximum Strain

For this type of cyclic loading, the residual strain after the first unloading from a specified strain is plotted against that strain in Figs. 3.4a and b. The strain prior to first unloading occurs on the envelope curve. The curves are essentially the same for tests with different ages and different water-cement ratios. These curves are initially higher than the curves for cycles to the envelope, but the overall shape is the same. However, in general, the ε_r-ε_{eu} relation appears to be independent of load history. This is demonstrated by the ε_r-ε_u curve shown in Fig. 3.5. The residual strains accumulated in the first and the last cycle to the same value of specified strain are included in this plot. The residual strain continues to accumulate and the stress continues to drop, with each cycle, as discussed in Chapter 2. When the specimen is subsequently loaded to a higher strain , the residual strain obtained upon the completion of unloading is essentially the same as that obtained for direct cycles to the envelope. The fact that the ε_r-ε_{eu} relation remains unchanged is strong evidence that the relation is unique.

3.2.5 Cycles to Common Points

For this type of cyclic loading, the residual strain after completion of the first unloading from the envelope is plotted against the envelope strain for four tests in Fig. 3.6. These curves concide with the ε_r-ε_{eu} curves obtained for cycles to a specified strain and have the same

general shape as those for cycles to the envelope.

Fig. 3.7 shows a typical ε_r-ε_u curve for cycles to common points. As the residual strain accumulates (with the decreasing peak strain and stress at the common points), the curve goes higher. When the specimen is again loaded to a larger strain on the envelope, the residual strain obtained upon the completion of unloading is essentially the same as that obtained for cycles to the envelope. This confirms the uniqueness of the ε_r-ε_{eu} relation.

3.3 Envelope Strain Upon Reloading as a Function of Residual Strain

To study the effect of load history on the relationship between the envelope strain upon reloading, ε_{er}, and the residual strain prior to reloading, ε_r, envelope strain versus residual strain (ε_{er}-ε_r) curves are constructed for different types of loading regimes.

The envelope curve is obtained, as described in Section 2.4.3 and as shown in Fig. 2.7. The strain at the point where the reloading curve joins the envelope represents ε_{er}. For those cycles whose peaks yield zero slope, but still remain below the envelope, the envelope strain is obtained by extrapolating the loading portion of the cycle to reach the envelope, as illustrated in Fig. 3.8. Those cycles which stay below the envelope curve, but do not yield a zero slope at their peaks, are not used in this portion of the analysis. For cycles with peaks above the envelope, the strain at which the peak of the cycle reaches zero slope is used as the envelope strain.

The relationship between the envelope strain and the residual strain is studied as follows for a number of loading regimes.

3.3.1 Cycles to the Envelope

ε_{er}-ε_r curves are shown in Figs. 3.9a and b for three 28-day

tests, and for one 14-day test and two 7-day tests, respectively.

The increase in envelope strain continues to become smaller with increasing residual strain, until ε_{er} reaches approximately 0.003. For larger values of envelope strain, the envelope strain increase becomes equal to the residual strain increase, i.e., the slope of the curve becomes equal to one.

The overall shape of the curves in Figs. 3.9a and b is the same. The curves match remarkably up to envelope strains of about twice the strain at the peak of the envelope. Comparing these plots with the ε_r-ε_{eu} curves (Fig. 3.1), the following observations are made: (i) The overall shape is the same for both types of curves, (ii) as expected, the envelope strain after reloading is larger than the envelope strain prior to unloading for the same residual strain, and (iii) at large envelope strains, the two types of curves become almost parallel straight lines.

3.3.2 Cycles to a Constant Maximum Strain

For these tests, only those cycles which reach the envelope are used. These cycles are the first cycles to the specified strains. The plots for one 30-day test with W/C = 0.5 and two 14-day tests with W/C = 0.6 are shown in Fig. 3.10.

The general observations for these curves are similar to those obtained for cycles to the envelope. It is further noted that water-cement ratio and age do not seem to effect the shape of the curves.

Comparing the ε_{er}-ε_r curves for cycles to the envelope and cycles to a constant maximum strain, the curves for cycles to the envelope are initially slightly higher, but the overall shape is the same. The similarity in shape indicates that the relationship of envelope strain upon reloading versus residual strain is fairly independent of the number of

cycles or the type of cyclic loading.

Comparing Fig. 3.10 with the ε_r-ε_{eu} curves in Figs. 3.4a and b, observations similar to those made for cycles to envelope in Section 3.3.1 can be made.

3.3.3 Cycles to Common Points

For these tests, only those cycles reaching the envelope are used. Envelope strain versus residual strain curves for four tests of the same age and water-cement ratio are shown in Fig. 3.11.

The overall shape of the curves is the same. As observed for the previous two types of tests, the slopes of the curves decrease rapidly until an envelope strain of about 0.003 is attained. For higher envelope strains the curve becomes a straight line with a slope of one.

The ε_{er}-ε_r curves for cycles to the common points are slightly lower than those for cycles to the envelope (Fig. 3.9), up to the strains at the peak of the envelope. For larger strains the curves match well. The curves for cycles to common points and cycles to a constant maximum strain (Fig. 3.10) match for all strains.

As observed for other loading regimes, the ε_{er}-ε_r curves and ε_r-ε_{eu} curves (Fig. 3.6) have a similar shape.

3.4 Initial Modulus of Elasticity as a Function of Unloading Strain

The "initial" modulus of elasticity, E_i, is taken as the secant modulus for the stress range of 625-1250 psi. This stress range was selected because it avoids the initial vertical portion of the loading curve and lies in the linear portion of the curve.

E_i-ε_u curves are shown in Figs 3.12, 3.13 and 3.14 for cycles to the envelope, cycles with a constant strain increment and cycles to

common points, respectively. For the first unloading from the envelope, at an ε_{eu} as large as 0.0005, a stress as high as 0.56 f'_m, the initial modulus was found to increase at the beginning of the next cycle, as shown in Table 3.2. For cycles to higher strains, the initial modulus begins to decrease at an accelerating rate. Finally, the rate of modulus decrease begins to slow beginning at strains equal to about one-and-a-half times the strain at the peak of the envelope.

For cycles to the common points, only those cycles which reach the envelope are used to obtain the values of the initial modulus of elasticity and the unloading strain. Therefore, the unloading strain is the envelope strain for both cycles to the envelope and cycles to the common points. As mentioned earlier, the unloading strain may be less than the envelope strain for cycles with a constant strain increment.

The general shape of the curves for the different types of tests is the same. The curves for cycles with a constant strain increment, and cycles to common points match. The curves for cycles to the envelope are slightly lower.

Log-log plots of the initial modulus versus the unloading strain are shown in Fig. 3.15 for a number of loading regimes. These curves begin with zero slope at a strain of approximately 0.0006. The values of E_i drop with increasing ε_u, indicating that the initial modulus does not reach an asymptotic value. The shape of the curves is the same, regardless of the type of loading. Even curves that may not reach the envelope on every cycle, such as cycles with a constant strain increment, have essentially the same shape as those for other loading regimes. Fig. 3.16 shows E_i versus ε_u for cycles to a specified strain and cycles to the common points. For cycles to the common points, the data for the first and last

cycles to the common points (based on the same unloading curve from the envelope) are included in the plot. For cycles to a specified strain, the first and last cycles to the same strain are included. The plots show that the initial modulus continues to decrease for cycles to the same maximum strain, and even for cycles to successively lower strains at the common points.

Table 3.3 shows the changes in the initial moduli of elasticity for cycles to specified maximum strain and Table 2.13 shows the corresponding drop in stress at the peaks of successive cycles. The last columns of the two tables give the total percentage drop in stress and initial modulus, respectively. A comparison of the two tables shows that the change in E_i is somewhat less sensitive to cycles of load than the drop in stress for this type of load regime.

3.5 Initial Modulus of Elasticity Versus Residual Strain

Plots of initial modulus versus residual strain are shown in Figs. 3.17, 3.18, 3.19 and 3.20 for cycles to the envelope, cycles with a constant strain increment, cycles to common points and cycles between fixed stress limits, respectively. The curves for cycles to common points are for cycles reaching the envelope.

The general shape of these curves is the same, regardless of the type of loading regime, except for cycles to the envelope, which yield slightly lower curves. The initial modulus versus the residual strain for a cycle to the common points test and a cycle to a specified strain test are plotted in Fig. 3.16. For cycles to common points, the plot includes the data for the first and last cycles intersecting the same unloading curve. For cycles to a specified strain, the plot includes the data for

the first and last cycle to the same strain.

The sudden dips in the plot of cycles to a specified strain and the small humps in the plot for cycles to common points show disproportionate changes in initial modulus and residual strain as the peaks of the cycles fall below the envelope. These effects do not significantly change the overall relationship between initial modulus and residual strain. It can still be said with a fair amount of accuracy that the initial modulus-residual strain relation is not significantly affected by the differences in the stress at the peaks of the cycles or the envelope stress.

3.6 Stress Drop Versus Number of Cycles for Cycles to a Constant Maximum Strain

The stress at the peak of each cycle is plotted versus the number of cycles to the same strain for four tests in Fig. 3.21. The log-log plot of the same data is shown in Fig. 3.22.

Fig. 3.21 shows that as cycles of load continue to the same strain, the stress at the peak of successive cycles continues to drop. The rate of stress drop decreases as cycling continues. Referring to the log-log plot in Fig. 3.22, the straight line relationships show that the stress drop does not stabilize. It is, also, observed that the straight lines relating the log of stress drop with the log of number of cycles are roughly parallel, independent of maximum strain, water-cement ratio and age.

3.7 Residual Strain Versus Number of Cycles for Cycles to a Constant Maximum Strain

The residual strain at the completion of a cycle to a constant maximum strain versus the number of cycles to the same strain is plotted

for two tests in Fig. 3.23. Fig. 3.24 shows log-log plots at selected values of strain for three tests.

Fig. 3.23 shows that the accumulation of residual strain continues at a decreasing rate, as cycling continues. This is true, for both tests. Fig. 3.24 shows that the log-log plots of residual strain versus the number of cycles are approximately linear. This indicates that the accumulation of residual strain does not stop as cycling continues to the same value of strain.

The lines in Fig. 3.24 are approximately parallel, although they correspond to residual strain accumulation for cycles to different values of strain and for specimens with different water-cement ratios and ages. Hence, the rate of degradation appears to be independent of these variables.

3.8 Maximum Strain Versus Number of Cycles

For cycles between fixed stress limits, the maximum strain increases with the number of cycles. However, the rate of strain increase varies.

Fig. 3.25 shows the change in maximum strain with the number of cycles. It is observed that the increase in strain per cycle first decreases and then increases.

As the maximum strain increases, the difference between the maximum stress and the envelope stress continues to increase until the peak of the envelope is reached. The rate of strain increase slows as the envelope stress rises above the maximum stress with each cycle. Under the descending branch of the envelope, the envelope stress drops with increasing strain, and therefore, the difference between the envelope stress and the maximum stress decreases. The strain increase per cycle now begins

to increase and continues this trend until the cycles intercept the envelope. This suggests that the strain increase per cycle is controlled by the ratio of the maximum stress at a given strain to the corresponding envelope stress. The higher the ratio, the greater strain increase per cycle.

Fig. 3.26, along with the data furnished by Table 2.10, shows the plot of maximum strain increase with number of cycles, for two tests. Both specimens were cycled to three different maximum stresses. The values of the maximum stresses were the same for both tests, and the specimens were cycled the same number of times for the first two maximum stress limits. The minimum stress limit was kept equal to zero for one specimen and equal to about half of the maximum stress for the other.

The curves shift to a higher position and acquire a larger slope as the maximum stress limit increases, indicating a higher rate of increase in maximum strain. The effect of a nonzero minimum stress limit becomes apparent at the highest maximum stress limit, when the rate of strain increase stays considerably lower than that for the specimen with the zero minimum stress.

This suggests that the degradation of mortar is faster, the higher the maximum stress and the lower the minimum stress, meaning that the total stress range of a cycle affects the damage.

3.9 Factors Controlling Degradation

The analysis of the test results in terms of the indications of damage brings to light a number of factors which seem to control the degradation of mortar. These factors are the maximum strain, the range of strain, the ratio of the maximum stress to the envelope stress at a

given strain, and the number of cycles of load. These factors will be studied in the following paragraphs, as they affect the behavior of mortar under different types of loading regimes.

3.9.1 Maximum Strain

During monotonic loading, the degradation of mortar continues to occur as the strain increases. The degradation of mortar is indicated by a continuously decreasing tangent modulus of elasticity and a continuously increasing Poisson effect with increasing strain. For cyclic loading, an increase in maximum strain results in an increase in residual strain and a decrease in the initial modulus of elasticity.

3.9.2 Range of Strain

For cyclic loading with a constant strain increment, the ε_r-ε_u curve achieves a slope greater than one in the descending branch of the envelope (Section 3.2). This happens when the strain increment is not large enough to carry the cycles to the envelope. When the ε_r-ε_u curve achieves a slope greater than one, the increase in residual strain exceeds the increase in maximum strain. If the maximum strain were to be the only factor controlling the degradation, the increase in residual strain would, at most, be equal to the increase in maximum strain.

As shown in Fig. 3.27, the total range of strain traversed by the specimen during a single cycle of load, $\Delta\varepsilon^r$ (equal to the absolute value of loading and unloading component of a cycle), is much larger than the maximum strain increment, $\Delta\varepsilon_u$. The fact that the increase in residual strain, $\Delta\varepsilon_r$, is greater than $\Delta\varepsilon_u$, is a strong indication that the range of strain, $\Delta\varepsilon^r$, also causes degradation of mortar.

For cyclic loading between fixed stress limits, the residual strain, ε_r, corresponding to a given value of maximum strain, ε_u, is

larger than that corresponding to the same value of the unloading envelope strain, ε_{eu} (Section 3.2), since the ε_r-ε_u line bridges the ε_r-ε_{eu} curve, as illustrated by the hypothetical example in Fig. 3.28. For cycles to the envelope, the total strain range traversed during cycles to a given strain is much smaller than the strain range traversed during cycles between fixed stresses, due to a lower number of cycles. This indicates that the greater the range of strain, the greater the damage.

For cyclic loading to a constant maximum strain, residual strain accumulates, peak stress drops and the modulus of elasticity decreases, as cycles of load continue to the same maximum strain. As the range of strain traversed during successive cycles increases, the amount of degradation also increases.

For cycles to common points, the integral effect of the range of strain is strongly evident in the residual strain increase and the initial modulus decrease even for a corresponding decrease in the maximum strain.

This discussion strongly suggests that the range of strain traversed during a cycle of load is a factor controlling the degradation of mortar.

3.9.3 Ratio of Maximum Stress to Envelope Stress (Maximum Stress Ratio)

For cycles between fixed stress limits, the increase in maximum strain is an indication of damage. The rate of increase in maximum strain appears to be controlled by the ratio of the maximum stress limit and the envelope stress at a given strain, as discussed in Section 3.8. The greater the ratio, the faster the increase in maximum strain per cycle, and therefore, the smaller the number of cycles to failure.

For cycles to a constant maximum strain, the stress drop occurs

and residual strain accumulates during successive cycles to the same maximum strain. As the ratio of the maximum stress at the peak of the present cycle versus the maximum stress achieved during first loading to the given strain decreases, less residual strain accumulates. The same phenomenon occurs during cycles to common points.

This discussion suggests that the maximum stress ratio is another factor controlling the degradation of mortar.

3.9.4 Number of Cycles

In all types of cyclic loading regimes discussed in Sections 3.9.2 and 3.9.3, the number of cycles acts as a controlling factor of degradation, along with the maximum stress ratio and the range of strain traversed.

For cycles between fixed stress limits,it was observed in Section 3.2.3 that the smaller the value of the maximum stress limit, the larger the accumulation of residual strain, for a given value of maximum strain. For these tests,as the maximum stress limit decreased, the strain accumulated per cycle decreased and, therefore, the number of cycles required to reach a certain value of maximum strain increased. Since the total range of strain traversed during the greater number of cycles was greater, the residual strain accumulation was larger.

3.10 Best Indicator of Damage

The criterion for the "best" indicator of damage is based on the "sensitivity" of the indicator to the damage caused by loading. The word "sensitivity" represents the capability to monitor degradation as early as it begins and to indicate the degree of damage caused by different loading regimes. The indicators of damage studied in the present chapter will be evaluated based on their sensitivity.

The indicators of damage are: The accumulation of residual strain, the decrease in the initial modulus of elasticity, the increase in maximum strain for cycles between specified stress limits, and the stress drop during cycles to a constant maximum strain. It is obvious that the increase in maximum strain and the stress-drop have limited usefulness, because they indicate damage for a single type of loading, only. The residual strain accumulation and initial modulus decrease occur with all of the loading regimes studied, except for cycles with a non-zero minimum stress-limit, and will be discussed.

Table 3.2 shows the value of residual strain upon unloading from the virgin stress-strain curve, and the initial modulus for the first reloading curve. A residual strain is observed for unloading strains as small as 0.00027. Upon reloading, an increase in the initial modulus is observed. This shows that both residual strain and initial modulus are highly capable of monitoring damage and/or structural change at a very early stage. Fig. 3.29 shows typical examples of the accumulation of residual strain and changes occurring in the initial modulus of elasticity with increasing strain for cycles to the envelope.

Previous investigators (5,25) have indicated that the initial modulus of elasticity and the energy dissipated in damage are highly sensitive to the degree of damage and have measured damage in cement paste and concrete at strains as low as 0.0004. The accumulation of residual strain may be added to the list of the "best" indicators.

It must be kept in mind that the accumulation of residual strain may include the effects of creep, in addition to the effects of cyclic loading. Since creep (the quantitative assessment of which was not made in this study) does not necessarily represent damage as defined at the

beginning of this chapter, the residual strain may be better considered as a "best" indicator of structural change in mortar. Further study is clearly warranted.

3.11 Nature of Degradation of Mortar

Structural changes in mortar produced by load may be of the following types:

(i) Local failure: Local compressive stress-strain state is beyond the peak of the envelope. Local failure manifests itself by the overall softening of the material (i.e., decrease in tangent modulus under monotonic loading and decrease in initial modulus under cyclic loading).

(ii) Compaction: Consolidation of the cement paste; manifests itself through permanent deformation and improvement in stiffness.

(iii) Cracking: Microcracks in the cement paste or at the paste-fine aggregate interface may occur. Cracking manifests itself by an increased Poisson effect and slight decrease in stiffness (6,16).

(iv) Sliding: Sliding of the material at a cracked surface manifests itself through similar increases in maximum and residual strain, without affecting the strength or stiffness, and an apparent increase in volume.

3.11.1 Monotonic Loading

The stress-strain curve has nonlinear ascending and descending branches with a continuous decrease in the material stiffness with increasing strain. This suggests that continuous local failure of mortar takes place, which may be accompanied by cracking. Since the Poisson's

ratio continues to increase, it shows that cracking and sliding are progressing.

3.11.2 Cyclic Loading

The initial modulus of elasticity increases and residual strain accumulates upon unloading from the virgin stress-strain curve (Table 3.2). This indicates that material compaction takes place. During further cyclic loading, the initial modulus of elasticity continuously decreases and residual strain continues to accumulate. This indicates that the process of failure is continuous during cyclic loading.

During monotonic or cyclic loading, hairline line cracks begin to appear on the surface of the specimen, as it crosses the peak of the envelope. Around one-and-a-half times the strain at the peak, the cracks become large and cut through the prismatic portion of the specimen. Cracks in cyclically loaded specimens are more in number and smaller in size, whereas in monotonically loaded specimens, cracks are less in number and larger in size.

At this stage, the descending branch of both the monotonic and cyclic envelopes begins to flatten. The rate of decrease of the initial modulus slows, and the increases in envelope strain and residual strain become approximately equal. The last observation indicates that sliding of the cracked surfaces is dominant at this stage.

The monotonic loading envelope yields a lower descending branch compared with the cyclic envelope. Since a larger number of cracks are observed in a cyclically loaded specimen, it seems that a larger volume of the specimen is subject to damage (distribution of damage) compared with a monotonically loaded specimen with the same maximum local state of damage (extent of damage). As shown by the hypothetical example in Fig.

3.30, the specimen sustaining the larger distribution of damage, yields a higher descending branch of the envelope curve.

The test results indicate that the residual strain is a function of the envelope strain, independent of the cyclic loading regime, but that the initial modulus of elasticity upon reloading is slightly lower for cycles to the envelope. As shown in Fig. 3.30, the specimen with the smaller distribution of damage has a lower slope, when reloaded from the same residual strain. It, therefore, seems that the strain range and the number of cycles affect the distribution of damage. A smaller distribution of damage is, therefore, expected in the specimen subjected to cycles to the envelope, compared with other cyclic loading regimes, due to the larger number of cycles involved in the latter cases. An even smaller distribution of damage occurs in a monotonically loaded specimen because the loading consists of only a single cycle.

3.12 Comparison of Monotonic and Cyclic Behavior of Cement Paste, Mortar and Concrete

3.12.1 Monotonic Loading

(1) The peak stress, and corresponding strain of mortar increase with increasing age and decreasing water-cement ratio, a property similar to that of cement paste and concrete (5,24,27).

(2) The stress-strain envelope yields a steeper descending branch with increasing strength, as observed for concrete (27). This indicates that the factors affecting damage are similar in nature for both mortar and concrete.

(3) The increase in Poisson's ratio takes place continuously with increasing compressive strain. The increase in Poisson's ratio under load implies that cracking and sliding are occurring.

The smooth change in Poisson's ratio indicates that the degradation of mortar is continuous under load. Spooner (26) has indicated that lateral expansion of cement paste relative to an ideal linearly elastic material occurs prior to reaching its peak stress, implying that the degradation of cement paste is progressive and of similar nature to that of concrete. It appears, therefore, that there are similarities in the nature of damage in cement paste, mortar and concrete.

3.12.2 Cyclic Loading

(1) The cyclic loading envelope for mortar has a flatter and higher descending branch than the monotonic envelope curve. The difference between the monotonic and cyclic envelopes is due to the different distributions of damage. Karsan and Jirsa (12) and Spooner and Dougill (25) indicate that the monotonic and cyclic envelopes for concrete are equivalent. Although the reason for this difference in behavior is not clear, the inclusion of coarse aggregate may result in a greater distribution of damage under monotonic load than is obtained with mortar.

(2) The shape of the loading component of the cycles of load for mortar beginning at small strains is highly nonlinear and convex to the left. The nonlinearity and convexity diminish as the strain at the beginning of the cycles increases. At large strains, the loading components are concave to the left. The same changes in the shape of the cyclic curves were obtained by Karsan and Jirsa for concrete.

(3) During cyclic loading, the initial modulus of elasticity upon

reloading appears to increase after unloading from the virgin stress-strain curve at stresses as large as 56% of the peak stress (Table 3.2). The increase in initial modulus during the first cycle, indicates that compaction of the material has occurred. No such increase was indicated by Spooner, et al., (26,27) during cyclic loading of cement paste and concrete, probably because they used cycles to relatively higher stresses.

(4) After the increase during the first reloading, the initial modulus of elasticity of mortar decreases continuously with increasing cycles. The initial moduli of cement paste and concrete during cyclic loading also decrease continuously, as indicated by Spooner, et al., (26,27). This indicates that the processes of damage in cement paste, mortar and concrete are similar and continuous during cyclic loading.

(5) The degradation of mortar is faster, the higher the maximum stress and the lower the minimum stress for cycles between fixed stresses. This behavior is similar to that of concrete, as studied by Karsan and Jirsa (12). This supports the point of view that the factors controlling the degradation of mortar and concrete are similar in nature.

(6) During successive cycles to the same strain, stress drop and residual strain accumulation continue to occur at a decreasing rate in mortar. The straight line log-log relationship between the residual strain and the number of cycles indicates that the damage never stops. Karsan and Jirsa, Whaley and Neville (29), and Neville and Hirst (18) have indicated that cycling below about 60 to 70 percent of the short-term strength of concrete, f'_c, is not detrimental to the strength

and stiffness of concrete. Spooner, et al., (25) have suggested that significant damage of concrete loaded to a specific strain occurs only during first cycle. The similar nature of damage in mortar and concrete (discussed in the earlier paragraphs) suggests that concrete will continue to degrade, even at stresses below 60 to 70 percent of f'_c. The degradation of cement paste mortar and concrete in the form of decreased initial moduli of elasticity for cycles as low as 40% of the short term strength was observed by Cook and Chindaprasirt (5). They observed, however, that while cyclic loading caused a reduction in the strength of concrete, it did not affect the strength of cement paste or mortar.

(7) The damage in mortar at a given strain is controlled by the number of cycles to reach that strain. The greater the number of cycles, the greater the damage. This implies that the total compressive strain is just one of the factors controlling the degradation. The same should be expected for concrete, since it continues to accumulate residual strain for several cycles, even though both the maximum stress and the maximum strain decrease with each cycle (12).

(8) Shah and Chandra (22) indicate that microcracking in concrete is a function of the compressive strain in the concrete and is independent of the method in which the strain is applied. Since the maximum strain may not completely control the degradation of concrete, as suggested in the preceeding paragraph, it seems very likely that factors other than microcracking may dominate the degradation of concrete during cyclic loading.

In summary, it appears that the process of degradation in cement paste, mortar and concrete is similar and continuous during both monotonic and cyclic loading. The strong similarity in the monotonic and cyclic behavior of mortar and concrete indicates that the nonlinear behavior of mortar may dominate the behavior of concrete. The damage in mortar is a function of both the total strain and the load history.

CHAPTER 4

ANALYTICAL REPRESENTATION OF THE CYCLIC BEHAVIOR OF MORTAR

4.1 General

An analytical model is developed to represent the behavior of mortar under cyclic compressive loading. The process of developing the model served as a useful tool in the analysis of the experimental data, as presented in Chapter 3. The representation is restricted to uniaxial behavior, and its adoption in a finite element representation of concrete will require generalization to biaxial or triaxial states of stress.

The key characteristics of the experimental behavior of mortar are incorporated in the model. A number of the relationships obtained in Chapter 3 are modified to simplify the model and to improve the realism of the stress-strain curves that are generated (see Table 4.1). The observed drop in stress for cycles to a constant maximum strain and the relationship between the residual strain and the unloading strain are generalized for all types of cyclic loading.

The model is compared with the experimental results for a number of cyclic loading regimes.

4.2 Stress-Strain Envelope for Cyclic Loading

A split representation, consisting of Saenz' (20) second and third order equations, is used for the ascending and descending branches of the envelope, respectively. This representation avoids the unrealistic variations in the convexity of the ascending branch that are obtained with changes in the steepness of the descending branch when the third order equation is used alone.

For $\varepsilon \leq \varepsilon_m$,

$$\frac{\sigma}{f'_m} = \frac{2.4\,\frac{\varepsilon}{\varepsilon_m}}{1+0.4\,\frac{\varepsilon}{\varepsilon_m}+\left(\frac{\varepsilon}{\varepsilon_m}\right)^2} \qquad (4.1.a)$$

For $\varepsilon > \varepsilon_m$,

$$\sigma = \frac{\varepsilon}{A+B\varepsilon+C\varepsilon^2+D\varepsilon^3} \qquad (4.1.b)$$

where $A = \frac{\varepsilon_m}{2.4 f'_m}$, $B = \frac{R+0.4}{2.4\ f'_m}$

$$C = \frac{1}{2.4}\,\frac{(1-2R)}{f'_m\varepsilon_m} \ , \ D = \frac{1}{2.4}\,\frac{R}{f'_m\varepsilon_m^{\,2}}$$

$$R = \frac{3.6\varepsilon_m^{\,2}}{(\varepsilon_m-0.006)^2} - \frac{\varepsilon_m}{0.006}$$

The stress, f'_m, and the strain, ε_m, correspond to the peak of the envelope. The average experimental values of f'_m and ε_m are used (Table 2.4).

For the sake of simplicity, it is assumed that (i) the initial modulus of elasticity at zero stress equals 2.4 times the secant modulus of elasticity at the peak, and (ii) in the descending branch of the envelope, the stress at a strain of 0.006 equals 0.4 times f'_m.

Fig. 4.1 shows the analytical envelope obtained using Eqs. (4.1.a) and (4.1.b).

4.3 Residual Strain Versus Envelope Strain

Analytical relationships for the residual strain, ε_r, versus the envelope strain prior to unloading, ε_{eu}, and the envelope strain after reloading, ε_{er}, are used in the construction of the loading and unloading

components of cycles of load.

4.3.1 ε_r Versus ε_{eu}

A split representation is used for the ε_r-ε_{eu} curve, consisting of a cubic equation up to a strain of 0.003 and a straight line with a slope of 1, thereafter. The average experimental data indicates that the straight line behavior begins at

$$\varepsilon_{eu} = 0.003 \text{ and } \varepsilon_r = 0.0013.$$

For $\varepsilon_{eu} \leq 0.003$, the curve is represented by

$$\varepsilon_r = 32.6 \times 10^3 \varepsilon^3 - 6.7\varepsilon^2 + 0.16\varepsilon \qquad (4.2.a)$$

For $\varepsilon_{eu} > 0.003$,

$$\varepsilon_r = \varepsilon_{eu} - 0.0017 \qquad (4.2.b)$$

The representation of ε_r versus ε_{eu}, obtained by using Eqs. (4.2.a) and (4.2.b) is compared with typical experimental results in Fig. 4.2

4.3.2 ε_r versus ε_{er}

The experimental results for ε_r versus ε_{er} are represented in the model as

$$\varepsilon_{er} = \varepsilon_r + 0.0019 \qquad (4.3)$$

$$\varepsilon_{er} \geq \varepsilon_m$$

For the purpose of simplicity, Eq. (4.3) differs from the experimental relationship (see Fig. 4.3). The average experimental results give an

envelope strain upon reloading of 0.003 corresponding to a residual strain of 0.001 at the beginning of the linear relationship. For smaller values of residual strain, a curvilinear relationship exists between ε_r and ε_{er}. The straight line represented by Eq. (4.3) gives $\varepsilon_{er} = 0.0029$ corresponding to $\varepsilon_r = 0.001$ rather than the experimental average ($\varepsilon_{er} = 0.003$). This slight modification gives better results for modelling the cyclic behavior of mortar between fixed stress limits. The restriction, $\varepsilon_{er} \geq \varepsilon_m$, is imposed, instead of using the experimental curvilinear relationship, to obtain a realistic representation of the shape of the loading component of the cycles reaching the envelope at strains smaller than ε_m, as explained in Sec. 4.6.1.

4.4 Residual Strain Versus Unloading Strain

For unloading from a point below the envelope, a straight line relationship between the residual strain, ε_r, and the unloading strain, ε_u, is used.

The method used to determine the ε_r-ε_u line is illustrated in Fig. 4.4. The strain intercepts, ε^i_{eb} and ε^i_{et}, on the ascending and descending branches of the envelope, Eqs. (4.1), corresponding to the unloading stress, σ_i, are calculated. The residual strains, ε^i_{rb} and ε^i_{rt}, corresponding to the envelope strains, ε^i_{eb} and ε^i_{et}, are obtained by using Eqs. (4.2). The straight line relating ε_r and ε_u is then given by,

$$\varepsilon^i_r - \varepsilon^i_{rb} = \left(\frac{\varepsilon^i_{rt}-\varepsilon^i_{rb}}{\varepsilon^i_{et}-\varepsilon^i_{eb}}\right)(\varepsilon_u-\varepsilon^i_{eb}) \qquad (4.4)$$

where the superscript "i" is used to indicate the values of the quantities ε_r, ε_{rb}, ε_{rt}, ε_{et} and ε_{eb} corresponding to the unloading stresses, σ_i,

$i = 1,2,3,\ldots$, for the same unloading strain, ε_u.

The slope of the ε_r-ε_u line changes with the change in the value of stress, σ_i, at the same unloading strain, ε_u, and the change in the shape of the envelope. The ε_r-ε_u lines illustrated in Fig. 4.4 are quite similar to the experimental results shown in Fig. 3.3.

4.5 Stress Upon Reloading to the Previous Unloading Strain

The stress at which the present cycle reaches the previous unloading strain, is obtained by using an equation similar to the experimentally derived relation between the stress drop and the number of cycles to the same strain. The equation is

$$\sigma = \sigma_{max} N^{-0.08} \qquad (4.5)$$

in which the stress, σ, corresponds to the Nth cycle and the stress, σ_{max}, corresponds to the first cycle. An exponent of -0.08, rather than -0.093 (experimental average), is used because it gives better results for modeling cyclic behavior of mortar between specified stress limits.

The reloading stress, $\sigma_{r\ell}$, for the previous unloading stress, σ_{pu}, and the previous unloading strain, ε_{pu}, is obtained as shown in Fig. 4.5. The envelope stress, σ_{max}, is obtained by substituting the strain, ε_{pu}, into the envelope equations, Eqs. (4.1). The value of N corresponding to the stress drop up to σ_{pu} is obtained by substituting the values of σ_{max} and σ_{pu} into Eq. (4.5) and solving for N. The value of N is not necessarily an integer. The reloading stress, $\sigma_{r\ell}$, is obtained by substituting N+1 for the number of cycles, N, in Eq. (4.5), with the same value of σ_{max}, and solving for σ, (Fig. 4.5). If $\sigma_{r\ell}$ has a value larger than σ_{er}, the stress at which the reloading curve joins the envelope, then $\sigma_{r\ell}$ is set equal to σ_{er}.

4.6 Shape of Load Cycles

4.6.1 Loading Component of A Cycle

A split representation is used consisting of a straight line up to the previous unloading strain and Saenz' second order equation for the remaining curve to the envelope.

For $\varepsilon \leq \varepsilon_{pu}$,

$$\sigma - \sigma_{min} = \left(\frac{\sigma_{r\ell} - \sigma_{min}}{\varepsilon_{pu} - \varepsilon_{min}}\right) (\varepsilon - \varepsilon_{min}) \qquad (4.6.a)$$

For $\varepsilon > \varepsilon_{pu}$,

$$\sigma - \sigma_{min} = \frac{(\varepsilon - \varepsilon_{min})\, E_i}{1 + \left(\frac{E_i}{E_m} - 2\right)\left(\frac{\varepsilon - \varepsilon_{min}}{\varepsilon_{er} - \varepsilon_{min}}\right) + \left(\frac{\varepsilon - \varepsilon_{min}}{\varepsilon_{er} - \varepsilon_{min}}\right)^2} \qquad (4.6.b)$$

$E_m = \frac{\sigma_{er} - \sigma_{min}}{\varepsilon_{er} - \varepsilon_{min}}$ = the secant modulus of elasticity of the cycle at the peak of the cycle.

The initial modulus of elasticity, E_i, at the point of reloading (σ_{min}, ε_{min}) is obtained by substituting $\sigma = \sigma_{r\ell}$ and $\varepsilon = \varepsilon_{pu}$ in Eq. (4.6.b) and solving for E_i. The envelope strain, ε_{er}, at the peak of the cycle, Eq. (4.6.b), is obtained by using Eq. (4.3), and the corresponding stress, σ_{er}, is obtained by substituting ε_{er} in Eqs. (4.1). The curve becomes horizontal at this strain . In practice, the loading component of the cycles reaching the envelope at strains smaller than the strain at the peak of the envelope does not yield a zero slope at its intersection with the envelope. For a realistic representation in this case, the strain at which Eq. (4.6.b) attains zero slope is assumed to equal the peak strain of the envelope. This assumption is incorporated into the ε_r-ε_{er} relation by

restricting $\varepsilon_{er} \geq \varepsilon_m$(Eq. 4.3) as shown in Fig. 4.3.

When unloading begins at a point below the envelope, the loading curve given by Eq. (4.6) is terminated at that point. The stress and strain at unloading $(\sigma_u, \varepsilon_u)$ correspond to the point of termination of the loading curve.

Fig. 4.6 shows the construction of the loading component of a cycle.

4.6.2 Unloading Component of A Cycle

An adaptation of Saenz' second order equation is used to represent the unloading component of a cycle. For the sake of simplicity, the tangent modulus of elasticity at the beginning of an unloading cycle (at $(\sigma_u, \varepsilon_u)$) is taken as $2\,\sigma_u/(\varepsilon_u - \varepsilon_r)$. The equation is given by,

$$\frac{\sigma_u - \sigma}{\sigma_u} = 2\,\frac{\left(\frac{\varepsilon_u - \varepsilon}{\varepsilon_u - \varepsilon_r}\right)}{1 + \left(\frac{\varepsilon_u - \varepsilon}{\varepsilon_u - \varepsilon_r}\right)^2} \qquad (4.7)$$

The residual strain, ε_r, is obtained by using Eqs. (4.2).

When reloading begins prior to the completion of unloading to zero stress, the stress and strain at the beginning of the reloading cycle $(\sigma_{min}, \varepsilon_{min})$ corresponds to the point of termination of the unloading curve Eq. (4.7).

Fig. 4.7 shows the construction of the unloading curve.

4.7 Comparison of the Experimental and Analytical Stress-Strain Response

4.7.1 Cyclic Envelope

Fig. 4.8 compares the experimental and analytical envelope curves for test 8-2/CP/29/0.6. The shape of the analytical curve compares

well with that of the test envelope.

Fig. 4.9 shows the experimental and analytical envelope curves for test 26-2/CMS/14/0.6. The analytical curve is slightly steeper than the experimental envelope. This is due to the simplifying assumption that a stress of 0.4 f'_m occurs at a strain of 0.006 for all ages and water-cement ratios. The shapes of the analytical and experimental curves are comparable.

4.7.2 Cycles to the Envelope

Local Behavior: Fig. 4.10 shows the shape of three cycles of load, beginning at a small strain, a medium strain and a large strain. The purpose is to compare the shapes of the analytical and experimental loading and the unloading curves. Since "local" behavior is being compared, the analytical representation employs the experimental values of stress and strain at the beginning and the end of the test cycles. For the cycle beginning at the small strain, the experimental loading curve is slightly more convex than the analytical loading curve, while the experimental unloading curve is less concave than the analytical unloading curve. For the cycle beginning at the medium strain, the shapes of the experimental and analytical loading and unloading components compare well. For the cycle beginning at the large strain, the overall shape of the experimental and analytical curves match fairly well. Since the initial portion of the analytical loading curve is a straight line, it cannot reproduce the convexity of the loading component at small strains or the concavity of the loading component at large strains.

Overall Behavior: Fig. 4.11 compares the analytical representation with the experimental stress-strain behavior of mortar subjected to a number of cycles to the envelope. The strain at unloading for the

analytical cycles is the same as for the experimental cycles. The analytical envelope is higher than the test envelope in the descending branch. This is due to the fact that tests with simple cycles to envelope yielded lower descending branches of the envelope than other types of cyclic loading. The overall stress-strain behavior of the model is similar to the test data.

4.7.3 Cycles to a Constant-Maximum Strain

Local Behavior: To compare the shape of the cycles, for cycles to a single strain, the experimental envelope and the experimental maximum stress at the given strain are incorporated into the analytical representation.

Fig. 4.12 shows the "local" experimental and analytical behavior of mortar for 22 cycles to a strain of 0.0042 for test 25-2/CMS/14/0.6. The plot shows the first three cycles and the last cycle only. The residual strain accumulation and the shape of the curves are in good agreement. The stress drop predicted by the analytical representation is slightly less than the test results. This is due to the fact that Eq. (4.5), which relates stress drop with the number of cycles to the same strain, utilizes a relationship which is less steep than the average experimental results (see Sec. 4.5).

Fig. 4.13 compares the local experimental and analytical behavior of mortar for 35 cycles to a strain of 0.0024 for test 38-3/CMS/29/0.5. Although, the values of the analytical residual strain are less than the experimental residual strain for all cycles, the pattern and amount of accumulation is comparable. The shape of analytical loading and unloading components of the cycles and the stress drop compare well with the test results.

Overall Behavior: Fig. 4.14 compares the overall experimental

and analytical behavior of mortar for cycles to a number of specified strains for test 25-2/CMS/14/0.6. It is observed that the analytical representation is quite similar to the experimental results.

4.7.4 Cycles Between Fixed-Stresses

Zero Minimum Stress Limit: Fig. 4.15 shows the experimental and analytical stress-strain response of mortar, for test 41-2/SL/15/0.6, cycled between zero and 3500 psi. The descending branch of the envelope is reached at the 10th cycle compared with the 9th cycle during the test. The model produced increments in maximum strain for successive cycles that accumulate first at a decreasing rate and then at an increasing rate. This coincides with the test results.

Fig. 4.16 compares the experimental and analytical stress-strain response for test 39-3/SL/28/0.6, cycled between zero and 3400 psi. The model predicts that the descending branch of the envelope will be reached in the 68th cycle, compared with the 74th cycle in the test The plots show the initial and final cycles, only. Similar to the previous example, the analytical prediction of the maximum strain increase has characteristics similar to those observed experimentally.

The two examples illustrate that the model successfully predicts the cyclic behavior of mortar between zero and a given value of compressive stress.

Non-Zero Minimum Stress Limit: Fig. 4.17 compares the experimental and analytical curves for test 41-1/SL/15/0.6, cycled between 1500 psi and 3500 psi. The analytical prediction of the number of cycles to the descending branch of the envelope (12 cycles) is less than that obtained in the test (17 cycles). Considering the variability of the material, the difference is not unreasonable. The shape of the

cycles and the maximum and minimum strain increase predicted by the model are similar to the experimental results.

Fig. 4.18 compares the experimental and analytical results for test 16-3/SL/29/0.6, cycled between 1440 psi and 3450 psi. The model predicts "failure" in the 68th cycle compared with test "failure" in the 70th cycle.

These two examples demonstrate the success of the representation for mortar cycled between fixed stress limits, with a non-zero minimum stress.

CHAPTER 5

SUMMARY AND CONCLUSIONS

5.1 Summary

The main purpose of this investigation was to study the behavior of the mortar constituent of concrete under cyclic uniaxial compressive load and to develop an analytical representation of its cyclic behavior.

Experimental tests were conducted using procedures similar to those developed by Karsan and Jirsa (11) in their study of concrete. Two mortar mixes were used. The proportions corresponded to concretes with water-cement ratios of 0.5 and 0.6. Forty-four groups of specimens were tested at ages ranging from 5 to 70 days.

The test specimens were fourteen inches high, with the middle six inch portion having a uniform two inch square cross-section, and with flared ends. The specimens were cured in a horizontal position, to minimize the problem of bleeding in the very fluid mortar. To ensure a good alignment of the testing machine platens with the ends of the specimens and, also, to prevent significant platen rotation during the tests, thin layers of high strength gypsum cement were used at both ends of the specimen with rigid, flat, non-rotating platens.

Specimens were loaded in compression using a closed-loop, electrohydraulic testing machine. The closed-loop-system of the testing machine was modified to allow the direction of the loading to be reversed at specified stress limits, while using strain control.

Average axial strain was measured using a specially designed variable gage length compressometer. A gage length of three inches gave satisfactory results. Strain-gages were installed on a few specimens to determine the variation of the total and incremental "Poisson's

ratio" with load history.

Complete stress-strain curves were obtained for monotonic and cyclic loading.

To investigate the effect of cyclic loading on the behavior of mortar, the following loading regimes were investigated:

(i) Cycles to the envelope,

(ii) Cycles with a constant strain increment,

(iii) Cycles between fixed stresses,

(iv) Cycles to common points, and

(v) Cycles to a constant maximum strain.

The results of the monotonic loading tests were compared for the same batch, different batches, different ages, and different W/C ratios. The variations in the value of the initial modulus of elasticity, peak stress and strain, and the stresses at twice and three times the strain at the peak were studied. The effect of the rate of loading on these properties was also investigated.

The effect of load history on the shape of the envelope curve, the accumulation of residual strain as a function of the maximum strain, the changes in the initial moduli of elasticity, the stress drop per cycle, and the existence of a stability limit below which no further damage occurs was studied.

The degradation of mortar under various types of loading regimes was assessed using a number of indications of damage. The best indicators of damage were evaluated, based on their sensitivity. The factors controlling the degradation of mortar were studied. The nature of the degradation of mortar under load was discussed. The monotonic and cyclic behavior of mortar was compared with the observations made by other investigators on the behavior of cement paste and concrete.

The similarities and differences were discussed.

The analytical model was developed using the key characteristics of the experimental behavior of mortar under cyclic loading. The process of developing the model served as a useful tool in the analysis of the experimental data. A number of experimental relationships were modified to simplify the model and to improve the realism of the stress-strain curves that were generated. The representation was restricted to uniaxial behavior, and its adoption in a finite element representation of concrete will require generalization to biaxial or triaxial states of stress. The model was compared with the experimental results for a number of cyclic loading regimes.

5.2 Conclusions

Based on the research presented in this report, the following general conclusions can be made:

1. For monotonic loading, the strength of mortar increases with increasing age and decreasing water-cement ratio.
2. A higher value of peak stress is accompanied by an increase in the corresponding strain and a steeper descending portion of the stress-strain curve.
3. The incremental "Poisson's ratio" continues to increase during monotonic loading with increasing compressive strain. The strain at the peak of the stress-strain curve does not appear to have any significance in this process.
4. The curvilinear relationships between residual strain and the envelope strain, both prior to unloading and upon reloading, have similar shapes and are independent of the type of loading history. Both relationships become almost straight lines

with a slope of one at envelope strains equal to about one-and-a-half times the strain at the peak stress.

5. The accumulation of residual strain has been measured for applied strains as small as 0.00027.
6. Upon unloading from the virgin stress-strain curve (for stresses as high as 56 percent of the peak stress), the initial modulus of elasticity of the reloading curve increases and, then, decreases continuously with further cycling. This shows that compaction of the material takes place during the first cycle, producing a beneficial effect on the stiffness of mortar.
7. For cycles to a constant maximum strain, log-log relationships between stress-drop and residual strain versus the number of cycles are linear, indicating that damage continues to occur and that a "stability limit" may not exist.
8. The process of degradation of mortar during monotonic as well as cyclic compressive loading is continuous and begins at very early stages of loading.
9. Cyclic loading, by itself, causes damage in mortar. The total range of strain traversed during cyclic loading is a factor contributing to the degradation.
10. For cyclic compression, the degradation of mortar is faster, the higher the maximum stress and the lower the minimum stress.
11. The descending branch of the cyclic loading envelope curve is higher than the monotonic loading envelope curve. It appears that the difference in behavior is due to the larger distribution of damage in cyclically loaded specimens.
12. The nature of degradation in mortar and concrete is similar to

that in cement paste.

13. The factors controlling the degradation of mortar and concrete are similar. Due to the strong similarity in monotonic and cyclic behavior of mortar and concrete, it appears that the nonlinear behavior of mortar may dominate the behavior of concrete.
14. In the descending branch of monotonic and cyclic envelopes, the deformation of mortar is dominated by sliding along macroscopic cracks. At this stage, the strength of mortar mainly consists of frictional resistance between the cracked surfaces.
15. The analytical model of mortar, matches well with the experimental response of mortar, for a number of cyclic loading regimes.

5.3 Recommendations for Future Study

The results of the present study strongly suggest that future research is needed in the following areas:

1. Since the nature of damage in mortar, as well as concrete, is similar to that in cement paste, experimental studies should be conducted to investigate the nature of damage in cement paste. A project at the University of Kansas is currently studying this question.
2. The degree of damage appears to be affected by the volume of aggregate. The nature of changes caused by the inclusion of aggregate in the process of degradation of cement paste, continues to require investigation. This may be accomplished by experimental as well as finite element studies. The analytical representation of mortar proposed in this study should be

generalized for biaxial and triaxial loading in order to be adopted in a finite element representation of concrete (16).

3. The cyclic loading of concrete to a constant maximum strain should be conducted to investigate the existence of a stability limit for concrete. Karsan and Jirsa (11) cycled the concrete to the "common points." The cycles used both a decreasing maximum stress and a decreasing maximum strain and, therefore, finally converged to an apparent stability limit.
4. The cyclic loading of mortar to relatively small compressive stresses should be conducted to investigate the existence of "cyclic creep" and the nature of degradation at low stresses.

REFERENCES

1. ACI Committee 224, "Control of Cracking in Concrete Structures," Concrete International: Design and Construction, Vol. 2, No. 10, Oct. 1980, pp. 35-76.

2. Andenaes, E., Gerstle, K., and Ko, H. Y., "Response of Mortar and Concrete to Biaxial Compression," Journal of Engineering Mechanics Division, ASCE, Vol. 103, No. EM4, Aug. 1977, pp. 515-526.

3. Buyukozturk, O., "Stress-Strain Response and Fracture of a Model of Concrete in Biaxial Loading," Thesis presented to Cornell University, June 1970, in partial fulfillment of the requirements for the degree of Doctor of Philosophy.

4. Carrasquillo, R. L., "Microcracking and Engineering Properties of High Strength Concrete," Report No. 80-1, Department of Structural Engineering, School of Civil and Environmental Engineering, Cornell University, Ithaca, New York, Feb. 1980.

5. Cook, D. J. and Chindaprasirt, P., "Influence of Loading History Upon the Compressive Properties of Concrete," Magazine of Concrete Research, Vol. 32, No. 111, June, 1980, pp. 89-100.

6. Darwin, D. and Slate, F. O., "Effect of Paste-Aggregate Bond Strength on Behavior of Concrete," Journal of Materials, JMLSA, Vol. 5, No. 1, Mar. 1970, pp. 86-98.

7. Derucher, K. N., "Application of the Scanning Election Microscope to Fracture Studies of Concrete," Building and Environment, Vol. 13, No. 2, 1978, pp. 135-141.

8. Hobbs, D. W., "The Strength and Deformation of Concrete Under Short Term Loading: A Review," Technical Report, No. 42.484, Sept. 1973, Cement and Concrete Association, London.

9. Hsu, T. C. and Slate, F. O., "Tensile Strength Between Aggregate and Cement Paste or Mortar," Journal of the American Concrete Institute, Proc. Vol. 60, No. 4, April, 1963, pp. 465-486.

10. Hsu, T. C., Slate, F. O., Sturman, G. M., and Winter, G., "Microcracking of Plain Concrete and the Shape of the Stress-Strain Curve," Journal of the American Concrete Institute, Proc. Vol. 60, No. 2, Feb. 1963, pp. 209-224.

11. Jeragh, A. A., "Deformational Behavior of Plain Concrete Subjected to Biaxial-Cyclical Loading," Thesis presented to New Mexico State University, Las Cruces, 1978, in partial fulfillment of the requirements for the degree of Doctor of Philosophy.

12. Karsan, I. D. and Jirsa, J. O., "Behavior of Concrete Under Compressive Loadings," Journal of the Structural Division, ASCE, Vol. 95,

No. ST12, Dec. 1979, pp. 2543-5263.

13. Kupfer, H. B. and Gerstle, K. H., "Behavior of Concrete Under Biaxial Stresses," Journal of the Engineering Mechanics Division, ASCE, Vol. 99, No. EM4, Aug. 1973, pp. 852-866.

14. Kupfer, H., Hilsdorf, H. K., and Rusch, H., "Behavior of Concrete Under Biaxial Stresses," Journal of the American Concrete Institute, Proc. Vol. 66, No. 2, Aug. 1969, pp. 656-666.

15. Liu, T. C. Y., "Stress-Strain Response and Fracture of Concrete in Biaxial Compression," Ph.D. Thesis and Research Report No. 339, Department of Structural Engineering, Cornell University, Ithaca, New York, Feb. 1971.

16. Maher, A. and Darwin, D., "Microscopic Finite Element Model of Concrete," Proceedings, First International Conference on Mathematical Modeling (St. Louis, Aug.-Sept. 1977), University of Missouri-Rolla, 1977, Vol. III, pp. 1705-1714.

17. Meyers, B. L., Slate, F. O., and Winter, G., "Relationship Between Time Dependent Deformation and Microcracking of Plain Concrete," Journal of the American Concrete Institute, Proc. Vol. 66, No. 1, Jan. 1979, pp. 60-68.

18. Neville, A.M. and Hirst, G. A., "Mechanism of Cyclic Creep of Concrete," Douglas McHenry Symposium on Concrete and Concrete Structures, SP55, American Concrete Institute, Detroit, 1978, pp. 83-101.

19. Perry, C. and Gillot, J. E., "The Influence of Mortar-Aggregate Bond Strength on the Behavior of Concrete in Uniaxial Compression," Cement and Concrete Research, Vol. 7, No. 5, Sept. 1977, pp. 553-564.

20. Saenz, L. P., Disc. of "Equation for the Stress-Strain Curve of Concrete," by Desayi and Krishnan, Journal of the American Concrete Institute, Proc. Vol. 61, No. 9, Sept. 1964, pp. 1229-1235.

21. Sinha, B. P., Gerstle, K. H. and Tulin, L. G., "Stress-Strain Relations for Concrete Under Cyclic Loading," Journal of the American Concrete Institute, Proc. Vol. 61, No. 2, Feb. 1964, pp. 195-211.

22. Shah, S. P. and Chandra, S., "Concrete Subjected to Cyclic and Sustained Loading," Journal of the American Concrete Institute, Proc. Vol. 67, No. 10, Oct. 1970, pp. 816-825.

23. Shah, S. P. and Winter, G., "Inelastic Behavior and Fracture of Concrete," Journal of the American Concrete Institute, Proc. Vol. 63, No. 9, Sept. 1966, pp. 925-980.

24. Spooner, D. C., "The Stress-Strain Relationship for Hardened Cement Pastes in Compression," Magazine of Concrete Research (London), Vol. 24, No. 79, June, 1972, pp. 85-92.

25. Spooner, D. C., and Dougill, J. W., "A Quantitative Assessment of Damage Sustained in Concrete During Compressive Loading," Magazine of Concrete Research (London), Vol. 27, No. 92, Sept. 1975, pp. 151-160.

26. Spooner, D. C., Pomeroy, C. D. and Dougill, J. W., "Damage and Energy Dissipation in Cement Pastes in Compression," Magazine of Concrete Research (London), Vol. 28, No. 94, Mar. 1976, pp. 21-29.

27. Spooner, D. C., Pomeroy, C. D. and Dougill, J. W., "The Deformation and Progressive Fracture of Concrete," Proc. British Ceramic Society, No. 25, May, 1975; Mechanical Properties of Ceramics (2), Joint Meeting of the Basic Sciences Section of the British Ceramic Society and the Materials and Testing Group of the Institute of Physics, London, England, Dec. 17-18, 1974, pp. 101-107.

28. Taylor, M.A. and Broms, B. B., "Shear-Bond Strength Between Coarse Aggregate and Cement Paste or Mortar," Journal of the American Concrete Institute, Proc. Vol. 61, No. 8, Aug. 1964, pp. 939-958.

29. Whaley, C. P. and Neville, A. M., "Non-elastic Deformation of Concrete Under Cyclic Compression," Magazine of Concrete Research (London), Vol. 25, No. 84, Sept. 1973, pp. 145-154.

TABLE 2.1

MIX DESIGNS

Ingredients	Water-Cement-Ratio 0.5 Concrete	0.5 Mortar	0.6 Concrete	0.6 Mortar
	pounds per cu.yd.	pounds	pounds per cu.yd.	pounds
Water	305	305	315	315
Cement	508	508	630	630
Fine Aggregate	1522	1522	1463	1463
Coarse Aggregate	1522	- - -	1463	- - -
Relative Proportions C:S:G	1:2.32:2.32	1:2.32:0	1:3:3	1:3:0
Slump	2 inch	too fluid to measure	2 inch	too fluid to measure

TABLE 2.2

MONOTONIC LOADING TESTS

(Test-Type-Designation = M)

	Test*	Moist cure (days)	E_i $\times 10^{-6}$	f'_m (psi)	ε_m	σ at $\varepsilon = 2\varepsilon_m$ (psi)	σ at $\varepsilon = 3\varepsilon_m$ (psi)
1	1-1/M/30/0.6	30	4.7	4800	0.0023	2100	1200
2	1-2/CEN/30/0.6	30	5.3	5100	0.0025	3000	900
3	2-1/M/28/0.6	28	4.7	4400	0.0022	2800	1600
4	2-2/M/28/0.6	28	3.7	3600	0.002	1600	- -
5	2-3/M/28/0.6	28	6.4	4300	0.0018	- -	- -
6	3-1/M/28/0.6	28	5.6	3800	0.0016	1800	600
7	3-2/M/28/0.6	28	4.3	3600	0.002	2200	500
8	4-1/M/28/0.6	28	3.7	3700	0.0029	- -	- -
9	5-1/M/28/0.6	28	5.7	4000	0.0019	2500	1150
10	6-1/M/28/0.6	28	4.9	4000	0.0019	2000	- -
11	7-1/M/28/0.6	28	4.8	4000	0.002	- -	- -
12	8-1/M/29/0.6	29	4.8	4200	0.0024	2600	1100
13	9-1/M/28/0.6	28	4.3	3900	0.0021	1100	500
14	10-1/M/28/0.6	28	3.9	3900	0.0022	- -	- -
15	11-1/M/28/0.6	28	4.4	3600	0.002	2400	1600
16	12-1/M/29/0.6	29	5.3	4000	0.0021	- -	- -
17	12-2/M/28/0.6	28	5.6	4300	0.0021	1600	- -
18	13-1/M/28/0.6	28	3.1	3300	0.0028	- -	- -
19	14-1/M/28/0.6	28	4.3	2900	0.0022	1300	- -
20	14-2/M/28/0.6	28	7.7	4100	0.0017	- -	- -
21	15-1/M/28/0.6	28	5.1	4400	0.0022	- -	- -
22	16-1/M/29/0.6	29	4.2	3900	0.002	- -	- -
23	17-1/M/29/0.6	29	4.6	3700	0.0018	- -	- -
24	18-1/M/28/0.6	28	4.8	3500	0.0022	1600	- -
25	18-2/MS/28/0.6	28	2.3	2900	0.0023	2100	- -
26	18-3/MS/28/0.6	28	3.6	3200	0.0022	2200	- -
27	19-1/M/29/0.6	26	3.8	4000	0.0027	2400	- -
28	19-2/M/28/0.6	26	4.3	3700	0.0023	- -	- -
29	20-1/M/29/0.6	26	3.9	4200	0.0024	2200	- -
30	20-2/M/28/0.6	26	6.4	3900	0.0019	2200	- -
31	21-1/M/28/0.6	28	4.8	4200	0.002	- -	- -
32	21-2/M/28/0.6	28	5.6	4600	0.002	2000	- -
33	21-3/MS/29/0.6	29	3.7	3900	0.0027	1300	- -

* See App. A

TABLE 2.2 (continued)

	Test	Moist cure (days)	E_i x10^{-6}	f'_m (psi)	ε_m	σ at ε $2\varepsilon_m$ (psi)	σ at ε $3\varepsilon_m$ (psi)
34	22-1/MS/28/.6	26	4.3	4500	0.0028	- -	- -
35	23-1/M/28/0.6	26	4.9	4500	0.0013	- -	- -
36	23-2/M/28/0.6	26	4.8	4700	0.0023	- -	- -
37	24-1/M/14/0.6	14	5.1	3700	0.0017	1600	800
38	25-1/M/14/0.6	14	4.0	3900	0.0023	1900	1000
39	26-1/M/14/0.6	14	4.8	3800	0.0019	1500	- -
40	27-2/MS/14/0.6	14	4.2	3800	0.0022	2700	1600
41	27-1/M/14/0.6	14	3.8	3500	0.002	- -	- -
42	40-1/CEN/14/0.6	14	4.2	4000	0.0022	2300	1100
43	28-1/M/15/0.6	15	4.2	3700	0.0019	1900	- -
44	29-1/M/5/0.6	5	5.0	3000	0.0013	2000	1400
45	30-1/M/8/0.6	8	3.8	3100	0.0017	2200	1600
46	30-2/M/7/0.6	7	4.2	2900	0.0017	2200	1600
47	31-1/CEN/7/0.6	7	5.4	3500	0.0021	2300	1300
48	32-1/CEN/7/0.6	7	4.2	3100	0.0019	1900	- -
49	33-1/M/28/0.5	28	5.4	4400	0.002	- -	- -
50	33-2/M/28/0.5	28	5.2	5500	0.0027		
51	33-3/M/29/0.5	29	4.9	4700	0.0033	2100	- -
52	34-1/M/28/0.5	28	5.5	5800	0.0032	4000	- -
53	35-1/M/28/0.5	28	4.9	5200	0.0025	2900	- -
54	35-2/MS/28/0.5	28	5.5	5200	0.0025	3200	- -
55	35-3/MS/29/0.5	29	4.8	5100	0.0027	- -	- -
56	36-1/M/29/0.5	29	4.8	4900	0.0021	- -	- -
57	36-2/M/30/0.5	30	5.7	5500	0.0023	2900	- -
58	37-1/M/28/0.5	28	4.8	4900	0.0024	- -	- -
59	38-1/M/29/0.5	29	6.5	5300	0.002	1300	- -
60	44-1/M/52/0.5	42	6.3	6500	0.0027	4000	3750
61	44-2/M/52/0.5	42	4.7	6600	0.0031	- -	- -

TABLE 2.3

COMPARISON OF MONOTONIC LOADING TESTS FOR SPECIMENS OF

THE SAME BATCH (SAME RATE OF LOADING)

Test*	E_i x10^{-6} (psi)	f'_m (psi)	ε_m	Strain Rate (Strain/min x10^{-3})	Approx. Time to Reach .004 Strain (min)	Stress at a Strain = 2xε_m (psi)	Stress at a Strain = 3xε_m (psi)
2-1/M/28/0.6	4.7	4400	0.0022	00.267	15	2800	1600
2-2/M/28/0.6	3.7	3600	0.002	00.267	15	1600	- -
2-3/M/28/0.6	6.4	4300	0.0018	00.267	15	- -	- -
Average	4.9	4100	0.002				
3-1/M/28/0.6	5.6	3800	0.0016	00.267	15	1800	600
3-2/M/28/0.6	4.3	3600	0.002	00.267	15	2200	500
Average	4.95	3700	0.0018				
12-1/M/29/0.6	5.3	4000	0.0021	00.267	15	- -	- -
12-2/M/28/0.6	5.6	4300	0.0021	00.267	15	1600	- -
Average	5.5	4150	0.0021				
14-1/M/28/0.6	4.3	3900	0.0022	00.267	15	1300	- -
14-2/M/28/0.6	7.7	4100	0.0017	00.267	15	- -	- -
Average	6.0	4000	0.002				
18-2/MS/28/0.6	2.3	2900	0.0023	0.03	120	2100	- -
18-3/MS/28/0.6	3.6	3200	0.0022	0.03	120	2200	- -
Average	3.0	3000	0.0022				
20-1/M/29/0.6	3.9	4200	0.0024	00.267	15	2200	
20-2/M/28/0.6	6.4	3900	0.0019	00.267	15	2200	
Average	5.2	4150	0.0021				
21-1/M/28/0.6	4.8	4200	0.002	00.267	15	- -	- -
21-1/M/28/0.6	5.6	4600	0.002	00.267	15	2000	- -
Average	5.2	4400	0.002				
23-1/M/28/0.6	4.9	4500	0.0013	00.267	15	- -	- -
23-2/M/28/0.6	4.8	4700	0.0023	00.267	15	- -	- -
Average	4.9	4600	0.0018				
30-1/M/8/0.6	3.8	3100	0.0017	00.267	15	2200	1600
30-2/M/7/0.6	4.2	2900	0.0017	00.267	15	2200	1600
Average	4.0	3000	0.0017				
33-1/M/28/0.5	5.4	4400	0.002	00.133	30	- -	- -
33-2/M/28/0.5	5.2	5500	0.0027	00.133	30	- -	- -
33-3/M/29/0.5	4.9	5700	0.0033	00.133	30	2100	- -
Average	5.2	5200	0.0027				

* See App. A

TABLE 2.4

AVERAGE PROPERTIES OF MORTAR FOR DIFFERENT AGES AND W/C RATIOS

No.	W/C	Age	Ascending Branch							Descending Branch						
			No. of Tests	Initial Modulus of Elasticity $E_i \times 10^{-6}$ (psi)		Peak Stress f'_m (psi)		Peak Strain ϵ_m		No. of Tests	$\sigma_{2\epsilon_m}$* (psi)		$\sigma_{2\epsilon_m}/f'_m$	No. of Tests	$\sigma_{3\epsilon_m}$** (psi)		$\sigma_{3\epsilon_m}/f'_m$
				Ave.	Coef. of Var.%	Ave.	Coef. of Var.%	Ave.	Coef. of Var.%		Ave.	Coef. of Var.%	Ave.		Ave.	Coef. of Var.%	Ave.
1	0.6	28	36	4.7	21	4030	11	0.0022	16	21	2050	24	0.52	9	1020	40	0.25
2	0.6	14	7	4.3	10	3770	4	0.0020	10	6	1980	21	0.52	4	1130	26	0.30
3	0.6	7	5	4.5	13	3120	7	0.0017	15	5	2120	7	0.68	4	1480	9	0.47
4	0.5	28	11	5.3	10	5230	7	0.0025	17	6	2730	31	0.50		- -		- -

* stress at twice the strain at the peak stress

** stress at three times the strain at the peak stress

TABLE 2.5

COMPARISON OF MONOTONIC LOADING TESTS WITH DIFFERENT LOADING RATES

Test*	E_i x10^{-6} (psi)	f'_m (psi)	ε_m	Strain Rate (Strain/min x10^{-3})	Approx. Time to Reach .004 Strain (min)	Stress at a Strain = 2xε_m (psi)	Stress at a Strain = 3xε_m (psi)
8-1/M/28/0.6	4.8	3500	0.0022	0.08	50	1600	- -
8-2/MS/28/0.6	2.3	2900	0.0023	0.03	120	2100	- -
8-3/MS/28/0.6	3.6	3200	0.0022	0.03	120	2200	- -
9-1/M/29/0.6	3.8	4000	0.0027	0.27	15	2400	- -
9-2/MS/28/0.6	4.3	3700	0.0023	0.03	120	- -	- -
21-1/M/28/0.6	4.8	4200	0.002	0.27	15	- -	
21-2/M/28/0.6	5.6	4600	0.002	0.27	15	2000	- -
21-3/M/29/0.6	3.7	3900	0.0027	0.03	120	1300	- -
27-1/M/14/0.6	3.8	3500	0.002	0.27	15	- -	
27-2/MS/14/0.6	4.2	3800	0.0022	0.03	120	2700	1600
35-1/M/28/0.5	4.9	5200	0.0025	0.13	30	2900	- -
35-2/MS/28/0.5	5.5	5200	0.0025	0.03	120	3200	- -
35-3/MS/29/0.5	4.8	5100	0.0027	0.03	120	- -	- -

* See App. A

TABLE 2.6

CYCLIC LOADING TO THE ENVELOPE

(TEST-TYPE-DESIGNATION: CEN)

Test*	Moist Cure (days)	E_i x10^{-6} (psi)	f'_m (psi)	No. of Loadings
1-2/CEN/30/0.6	30	5.3	5100	2
3-3/CEN/28/0.6	28	5.3	3200	21
4-2/CEN/29/0.6	29	5.1	4000	21
5-2/CEN/28/016	28	3.2	4200	21
39-1/CEN/28/0.6	28	3.8	3700	2
9-3/CEN/28/0.6	26	4.7	3560	8
22-2/CEN/28/0.6	26	5.0	4300	3
40-/CEN/14/0.6	14	4.2	4000	3
31-1/CEN/7/0.6	7	5.4	3500	5
32-1/CEN/7/0.6	7	4.2	3100	4
34-2/CEN/28/0.5	28	4.8	6100	2
34-3/CEN /28/0.5	28	7.1	5600	2

* See App. A

TABLE 2.7

COMPARISON OF RESULTS FOR MONOTONIC LOADING AND

CYCLIC LOADING TO THE ENVELOPE

Test*	E_i x10^{-6} (psi)	f'_m (psi)	ε_m	Strain Rate (Strain/min x10^{-3}	Approx Time to Reach .004 Strain (min)	Stress at a Strain = $2\varepsilon_m$ (psi)$_m$	Stress at a Strain = $3\varepsilon_m$ (psi)$_m$	No. of Loadings
1-1/M/30/0.6	4.7	4800	0.0023	0.27	15	2100	1200	1
1-2/CEN/30/0.6	5.3	5100	0.0025	0.27	20	3000	900	2
3-1/M/28/0.6	5.6	3800	0.0016	0.27	15	1800	600	1
3-2/M/28/0.6	4.3	3600	0.002	0.27	15	2200	500	1
3-3/CEN/28/0.6	5.3	3200	- -	0.27	85	2500	1250	21
4-1/M/28/0.6	3.7	3700	0.0029	0.27	15	- -	- -	1
4-2/CEN/29/0.6	5.1	4000	- -		120	1900	1000	21
5-1/M/28/0.6	5.7	4000	0.0019	0.27	15	2500	1150	1
5-2/CEN/28/0.6	3.2	4200	- -	0.27	70	3800	1900	21

* See App. A

TABLE 2.8

CYCLIC LOADING WITH A CONSTANT STRAIN INCREMENT BETWEEN SUCCESSIVE CYCLES

(TEST-TYPE-DESIGNATION = CSI)

Test*	Moist Cure (days)	E_i x10^{-6} (psi)	f'_m (psi)	N	Magnitude and Type of the Strain Increment/Cycle
7-2/CSI/29/0.6	29	3.9	3800	15	Incr. of 5.0x10^{-4} strain/cycle
7-3/CSI/28/0.6	28	4.2	3800	7	Incr. of 5.0x10^{-4} strain/cycle
8-3/CSI/28/0.6	28	5.3	4000	14	Incr. of 5.0x10^{-4} strain/cycle
9-3/CSI/29/0.6	29	4.8	4200	32	Loaded up to 5.0x10^{-4} strain and then incr.of 2.5x10^{-4} strain/cycle
19-3/CSI/28/0.6	26	4.7	3560	8	Loaded up to 9x10^{-4} strain and then incr. of 3x10^{-4} strain/cycle
20-3/CSI/29/0.6	26	4.0	3800	35	Loaded up to 5.0x10^{-4} strain then incr. of 1.3x10^{-4} strain/cycle
28-2/CSI/14/0.6	14	4.8	3500	13	Incr. of 3.3x10^{-4} strain/cycle
31-2/CSI/7/0.6	7	3.6	3200	9	Incr. of 3.3x10^{-4} strain/cycle
32-2/CSI/7/0.6	7	3.5	3000	23	Loaded up to 3.3x10^{-4} strain and then incr. of 1.67x10^{-4} strain/cycle
36-3/CSI/29/0.5	29	4.8	5600	13	Loaded up 2.7x10^{-4} strain and then 3.3x10^{-4} strain/cycle
37-2/CSI/28/0.5	28	5.0	4800	22	Loaded up to 3.3x10^{-4} strain and then 1.67x10^{-4} strain/cycle

* See App. A

TABLE 2.9

COMPARISON OF RESULTS FOR MONOTONIC LOADING AND CYCLIC LOADING WITH A CONSTANT STRAIN INCREMENT

Test*	E_i $\times 10^{-6}$ (psi)	f'_m (psi)	ε_m	Approx time to Reach 0.004 Strain (min)	Stress at $2\varepsilon_m$ (psi)	Stress at $3\varepsilon_m$ (psi)	No. of Loadings
9-1/M/28/0.6	4.3	3900	0.0021	15	1100	500	1
9-3/CSI/29/0.6	4.8	4200	- - -	120	3400	1900	32
20-1/M/29/0.6	3.9	4200	0.0024	15	2200	- -	1
20-2/M/28/0.6	6.4	3900	0.0019	15	2200	- -	1
20-3/CSI/29/0.6	4.0	3800	- - -	120	2100	- -	35
28-1/M/15/0.6	4.2	3700	0.0019	15	1900	- -	1
28-2/CSI/14/0.6	4.8	3500	- - -	90	3300	2700	13
36-2/M/30/0.5	5.7	5300	0.0023	15	2900	- -	1
36-3/CSI/29/0.5	4.8	5600	- - -	70	2500	- -	13
8-1/M/29/0.6	4.8	4200	0.0024	15	2600	1100	1
8-3/CSI/28/0.6	5.3	4000	- - -	70	1600	500	14

* See App. A

TABLE 2.10

CYCLIC LOADING BETWEEN FIXED MAXIMUM AND MINIMUM STRESSES

(TEST-TYPE-DESIGNATION = SL)

	Test***	Moist Cure (days)	E_i x10^{-6} (psi)	σ_{max_1} (psi)	σ_{min_1} (psi)	No.of cycles N_1	σ_{max_2} (psi)	σ_{min_2} (psi)	No.of cycles N_2	σ_{max_3} (psi)	σ_{min_3} (psi)	No.of cycles N_3
1.	5-3/SL/29/0.6	29	3.8	2900	0	1	3200	510	5	3700	510	13
2.	10-2/SL*/29/0.6	29	5.2	2400	0	2	2900	0	8			
3.	39-2/SL*/28/0.6	28	4.3	3200	0	23						
4.	39-3/SL/28/0.6	28	4.2	3380	0	74						
5.	11-2/SL/28/0.6	28	4.3	3100	0	4						
6.	11-3/SL*/28/0.6	28	4.1	3000	0	31						
7.	12-3/SL*/29/0.6	29	4.3	3300	0	9						
8.	13-2/SL*/28/0.6	28	4.6	3500	1500	12						
9.	13-3/SL*/29/0.6	29	3.9	3500	0	12						
10.	15-2/SL*/28/0.6	28	5.3	3700	1500	9	3700	0	1			
11.	15-3/SL*/28/0.6	28	4.9	3800	0	10						
12.	16-2/SL/29/0.6	29	4.9	3700	1400	15	4000	1400	7			
13.	16-3/SL/29/016	29	4.4	3450	1440	69						
14.	22-2/SL*/29/0.6	26	4.6	3900	0	1	3900	1900	10			
15.	41-1/SL/15/0.6	15	4.5	3500	1500	16						
16.	41-2/SL/15/0.6	15	4.0	3500	0	8						
17.	42-1/SL/13/0.6	13	4.3	3700	0	15						
18.	42-2/SL/13/0.6	13	4.9	3800	1560	8						
19.	38-2/CMS**/30/0.5	30	4.8	3500	0	34						
20.	43-1/SL*/67/0.5	64	5.0	4800	0	27						
21.	43-2/SL/68/0.5	64	5.1	4400	2200	10	5000	2200	14	6000	3000	13
22.	43-3/SL/70/0.5	64	6.7	4400	0	10	5000	0	14	6000	0	6

* a number of cycles followed by monotonic loading to failure

** a number of cycles between fixed stresses followed by cycles to a constant maximum strain

*** See App. A

TABLE 2.11

COMPARISON OF RESULTS FOR MONOTONIC LOADING AND CYCLIC LOADING BETWEEN FIXED MAXIMUM AND MINIMUM STRESSES

Test *	E_i x10^{-6} (psi)	f'_m (psi)	ϵ_m	Approx. Time of Reach .004 Strain (min)	Stress at $2\epsilon_m$ (psi)	Stress at $3\epsilon_m$ (psi)	No.of Loadings
5-1/M/28/0.6	5.7	4000	0.0019	15	2500	1150	1
5-3/SL/29/0.6	3.8	- -	- - -	120	3300	2200	20
11-1/M/28/0.6	4.4	3600	0.002	15	2400	1600	1
11-3/SL*/28/0.6	4.1	- -	- - -	240	2900	1300	31
12-2/M/28/0.6	5.6	4300	0.0021	15	1600	- -	1
12-3/SL*/29/0.6	4.3	- -	- - -	- -	1700	940	9

* See App. A

TABLE 2.12

CYCLIC LOADING TO A CONSTANT MAXIMUM-STRAIN

(TEST-TYPE-DESIGNATION: CMS)

Test*	Moist Cure (days)	E_i x10^{-6} (psi)	f'_m (psi)	Cycles, N, to a Constant Maximum Strain, ϵ_{max}											
				ϵ_{max}	N	ϵ_{max}	N	ϵ_{max}	N	ϵ_{max}	N	ϵ_{max}	N	ϵ_{max}	N
25-2/CMS/14/0.6	14	4.8	3600	0.001	13	0.0017	20	0.0023	18	0.003	15	0.004	21		
26-2/CMS/14/0.6	14	3.8	3700	0.0009	15	0.0016	20	0.0024	42	0.0033	18	0.004	22	0.0053	28
38-2/CMS/30/0.5	30	4.8	5300	0.0024	21	0.0031	21	0.0037	17						
38-3/CMS/29/0.5	29	6.7	5300	0.0014	25	0.0021	35								

* See App. A

TABLE 2.13

PEAK-STRESSES FOR CYCLIC LOADING TO A CONSTANT MAXIMUM STRAIN

Test*	ε_{max}	Peak Stress for Cycle Number							Last	No.of cycles	% Stress Drop
		1	2	3	4	5	6	7			
25-2/CMS/14/0.6	0.001	3130	2910	2710	2660	- -	- -	- -	2420	13	23
	0.0017	3480	3280	3160	3080	3000	2910	2860	2600	20	25
	0.0023	3610	3380	3330	3260	3200	3160	3120	2990	18	17
	0.003	3590	3340	3210	3110	3030	2960	2930	2710	15	25
	0.004	3100	2840	2700	2600	2520	2460	2410	2110	21	32
26-2/CMS/14/0.6	0.0009	2880	- -	- -	- -	- -	- -	- -	2480	15	14
	0.0016	3580	3390	3280	3210	3170	3130	3080	2830	20	21
	0.0024	3630	2430	3300	3200	3150	3100	3040	2540	42	30
	0.0044	3060	- -	- -	- -	- -	- -	- -	2130	22	30
	0.0053	2470	2260	2120	2030	1980	1910	1870	1520	28	38
38-2/CMS/30/0.5	0.024	5140	4890	4690	4550	4480	4380	4330	3930	21	24
	0.0031	4960	4700	4600	4490	4390	4310	4260	3890	21	22
	0.0037	4660	4380	4300	4200	4100	4030	3980	3500	17	25
38-3/CMS/29/0.5	0.0014	4500	4330	4140	4060	3990	- -	- -	3500	25	22
	0.0021	4800	4580	4460	4400	4340	- -	- -	3790	35	21

* See App. A

TABLE 2.14

COMPARISON OF RESULTS FOR MONOTONIC LOADING AND

CYCLIC LOADING TO A CONSTANT MAXIMUM STRAIN

Test*	E_i $\times 10^{-6}$ (psi)	f'_m (psi)	ε_m	Approx. Time to Reach 0.004 Strain (min)	Stress at $2\varepsilon_m$ (psi)	Stress at $3\varepsilon_m$ (psi)	No.of Loadings
25-1/M/14/0.6	4.0	3900	0.0023	15	1900	1000	1
25-2/CMS/14/0.6	4.8	3600	- - -	215	2500	- -	98
26-1/M/14/0.6	4.8	3800	0.0019	15	1500	- -	1
26-2/CMS/14/0.6	3.8	3700	- -	240	3100	2000	154
38-1/M/29/0.5	6.5	5300	0.002	30	1300	- -	1
38-2/CMS/30/0.5	4.8	5300	- -	550	4400	- -	94
38-3/CMS/29/0.5	6.7	5300	- -	360	- -	- -	85

* See App. A

TABLE 2.15

CYCLIC LOADING TO COMMON POINTS

(TEST-TYPE-DESIGNATION: CP)

Test*	Moist Cure (days)	E_i $\times 10^{-6}$ (psi)	f'_m (psi)	No.of load-ings
6-2/CP/28/0.6	28	4.8	4100	36
8-2/CP/29/0.6	29	4.0	4200	40
9-2/CP/29/0.6	29	3.9	4200	36
14-3/CP/28/0.6	28	5.0	3900	33
40-2/CP/14/0.6	14	4.2	3900	13

* See App. A

TABLE 2.16

COMPARISON OF RESULTS FOR MONOTONIC LOADING AND

CYCLIC LOADING TO THE COMMON POINTS

Test*	E_i x10^{-6} (psi)	f'_m (psi)	ε_m	Approx. Time to Reach .004 Strain (min)	Stress at $2\varepsilon_m$	Stress at $3\varepsilon_m$	No. of load-ings
6-1/M/28/0.6	4.4	4000	0.0019	15	2000	- -	1
6-2/CP/28/0.6	4.8	4100	- - -	100	3800	2500	36
8-1/M/29/0.6	4.8	4200	0.0024	15	2600	1100	1
8-2/CP/29/0.6	4.0	4200	- - -	100	2200	1100	40
9-1/M/28/0.6	4.3	3900	0.0021	15	1100	500	1
9-2/CP/29/0.6	3.9	4200	- - -	100	3600	900	36
40-1/CEN/14/0.6	4.2	4000	0.0022	30	2300	1100	3
40-2/CP/14/0.6	4.2	3900	- - -	120	2800	- -	13

* See App. A

TABLE 2.17

COMPARISON OF RESULTS FOR DIFFERENT LOADING REGIMES

Test*	E_i x10^{-6} (psi)	f'_m (psi	ε_m	Approx. Time to Reach .004 Strain (min)	Stress at $2\varepsilon_m$ (psi)	Stress at $3\varepsilon_m$ (psi)	No. of load-ings
5-1/M/28/0.6	5.7	4000	0.0019	15	2500	1150	1
5-2/CEN/28/0.6	3.2	4200	- - -	70	3800	1900	21
5-3/SL/29/0.6	3.8	- -	- - -	120	3300	2200	20
8-1/M/29/0.6	4.8	4200	0.0024	15	2600	1100	1
8-2/CP/29/0.6	4.0	4200	- - -	100	2200	1100	40
8-3/CSI/28/0.6	5.3	4000	- - -	70	1600	500	14
9-1/M/28/0.6	4.3	3900	0.0021	15	1100	500	1
9-2/CP/29/0.6	3.9	4200	- - -	100	3600	900	36
9-3/CSI/29/0.6	4.8	4200	- - -	120	3400	1900	32
39-1/CEN/28/0.6	3.8	3700	- - -	25	1600	- -	2
39-3/SL/28/0.6	4.2	3400	- - -	370	3300	1400	74

* See App. A

TABLE 2.18

TESTS TO MEASURE THE POISSON'S RATIO

Test*	Moist Cure (days)	E_i x10^{-6} (psi)	f'_m (psi)	ε_m	Device to Measure	
					Long.strain	Lat. Strain
9-1/M/29/0.6	26	3.8	4000	0.0027	Compressometer	2 Strain gages
9-3/CEN/28/0.6	26	4.7	3560	0.0015	Compressometer	Strain gage
14-2/M/52/0.5	42	4.7	6500	0.0031	Compressometer and strain gage	Strain gage

* See App. A

TABLE 2.19

TOTAL AND INCREMENTAL POISSON'S RATIOS FOR CYCLIC LOADING
(TEST: 9-3/CEN/38/0.6)

Stress (psi)	Strain x 10^4		Poisson's Ratio	
	Long.	Lateral	Total	Incremental
2000	3.9	0.67	0.17	0.15
2500	5.3	0.88	0.17	0.15
2800	6.3	1.03	0.16	0.13
2800	8.15	1.18	0.14	0.38
2500	7.9	1.10	0.13	0.26
2000	7.3	0.95	0.12	0.18
1500	6.4	0.79	0.12	0.16
1000	5.2	0.63	0.12	0.13
500	3.75	0.48	0.13	0.11
300	3.2	0.42	0.13	0.11
0	2.2	0.32	0.15	
300	2.7	0.37	0.14	0.11
2000	6.0	0.77	0.13	0.14
2500	7.3	0.98	0.14	0.17
2800	8.2	1.11	0.14	0.16
3200	9.8	1.40	0.13	0.19
3100	12.5	1.86	0.15	0.06
2500	11.5	1.73	0.15	0.16
2000	12.15	1.55	0.13	0.28
1500	9.1	1.32	0.15	0.18
500	6.7	0.9	0.14	0.18
0	5.4	0.68	0.13	0.18

TABLE 2.19 (continued)

Stress (psi)	Strain x 10^4 Long.	Lateral	Poisson's Ratio Total	Incremental
0	4.85	0.67	0.14	- -
500	5.9	0.8	0.14	0.14
1500	7.85	1.1	0.14	0.14
2000	9.3	1.3	0.14	0.16
2500	11.0	1.54	0.14	0.13
3000	13.1	1.77	0.14	0.10
3250	14.5	1.90	0.13	0.11
3250	16.5	2.17	0.13	0.06
2500	14.8	2.00	0.14	0.15
1500	11.9	1.53	0.13	0.16
500	9.05	1.09	0.12	0.16
0	7.6	0.86	0.11	0.16
500	8.1	0.97	0.12	0.1
1000	8.9	1.12	0.13	0.21
1500	9.85	1.33	0.14	0.18
2000	11.45	1.56	0.14	0.16
2500	13.0	1.85	0.14	0.16
3000	15.5	2.13	0.14	0.16
3150	16.2	2.40	0.15	0.17
3150	19.85	2.99	0.15	0.15
2500	19.0	2.83	0.15	0.19
1500	16.45	2.32	0.14	0.2
500	12.35	1.66	0.14	0.13
0	9.9	1.32	0.13	0.13
1000	12.2	1.67	0.14	0.15
2000	15.4	2.28	0.15	0.24
2500	17.0	2.73	0.16	0.29
2900	18.7	3.18	0.17	0.22
2800	22.7	4.32	0.19	0.08
1500	20.4	4.16	0.20	0.15
500	16.7	3.35	0.20	0.22
0	13.2	2.62	0.20	- -

TABLE 3.1

SLOPE OF RESIDUAL STRAIN VERSUS UNLOADING STRAIN LINE FOR CYCLES BETWEEN FIXED STRESSES

Test*		Initial Strain	σ_{max}/f'_m %	Slope	Comments
11-3/SL/28/0.6		0.0012	70	0.78	bridges ε_r-ε_{eu} curve-straight line
12-3/SL/29/0.6		0.0012	78	0.84	begins from ε_r-ε_{eu} curve-straight line
43-1/SL/67/0.5		0.00147	65	0.84	begins from ε_r-ε_{eu} curve-straight line
39-2/SL/28/0.6		0.0009	76	0.78	bridges ε_r-ε_{eu} curve-fairly straight line
39-3/SL/28/0.6		0.0012	84	0.73	Bridges ε_r-ε_{eu} curve-straight line except at the end where data is not pertinent to the type of test (last cycle has a considerably higher load than the previous ones)
41-2/SL/15/0.6		0.0015	90	0.65	lower than ε_r-ε_{eu} curve-straight line
42-1/SL/13/0.6		0.0016	96	0.65	bridges ε_r-ε_{eu} line
13-3/SL/29/0.6		0.0013	82	0.73	bridges ε_r-ε_{eu} curve-straight line
15-3/SL/29/0.6		0.0012	89	0.73	bridges ε_r-ε_{eu} curve-straight line
43-3/SL/70/0.5	(a)	0.00093	64	1.0	beginning at ε_r-ε_{eu} curve-
	(b)	0.0014	73	0.92	three straight lines
	(c)	0.0021	87	0.75	components

* See App. A

TABLE 3.2

RESIDUAL STRAIN AND INITIAL MODULI FOR FIRST UNLOADING AND RELOADING

Test*	f'_m (psi)	σ/f'_m	Unloading Strain	Initial Modulus $\times 10^{-6}$ (psi) For Virgin Curve	Initial Modulus $\times 10^{-6}$ (psi) Upon Reloading	Residual Strain After Unloading
1-2/CEN/30/0.6	5100	0.41	.00043	5.3	5.9	.00007
37-2/CSI/28/0.5	4800	0.40	.00033	5.0	5.6	.00005
20-3/CSI/29/0.6	3800	0.52	.0005	4.0	4.8	.00012
7-2/CSI/29/0.6	3800	0.54	.0005	3.9	4.8	.00017
36-3/CSI/29/0.5	5600	0.29	.00027	3.6	4.2	.00003
7-3/CSI/28/0.6	3800	0.56	.0005	4.2	4.5	.00007
9-3/CSI/29/0.6	4200	0.39	.0005	4.8	4.9	.00008

* See App. A

TABLE 3.3

CHANGES IN INITIAL MODULUS OF ELASTICITY FOR

CYCLES TO CONSTANT MAXIMUM STRAIN

Test*	Strain	Initial Modulus, E_i^j, for Cycle, j: E_i^1	E_i^2	E_i^3	E_i^4	E_i^ℓ	Total No. of Cycles	% E_i Drop
		$\times 10^{-6}$ (psi)						
25-2/CMS/14/0.6	0.001	4.5	4.5	4.5	- -	3.8	13	15
	0.0017	3.5	3.2	3.2	- -	3.2	20	9
	0.0023	2.74	2.74	- -	- -	2.74	18	0
	0.003	2.26	2.13	2.13	- -	2.08	15	8
	0.004	1.92	1.74	1.65	1.6	1.6	21	17
26-2/CMS/14/0.6	0.0009	4.16	4.16	4.0	- -	3.48	15	16
	0.0016	3.2	3.1	- -	- -	2.73	20	15
	0.0024	2.4	2.4	2.3	2.3	2.13	42	11
	0.0044	1.5	1.5	1.5	1.4	1.4	22	7
	0.0053	1.3	1.3	1.3	1.3	1.3	28	0
38-2/CMS/30/0.5	0.0024	4.3	3.9	3.7	3.7	3.7	21	14
	0.0031	3.4	3.4	3.2	3.1	3.1	21	7
	0.0037	2.9	2.8	2.7	2.7	2.5	17	10
38-3/CMS/29/0.5	0.0014	6.1	6.1	6.0	- -	5.9	25	3
	0.0021	5.5	5.5	5.5	- -	5.5	35	0

ℓ last cycle to maximum strain

* See App. A

TABLE 4.1

COMPARISON OF CHARACTERISTICS OF ANALYTICAL MODEL

WITH EXPERIMENTAL DATA

Mortar Property Properties of Envelope	Value or Characteristics Analytical	Average Experimental
1. E_i	2.4 ε_m	see Table 2.4
2. f'_m, ε_m	same as experimental value	see Table 2.4
3. stress at 0.006 strain	0.4 f'_m	stress taken only at multiples of ε_m see Table 2.4
Relationships		
1. ε_r-ε_{eu} curve		
$\varepsilon_{eu} < 0.003$	curvilinear	curvilinear
$\varepsilon_{eu} = 0.003$	$\varepsilon_r = 0.0013$	$\varepsilon_r = 0.0013$
$\varepsilon_{eu} > 0.003$	straight line with a slope of 1	straight line with a slope of 1
2. ε_{er}-ε_{em} curve		
$\varepsilon_{er} < \varepsilon_m$	$\varepsilon_{er} = \varepsilon_m$	varies (curvilinear relation)
$\varepsilon_{er} \geq \varepsilon_m$	straight line with a slope of 1 passing through point $(\varepsilon_r, \varepsilon_{er}) = (0.001, 0.0029)$	curvilinear up to $(\varepsilon_r, \varepsilon_{er}) = (0.001, 0.003)$, then straight line with a slope of 1
3. $\sigma_{r\ell}$ vs N line $\sigma_{r\ell} = \sigma_{max} N^A$	A = -0.08	A = -0.093
	$\frac{\sigma_r}{\sigma_{max}} \leq \frac{\sigma_{er}}{\sigma_{max}}$	-
Shape of the Cycles		
1. loading component		
$\sigma \leq \sigma_{r\ell}$	straight line	mostly curved
$\sigma > \sigma_{r\ell}$	curved	curved
$\sigma = \sigma_{er}$	slope = zero	slope may be greater than, equal to or less than zero with increasing ε_{er}
2. unloading component shape	curved	curved
$\varepsilon = \varepsilon_r$	slope = zero	slope may be greater than, or equal to zero with increasing ε_{er}

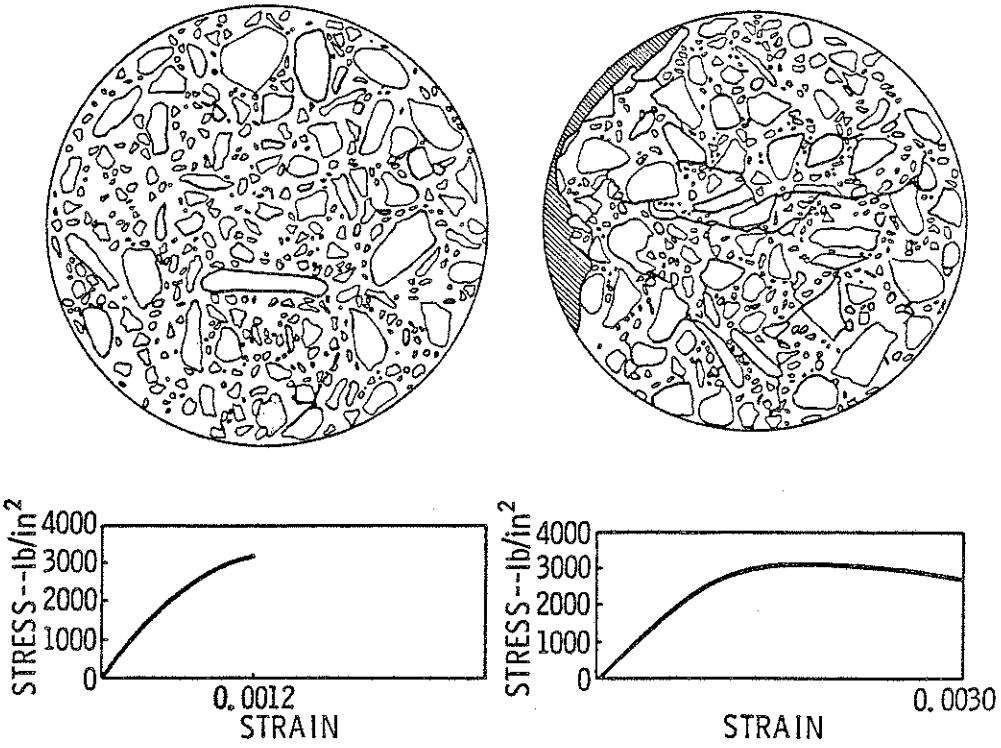

Fig. 1.1 Cracking Maps and Stress-Strain Curves for Concrete Loaded in Uniaxial Compression (1)

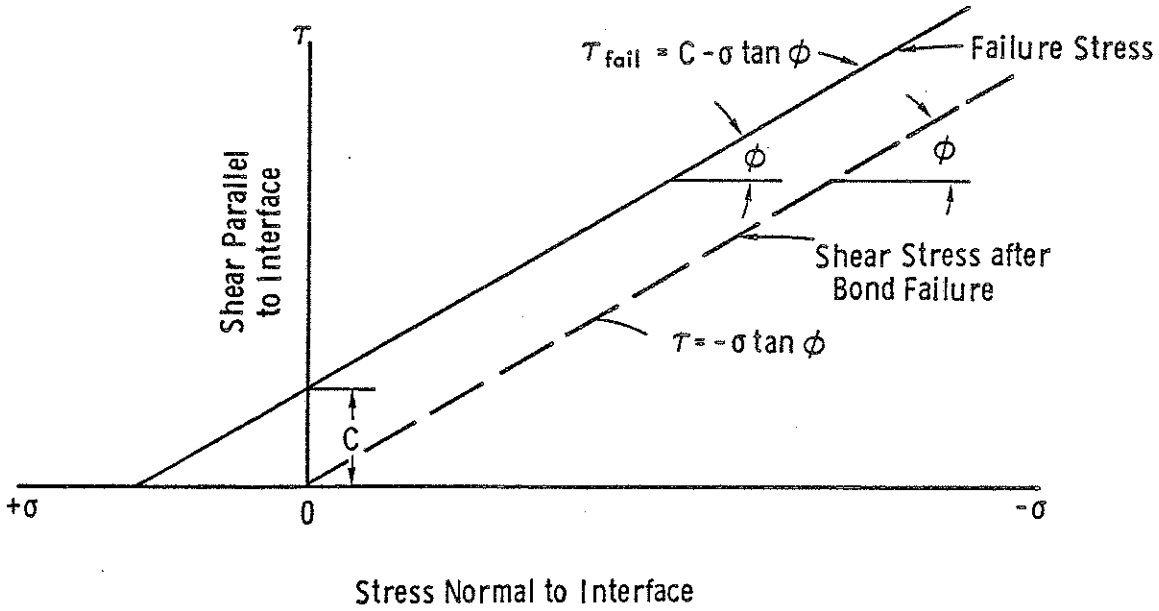

Fig. 1.2 Mohr-Coulomb Strength Envelope for the Interfacial Bond Between Mortar and Coarse Aggregate (28)

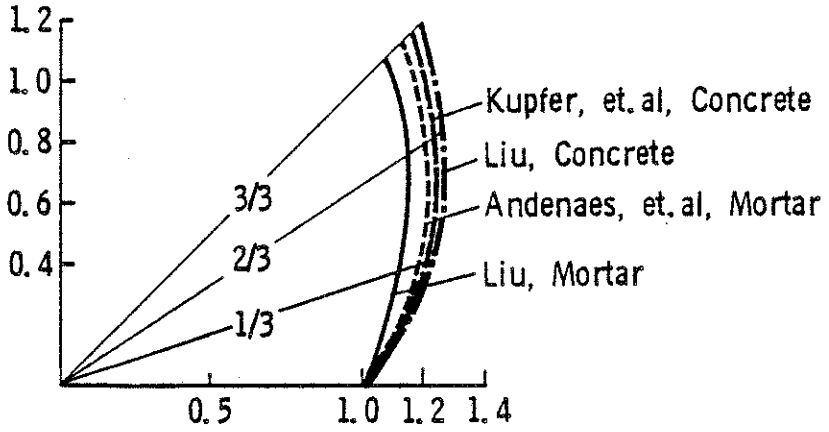

Fig. 1.3 Biaxial Strength Envelopes for Mortar and Concrete (2,14,15)

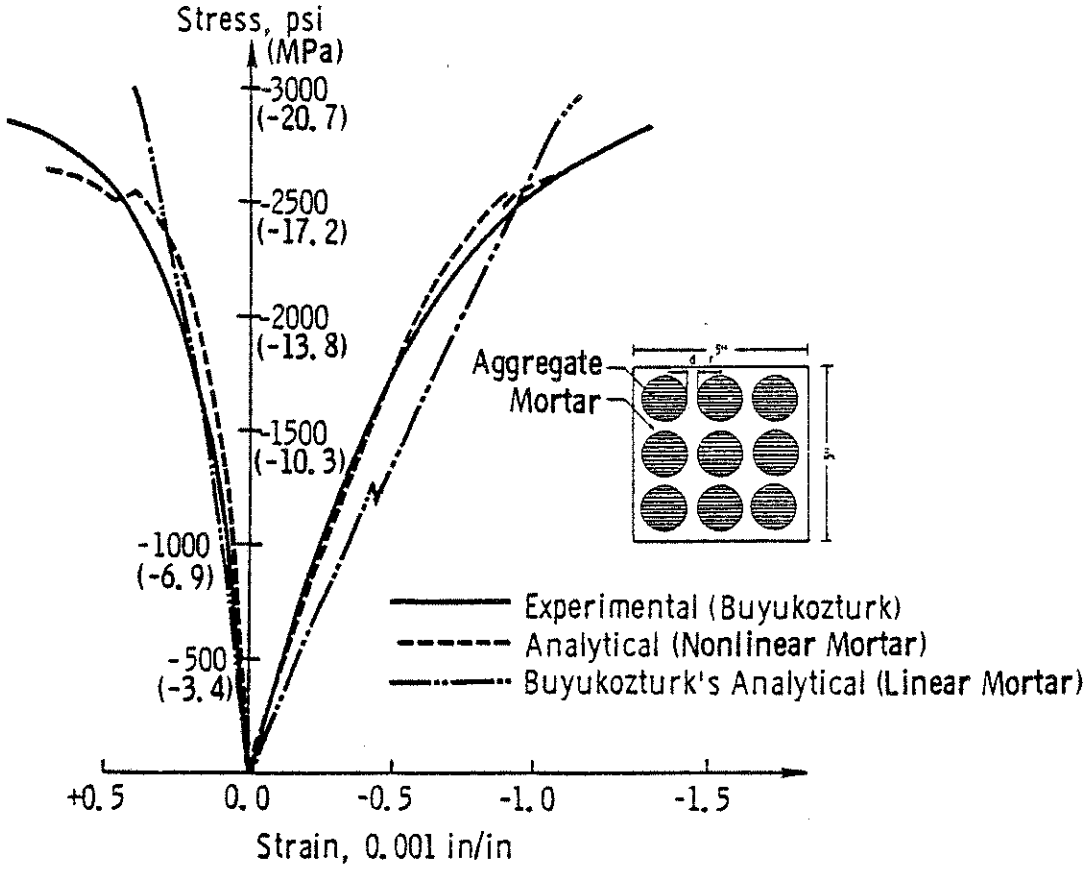

Fig. 1.4 Stress-Strain Curves for Concrete Model (1)

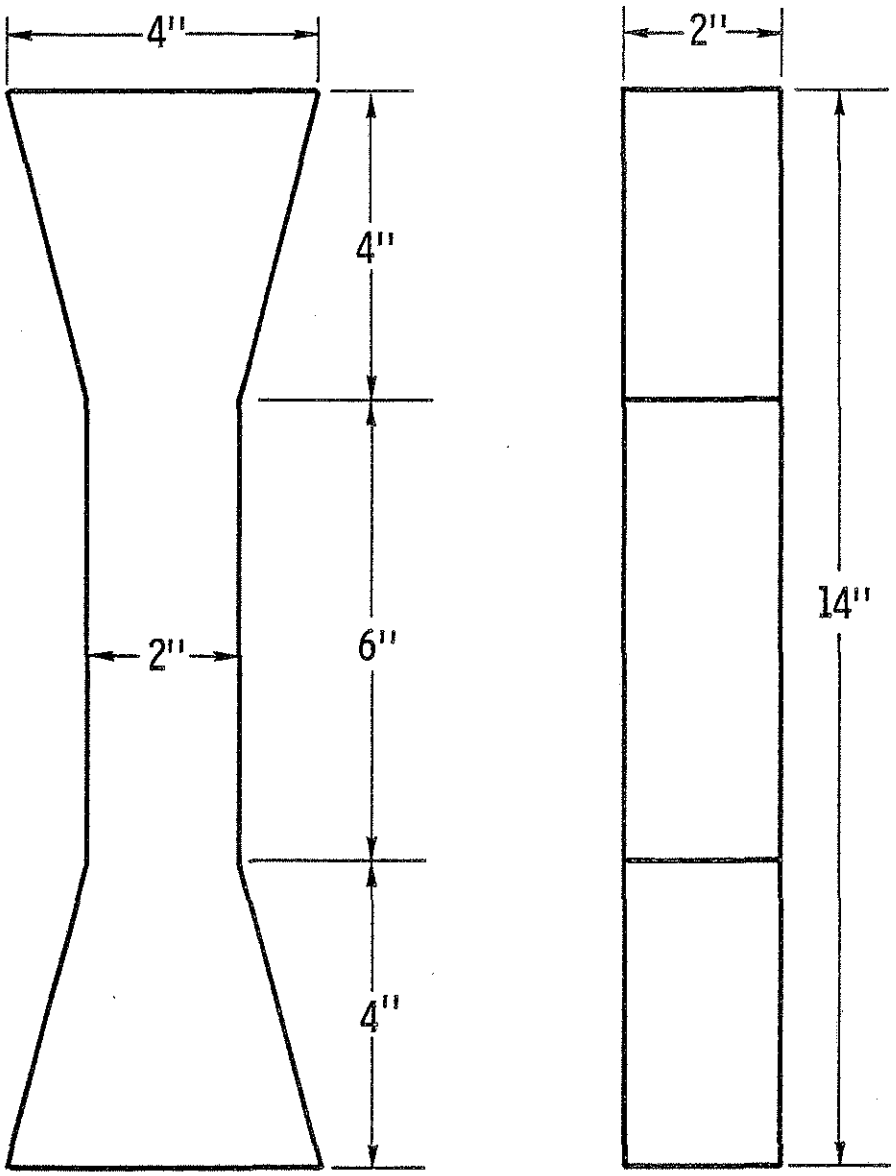

Fig. 2.1 Shape of Test Specimen

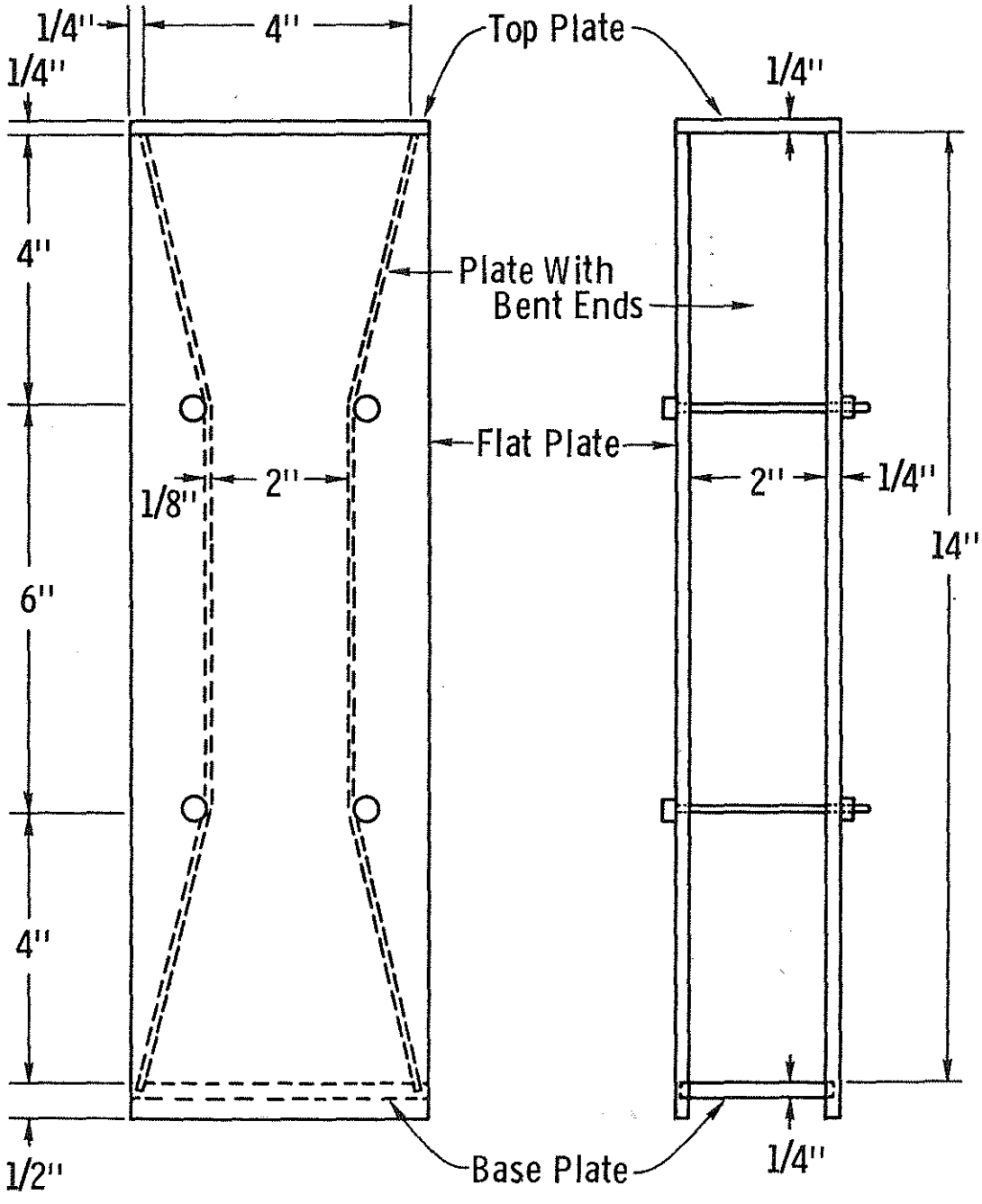

(a) View From The Top (b) Side View

Fig. 2.2 Steel Mold

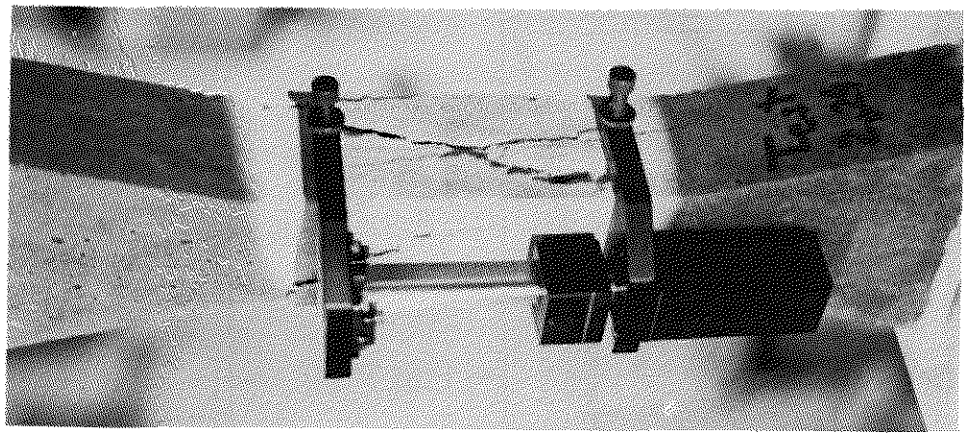

(b)

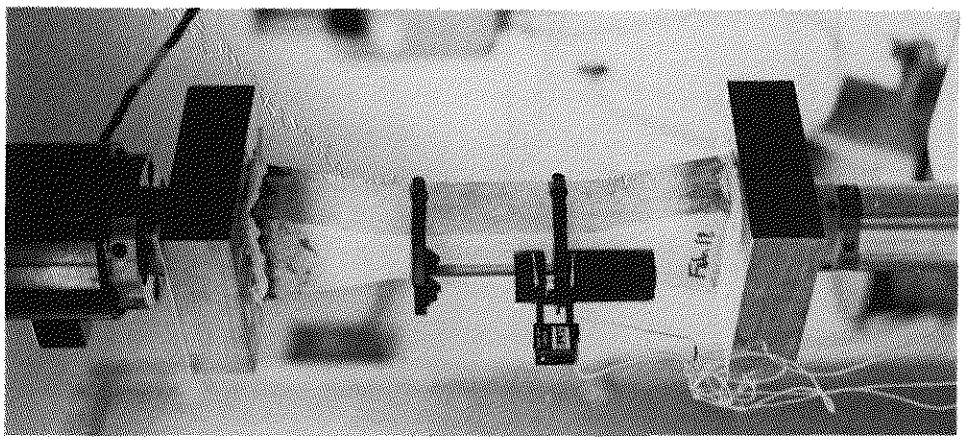

(a)

Fig. 2.3 Test Specimens: (a) Before Testing, (b) After Failure

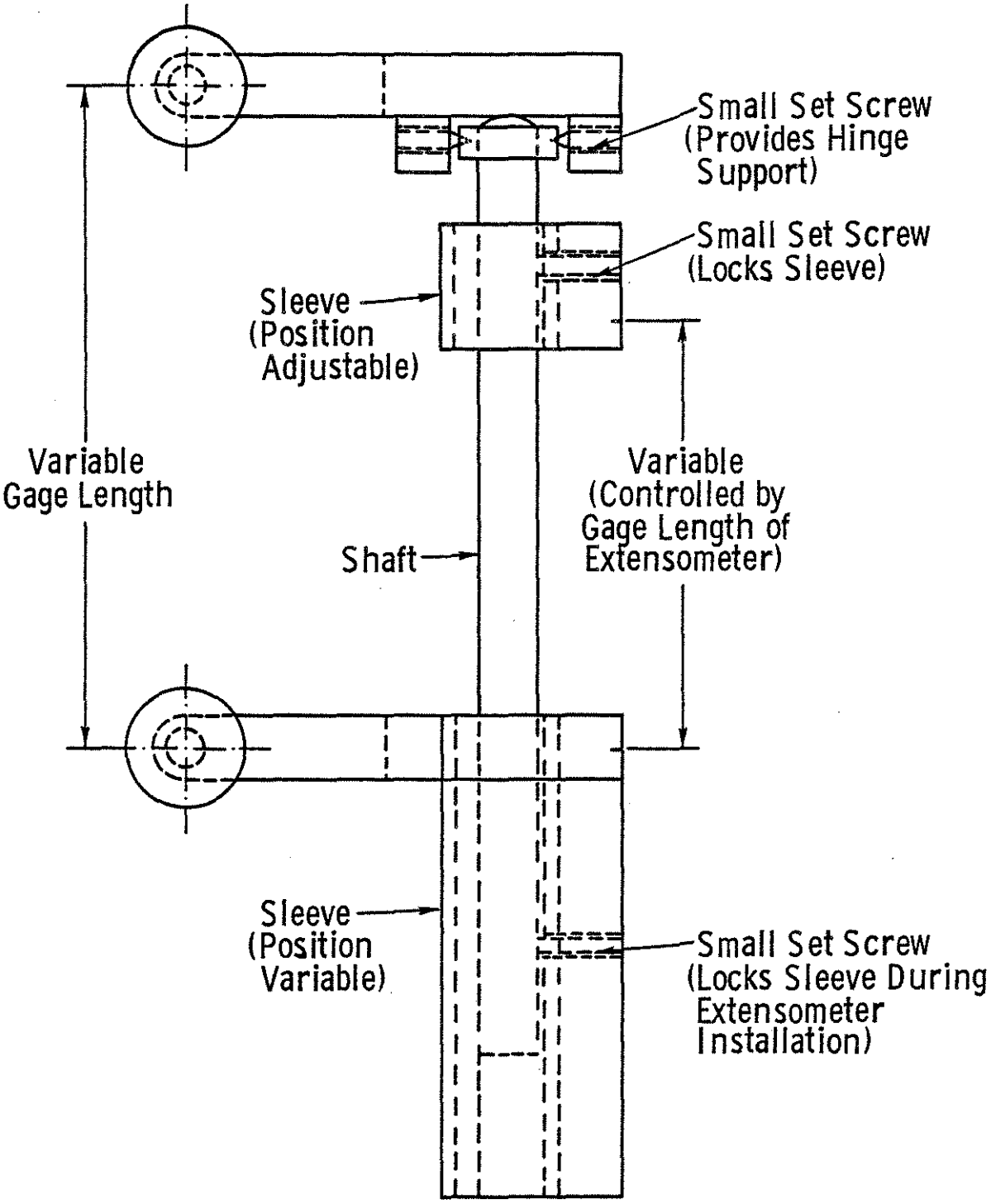

Fig. 2.4 Compressometer

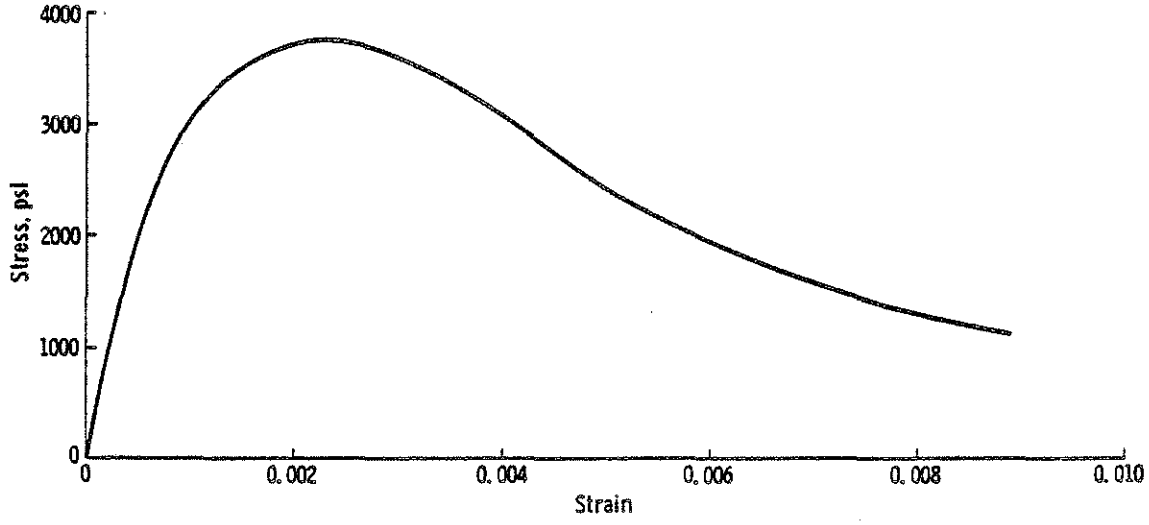

Fig. 2.5a Monotonic Envelope

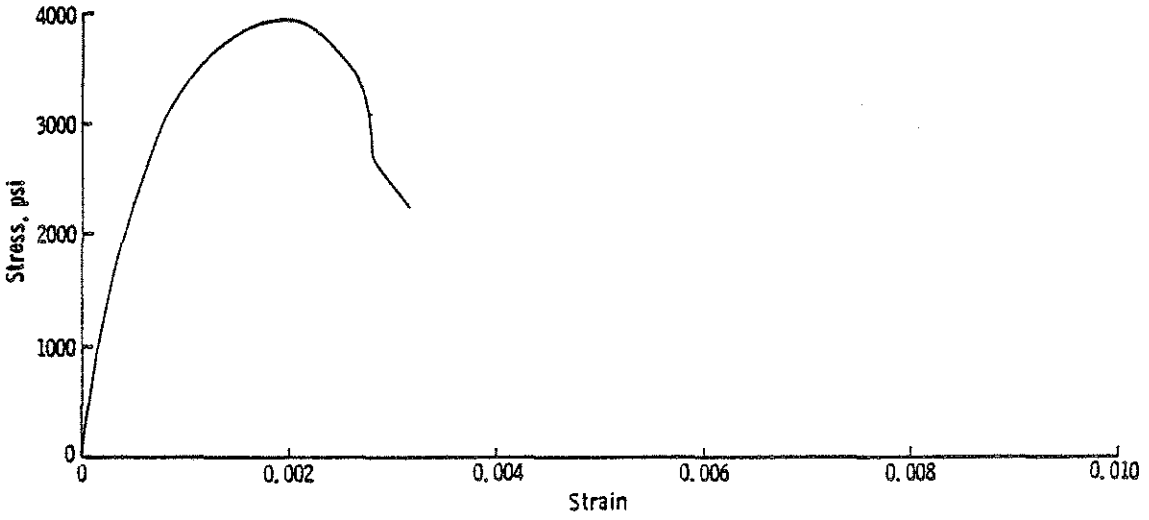

Fig. 2.5b Shape of Envelope Due to Cracking Outside the Gage Length of the Compressometer

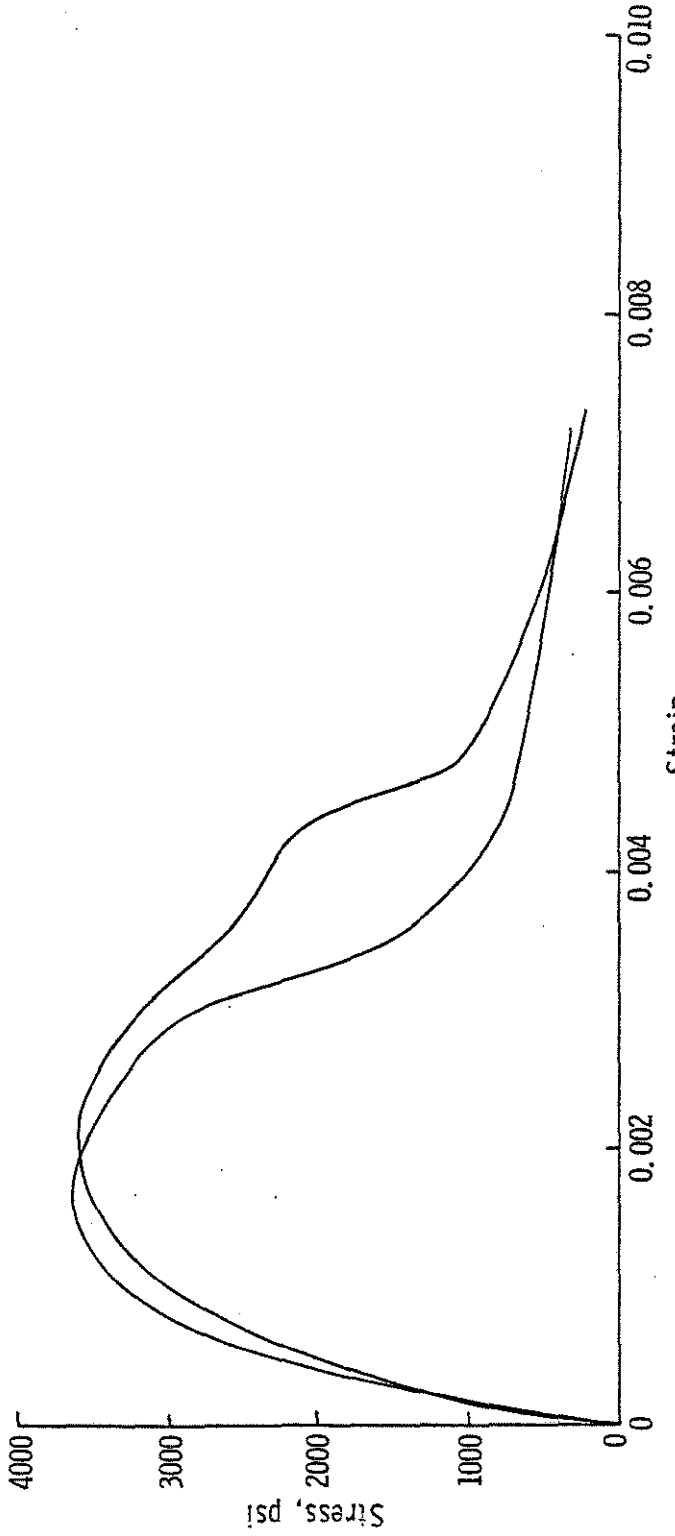

Fig. 2.6 Comparison of Monotonic Envelopes for the Same Batch

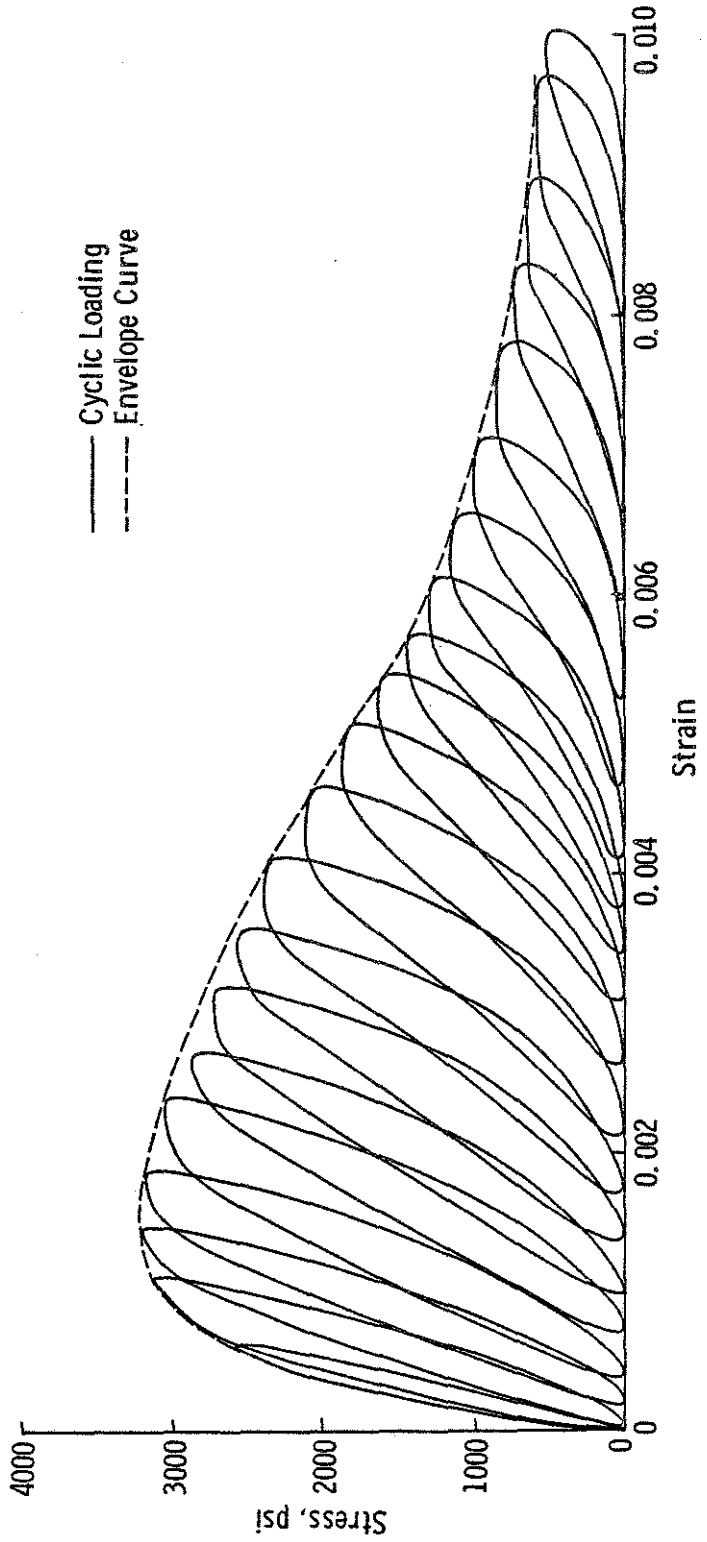

Fig. 2.7 Mortar Under Cyclic Loading

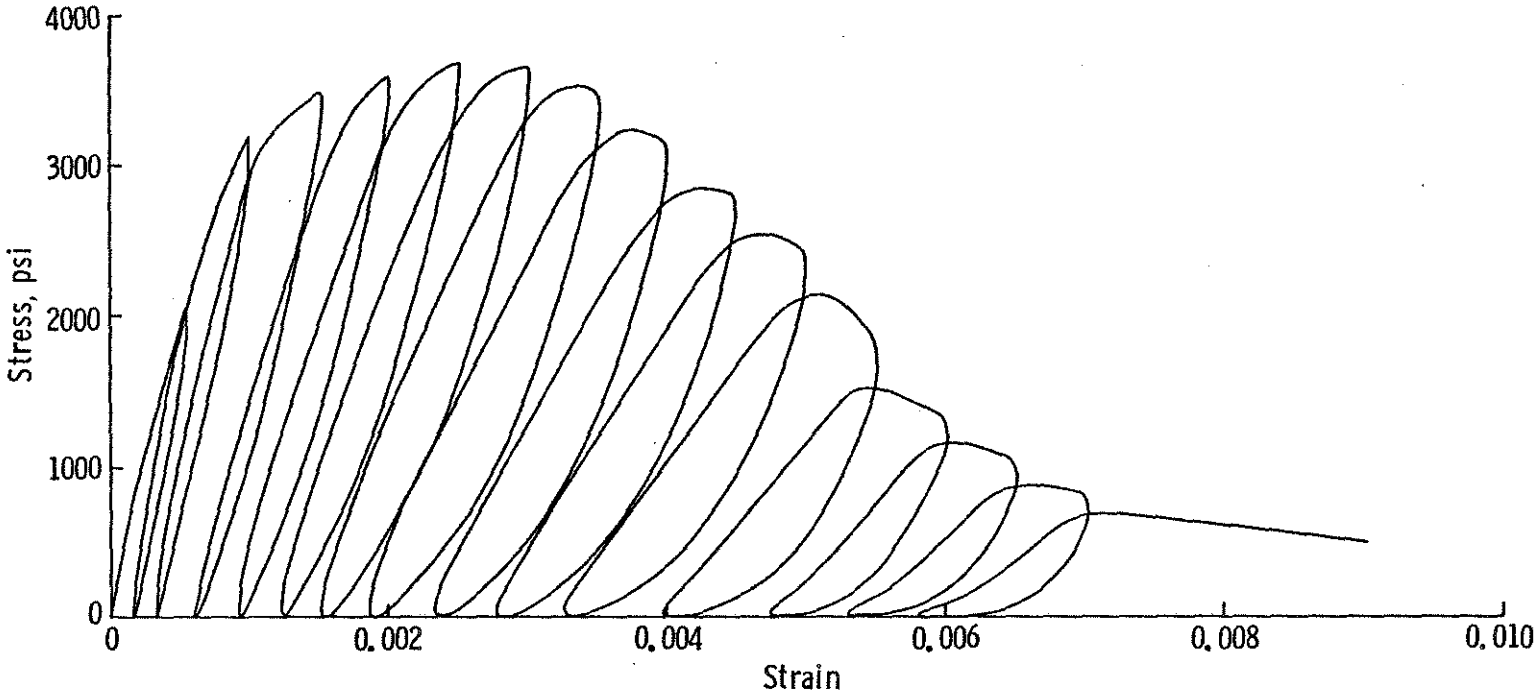

Fig. 2.8 Cycles with a Constant Strain Increment

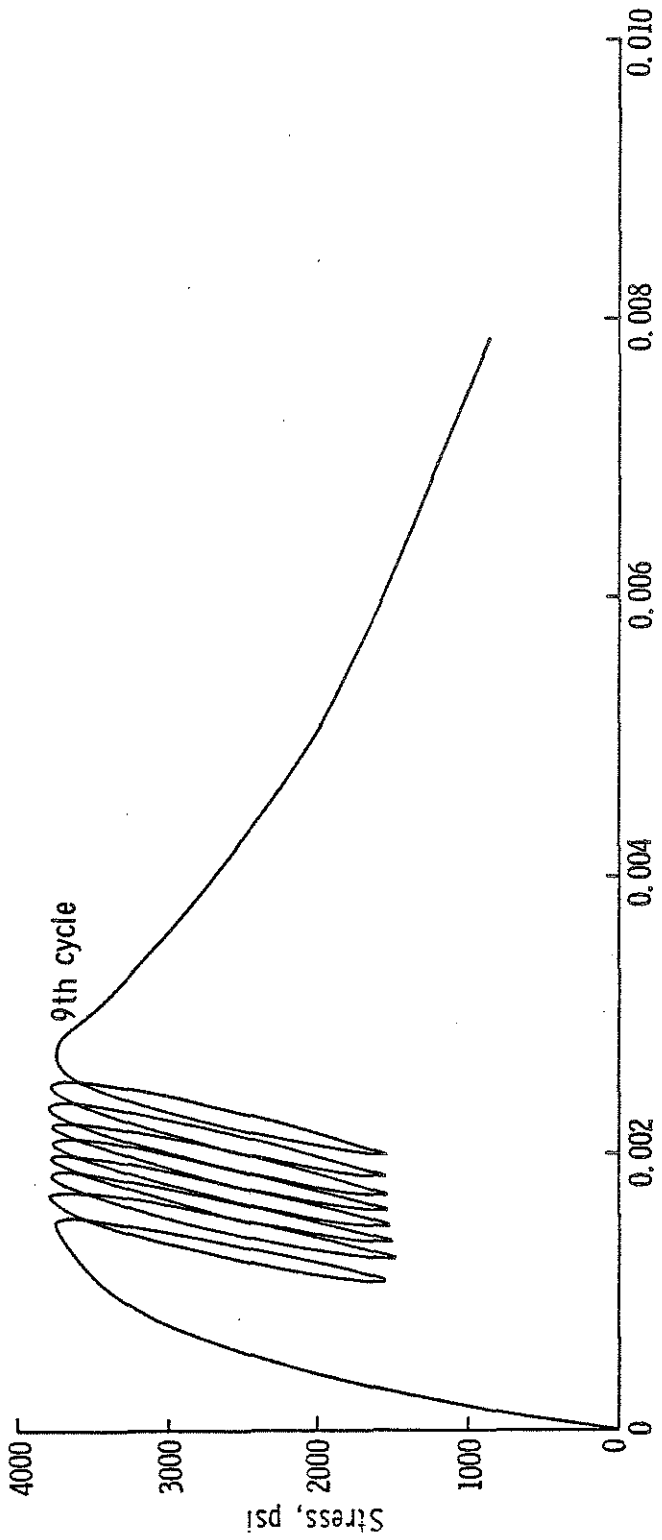

Fig. 2.9 Cycles between Fixed Stresses

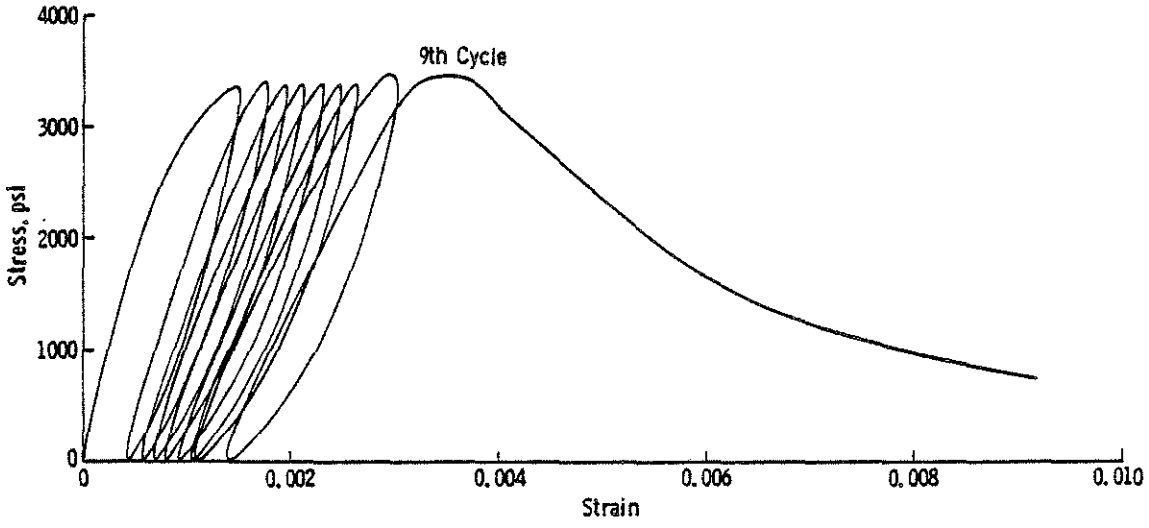

(a)

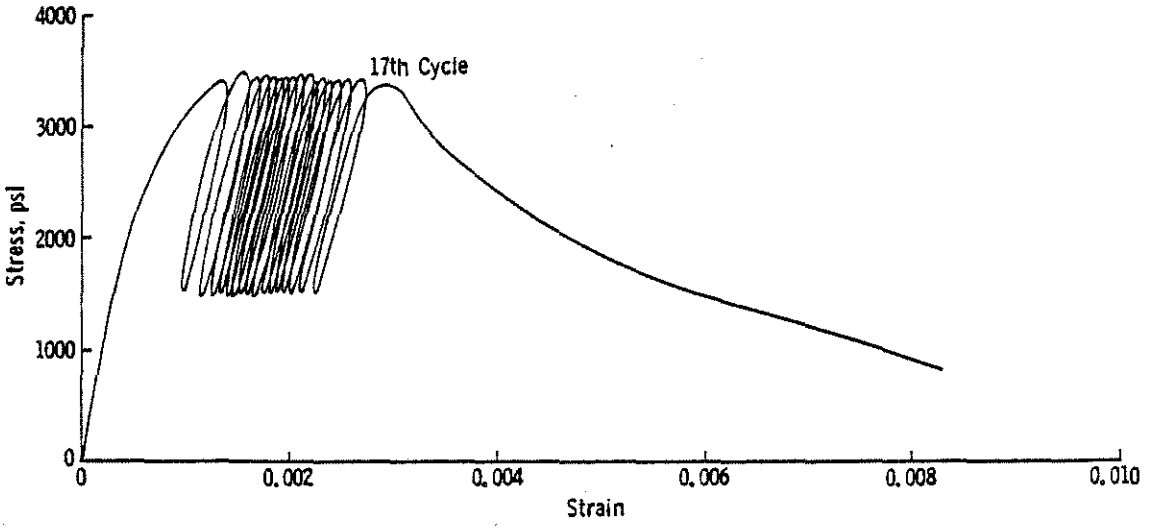

(b)

Fig. 2.10 Effect of Minimum Stress on the Number of Cycles to Failure for the Same Maximum Stress

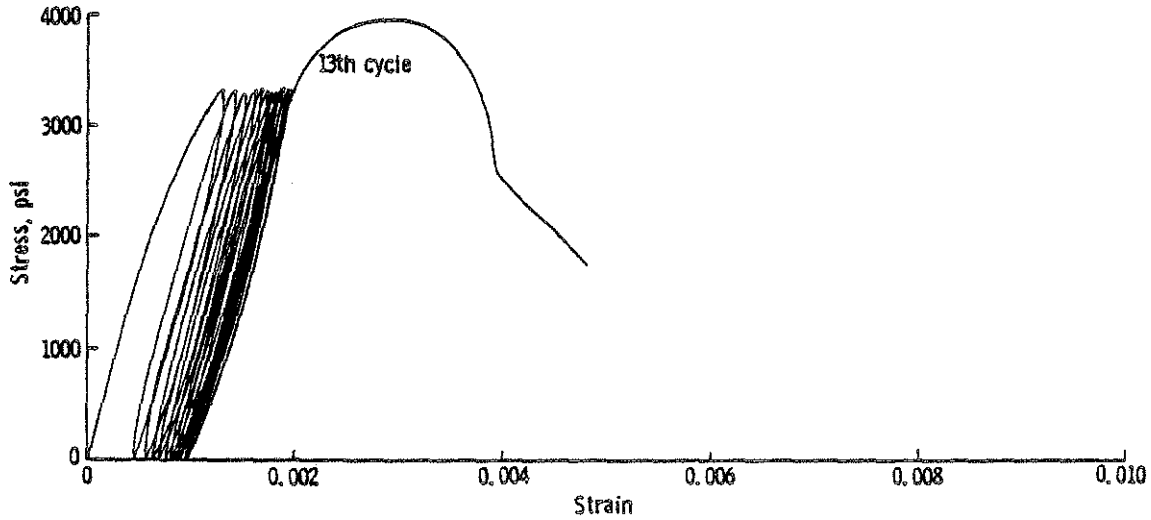

(a)

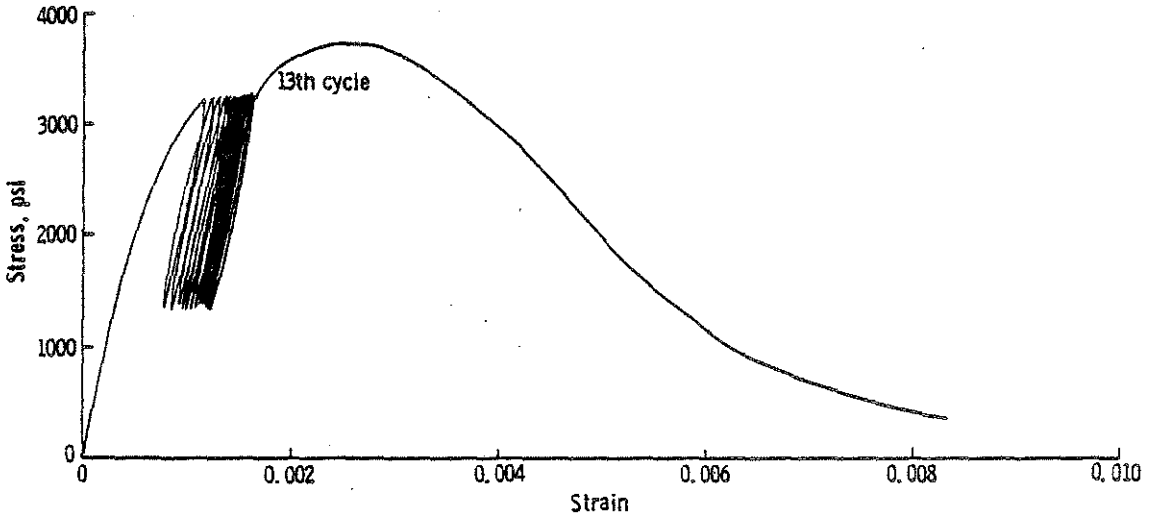

(b)

Fig. 2.11 Effect of Minimum Stress on the Strain Increase for the Same Maximum Stress

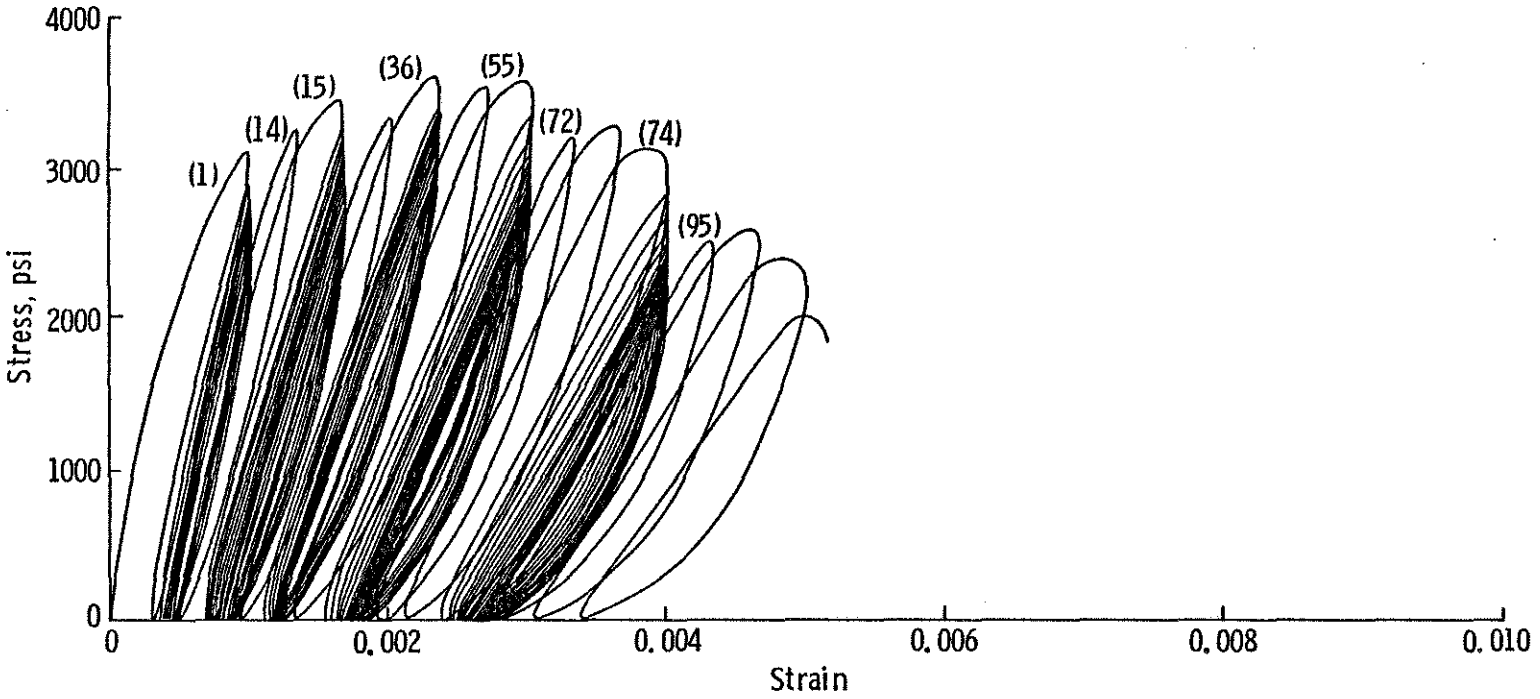

Fig. 2.12 Cycles to a Constant Maximum Strain

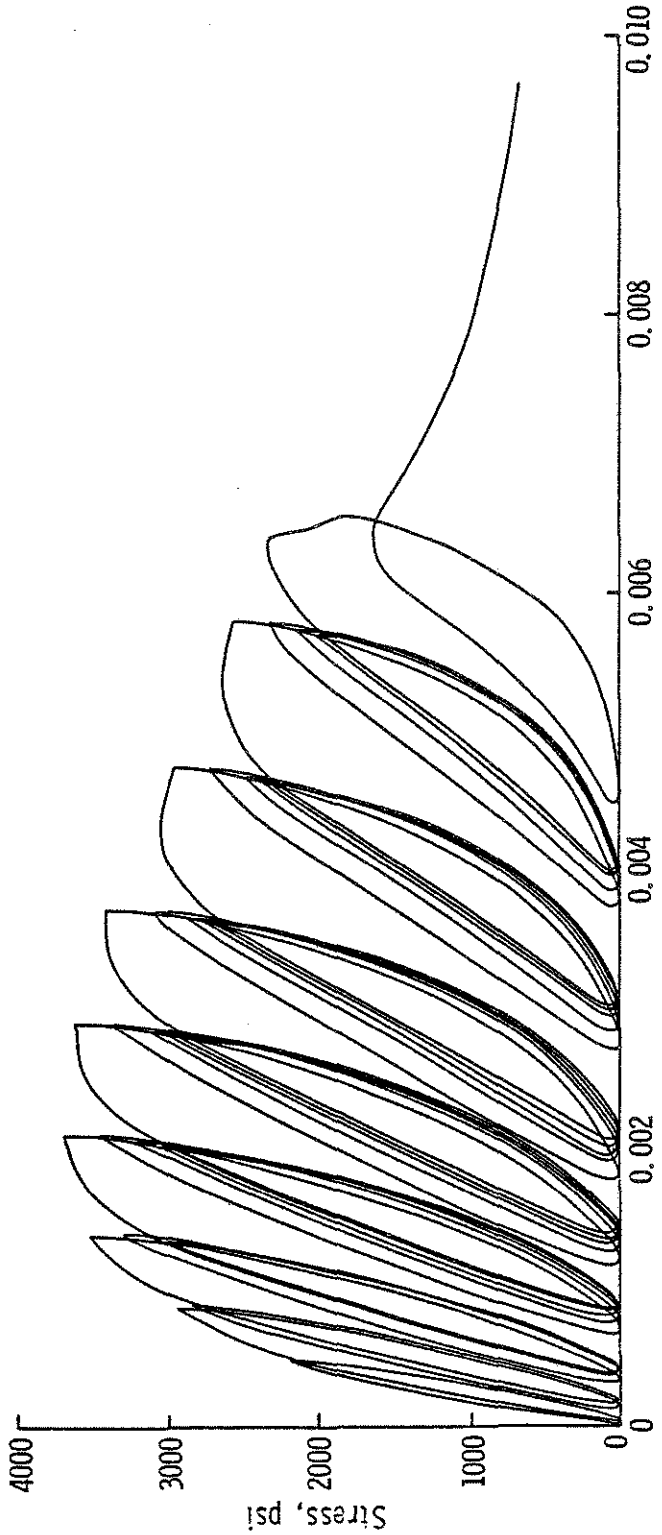

Fig. 2.13 Cycles to Common Points

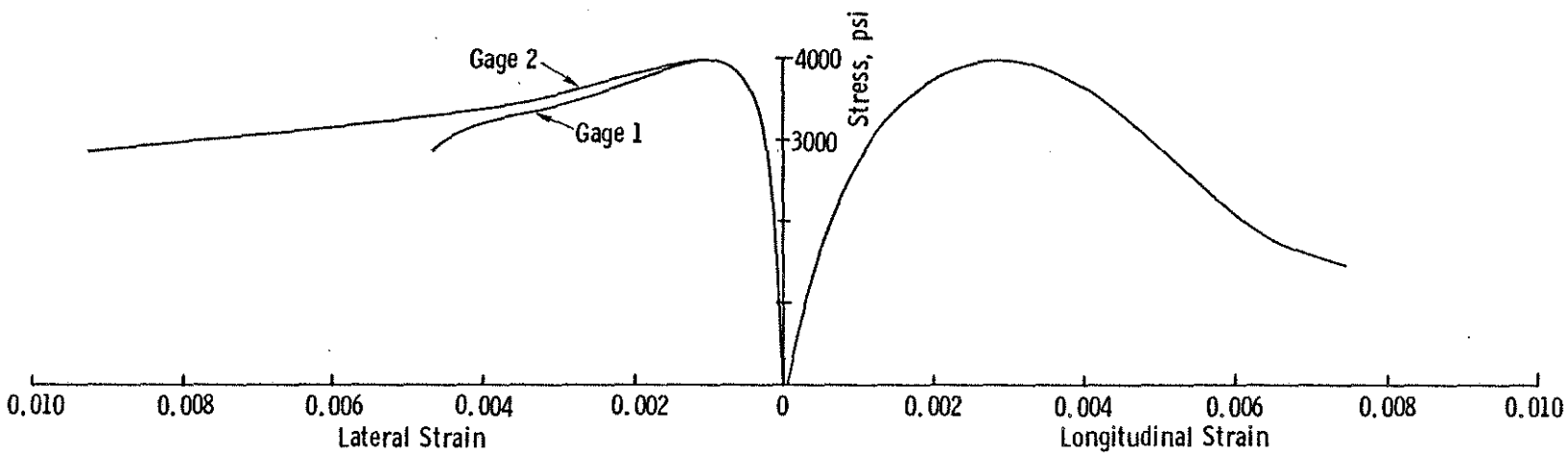

Fig. 2.14 Stress versus Longitudinal and Lateral Strain for Test 9-1/M/29/0.6

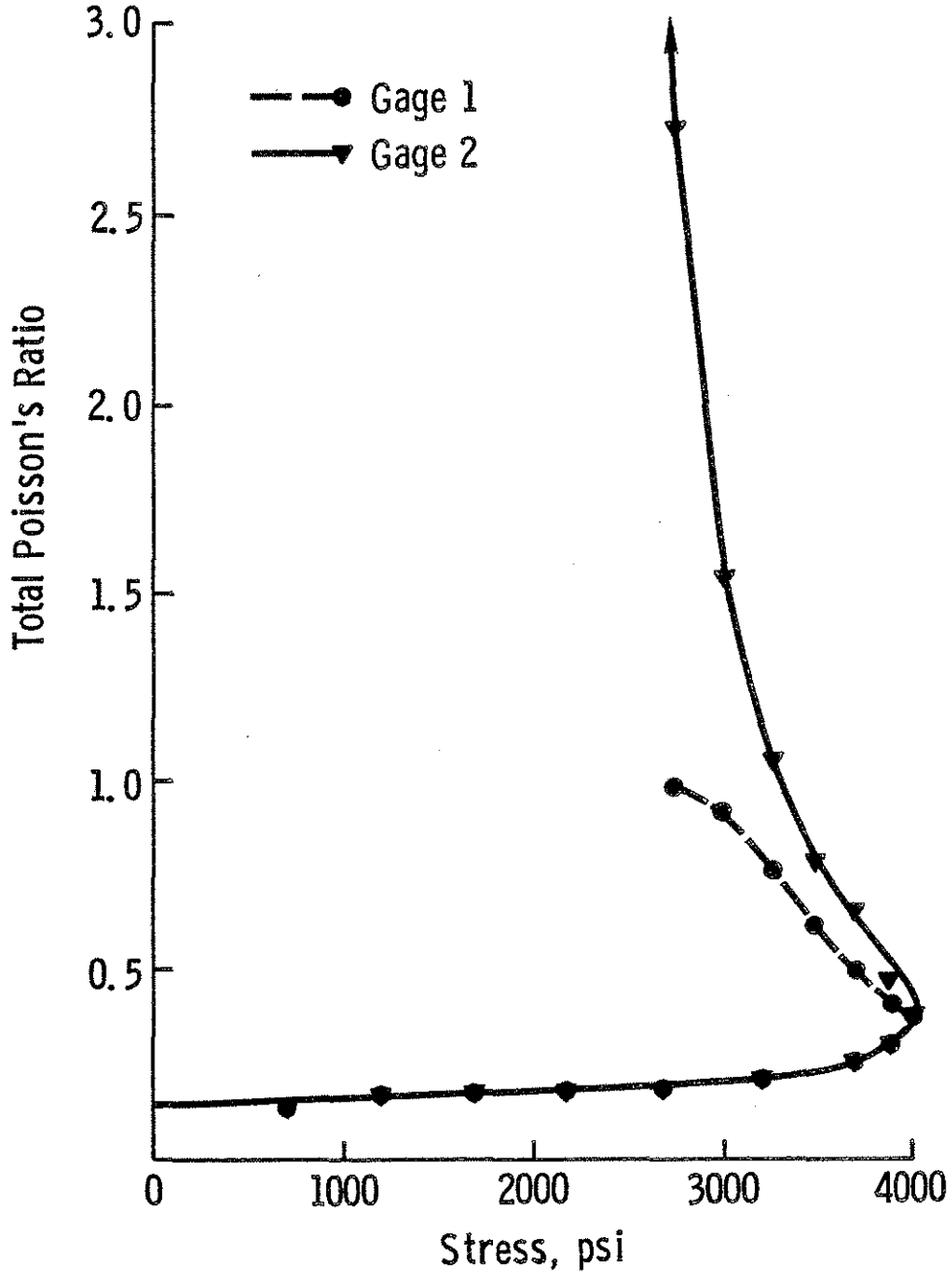

Fig. 2.15 Total Poisson's Ratio versus Stress for Test 9-1/M/29/0.6

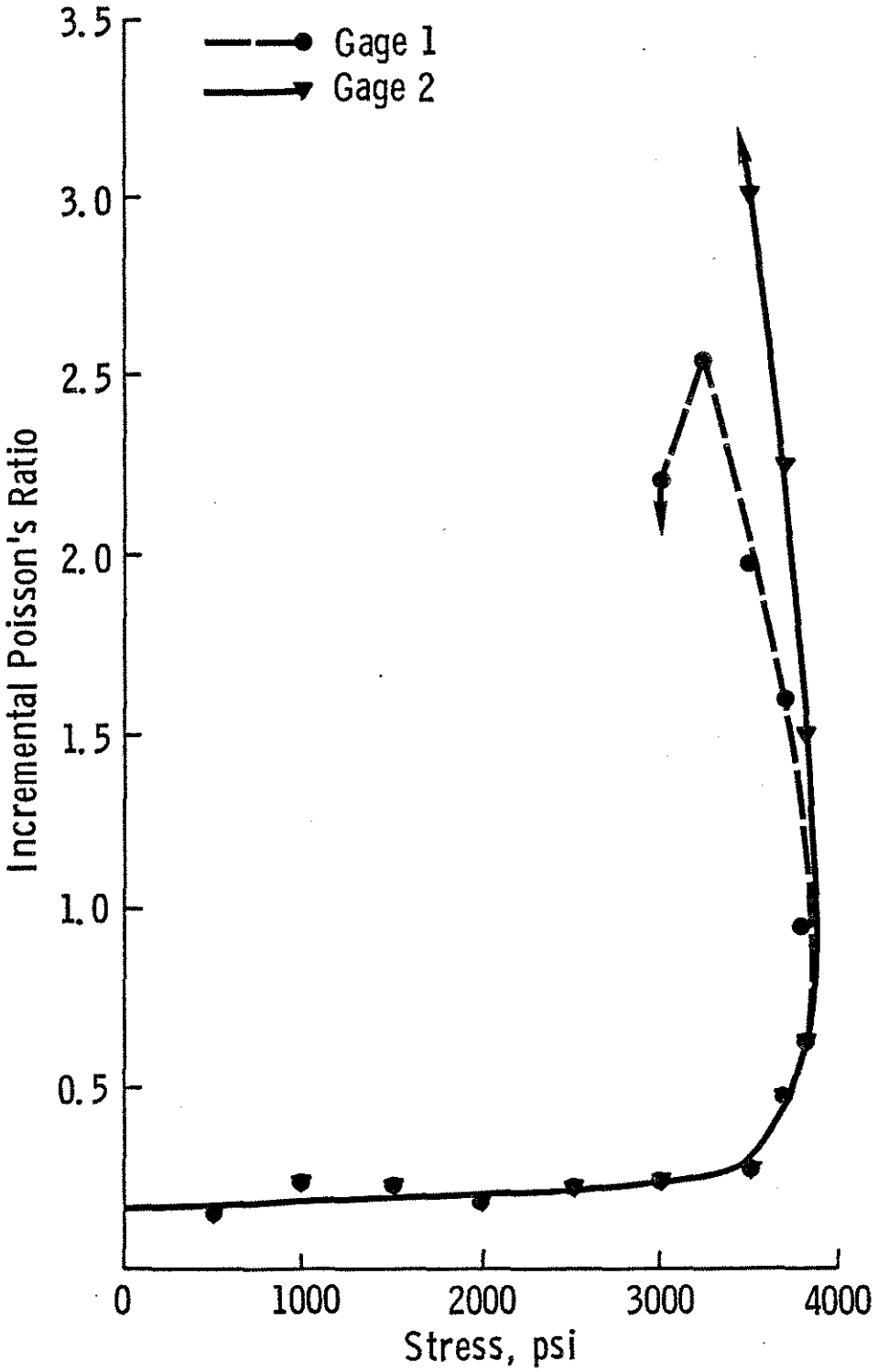

Fig. 2.16 Incremental Poisson's Ratio versus Stress for Test 9-1/M/29/0.6

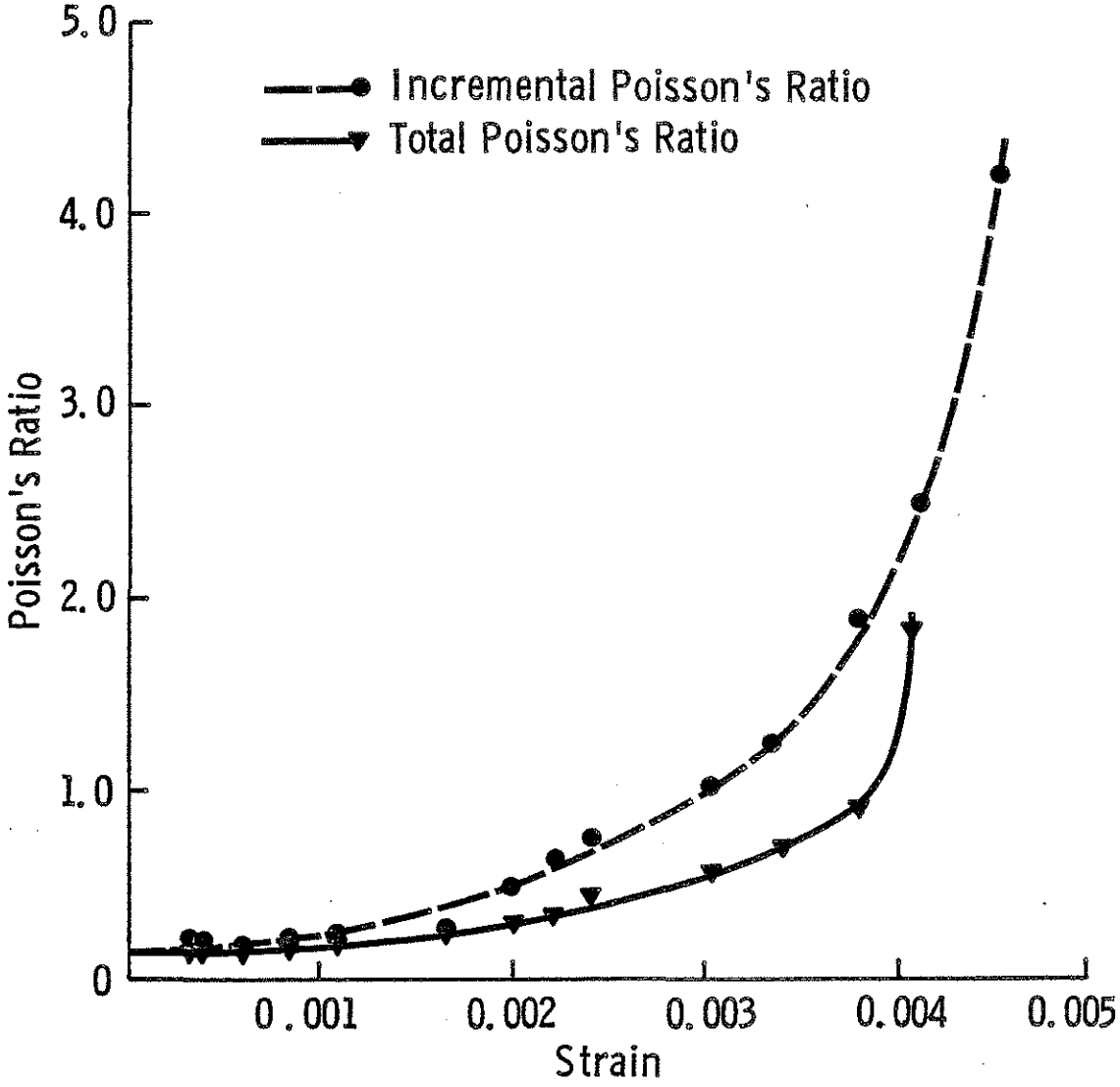

Fig. 2.17 Average Total and Incremental Poisson's Ratios versus Strain for Test 9-1/M/29/0.6

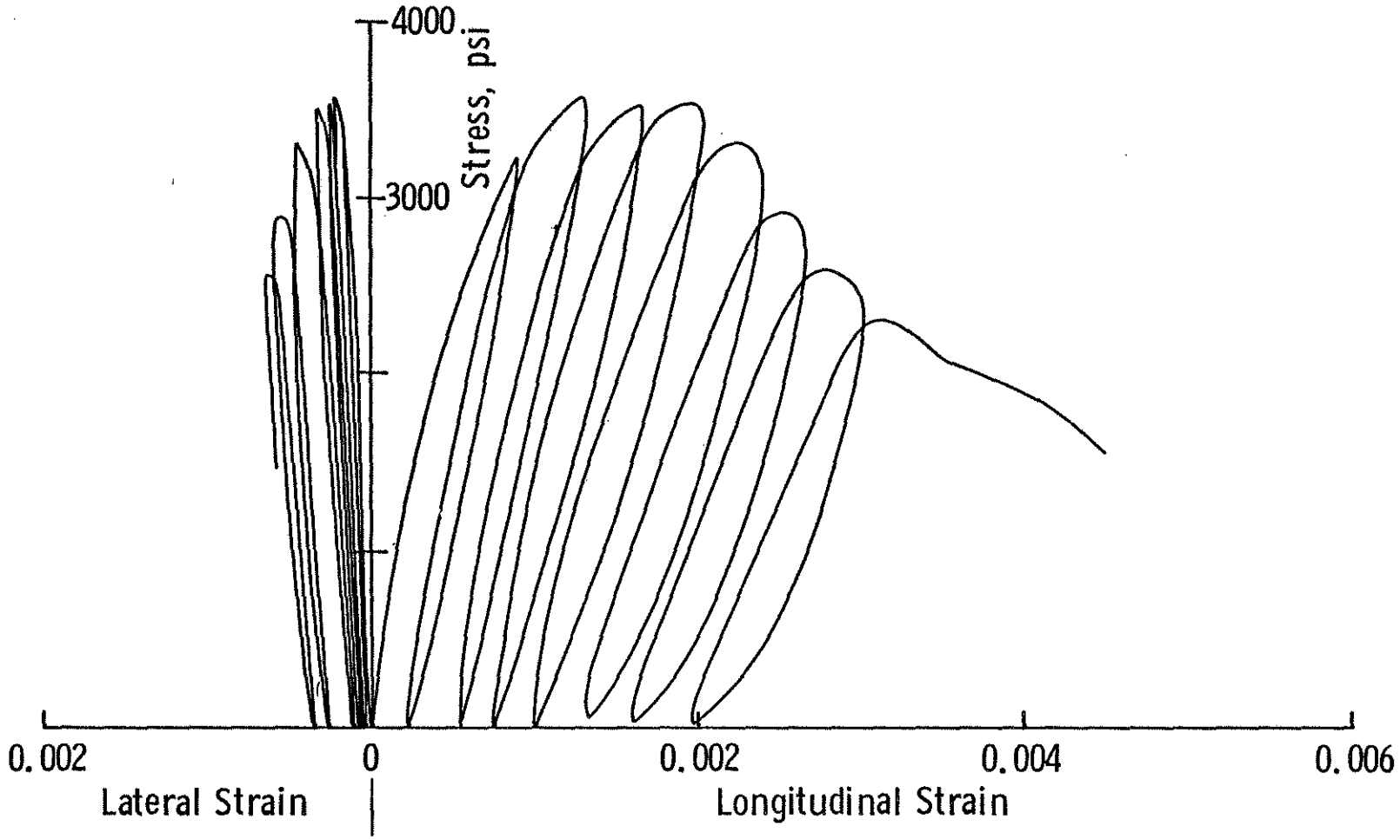

Fig. 2.18 Stress versus Longitudinal and Lateral Strain for Test 9-3/CEN/28/0.6

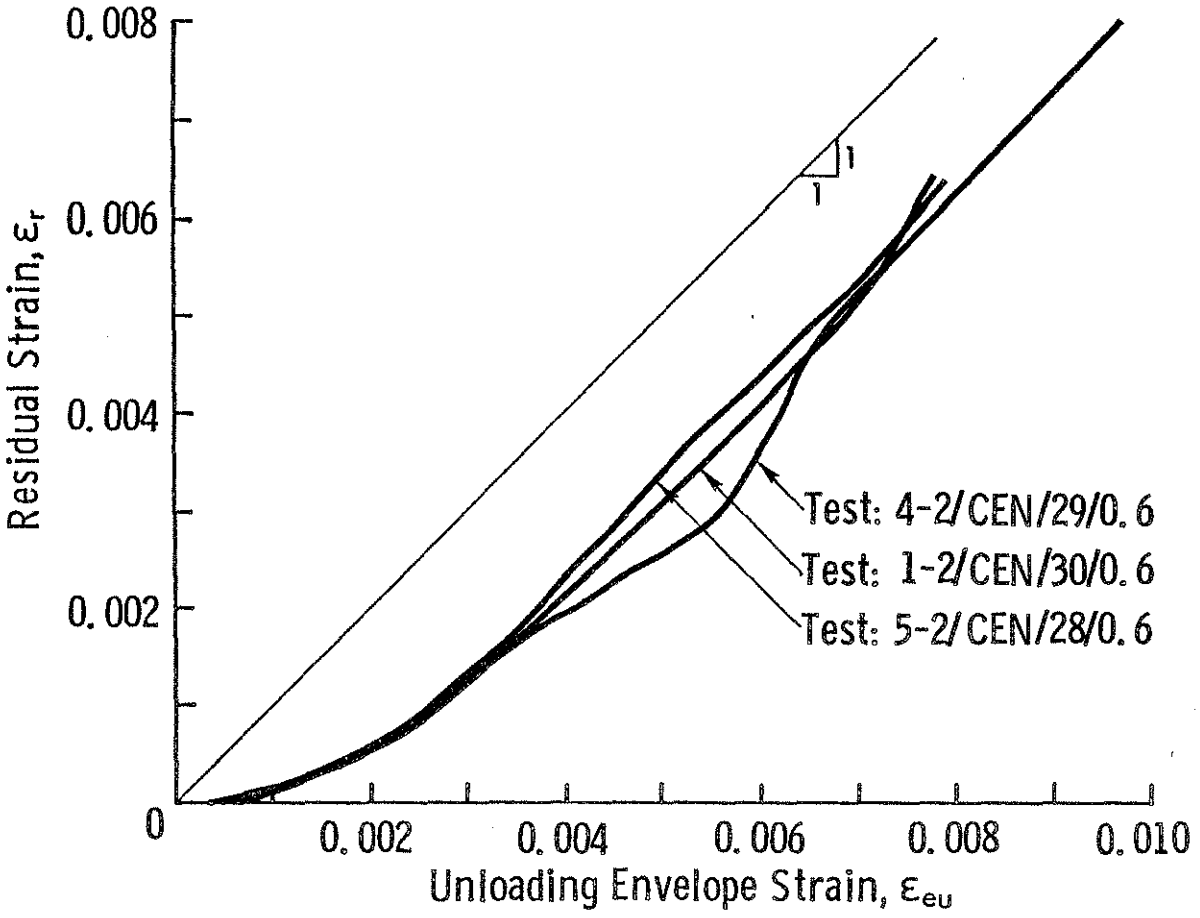

Fig. 3.1 Residual Strain versus Unloading Envelope Strain for Cycles to the Envelope

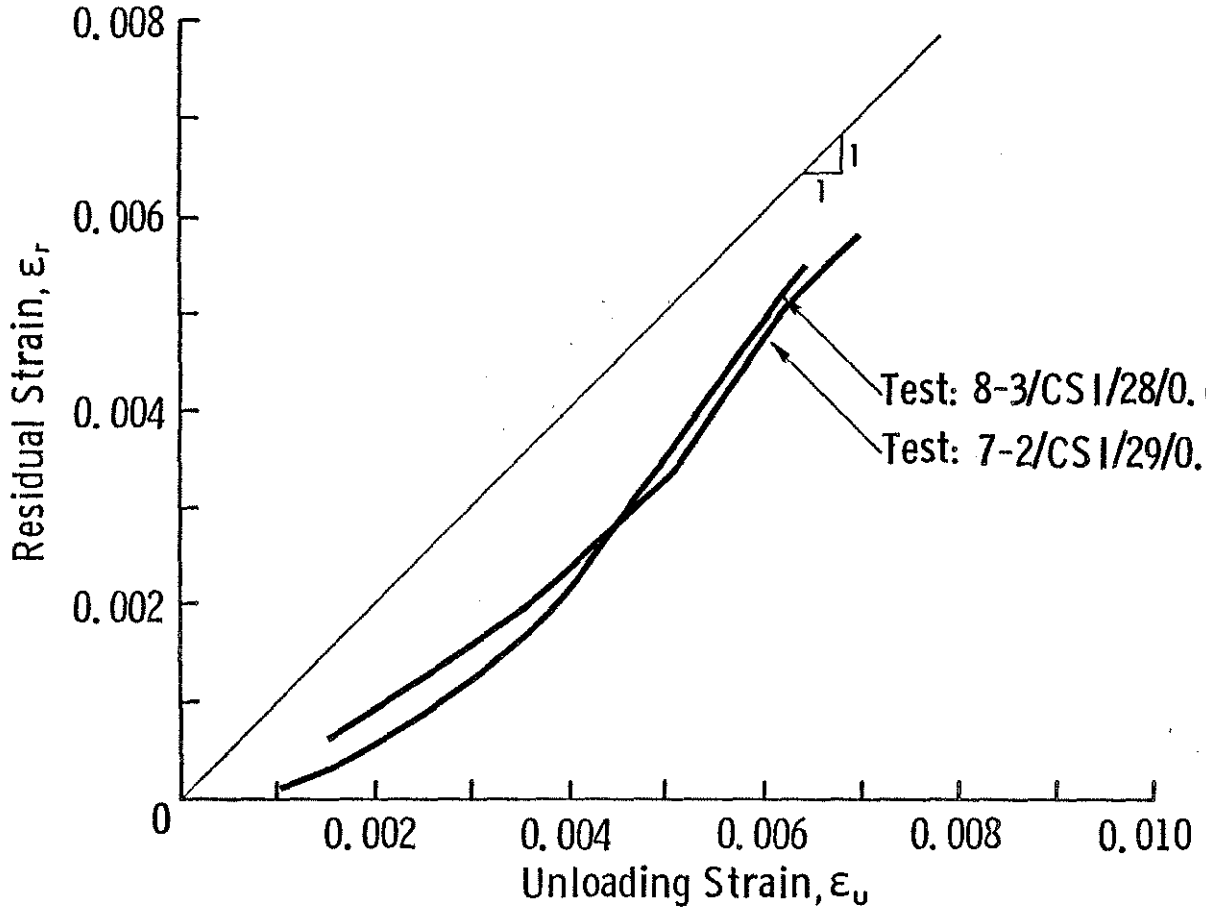

(a)

Fig. 3.2 Residual Strain versus Unloading Strain for Cycles with a Constant Strain Increment

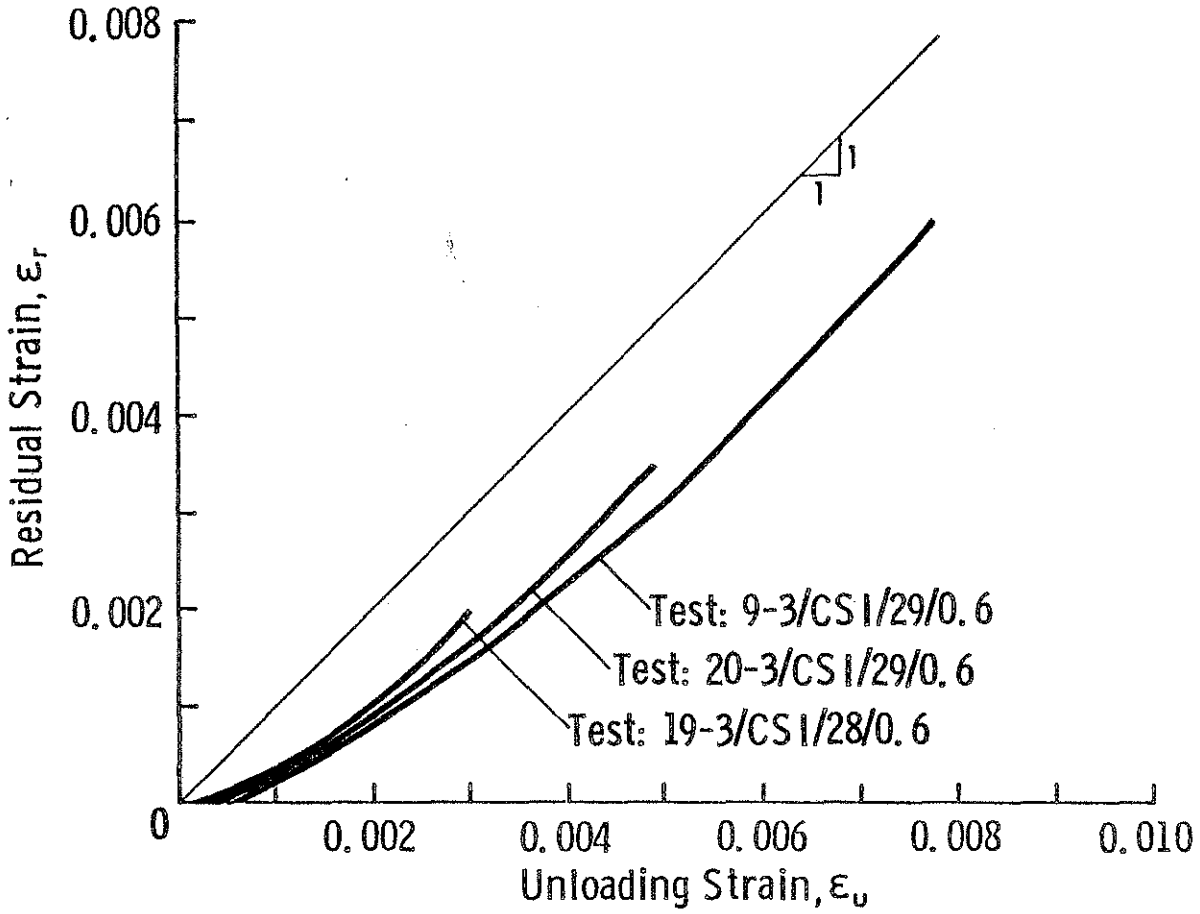

(b)

Fig. 3.2 Residual Strain versus Unloading Strain for Cycles with a Constant Strain Increment (cont'd)

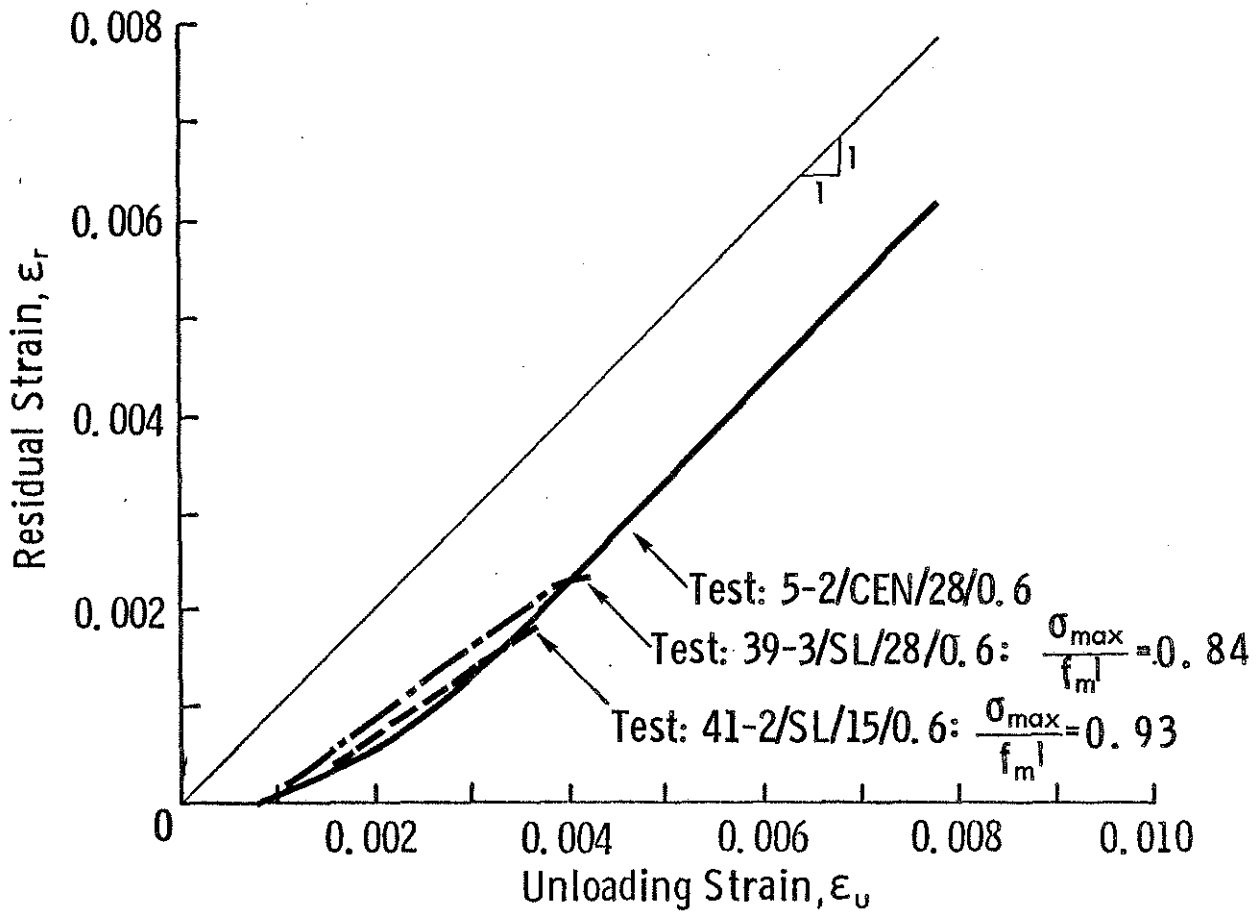

Fig. 3.3 ε_r-ε_u Line Bridging ε_r-ε_{eu} Curve

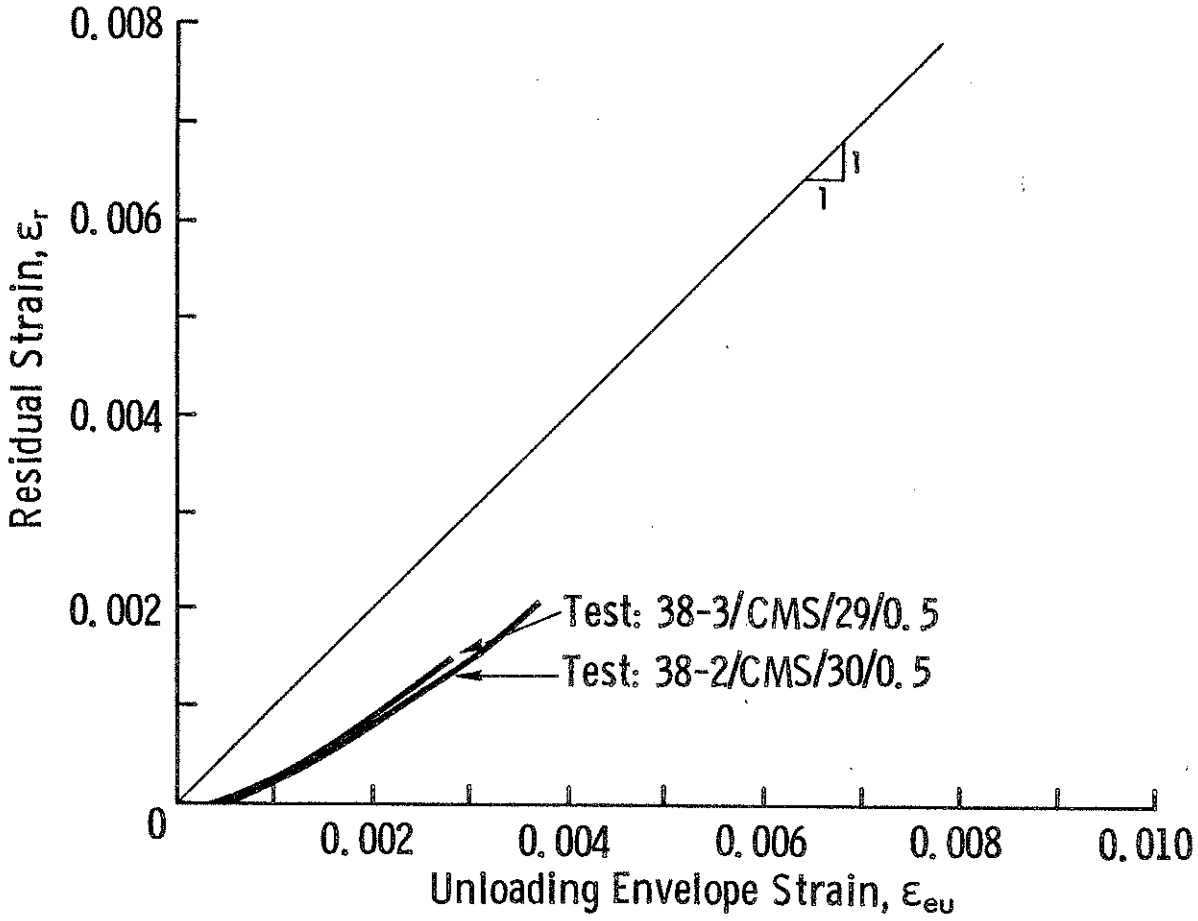

(a)

Fig. 3.4 Residual Strain versus Unloading Strain for Cycles to a Constant Maximum Strain (First Cycle)

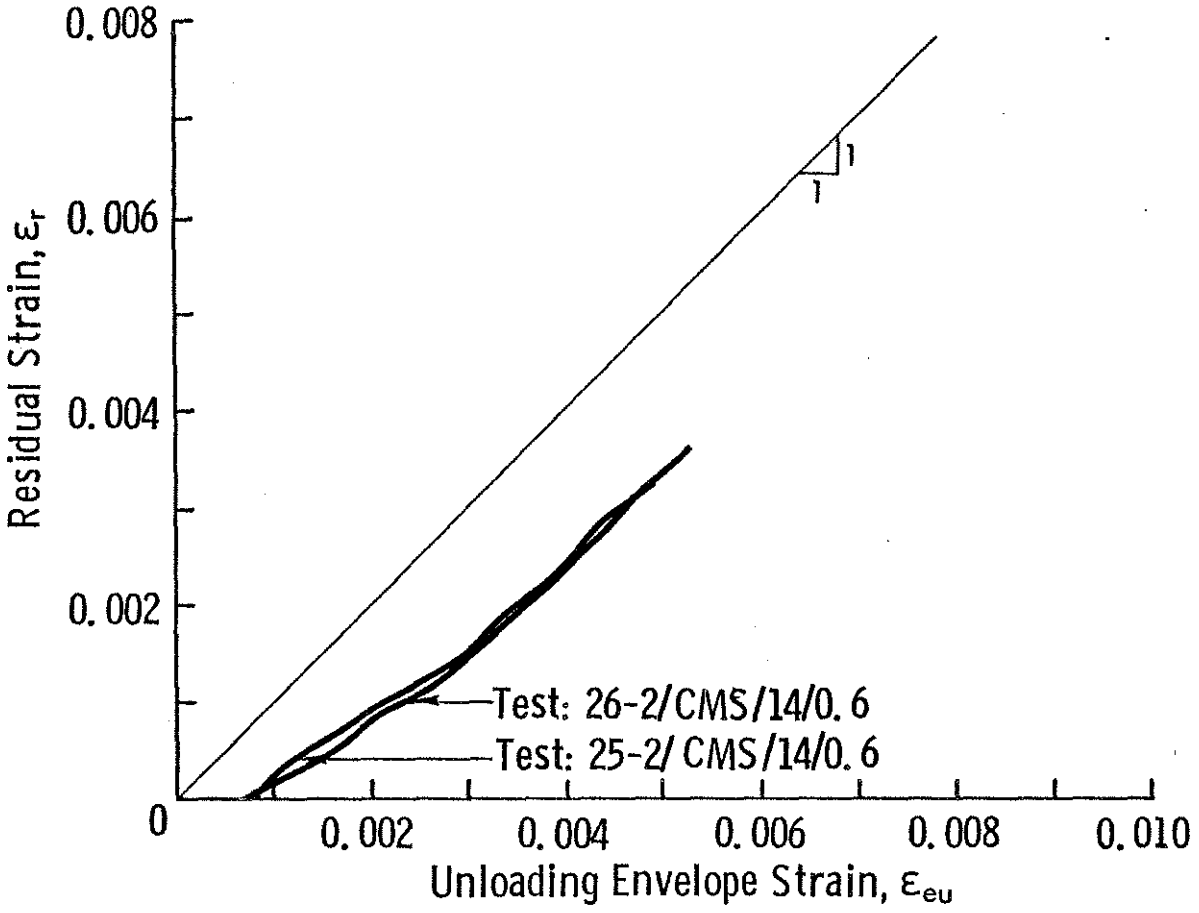

(b)

Fig. 3.4 Residual Strain versus Unloading Strain for Cycles to a Constant Maximum Strain (First Cycle) (cont'd)

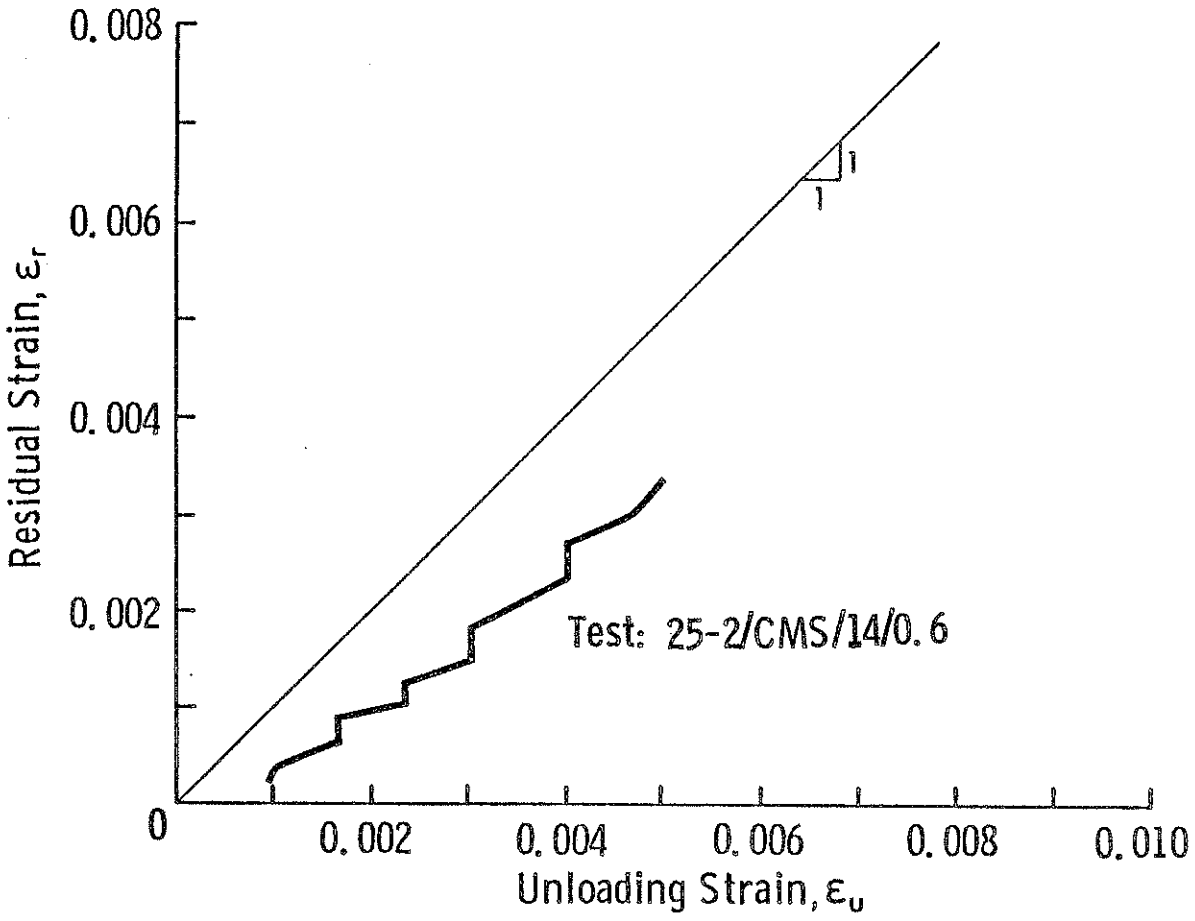

Fig. 3.5 Residual Strain versus Unloading Strain for Cycles to a Constant Maximum Strain

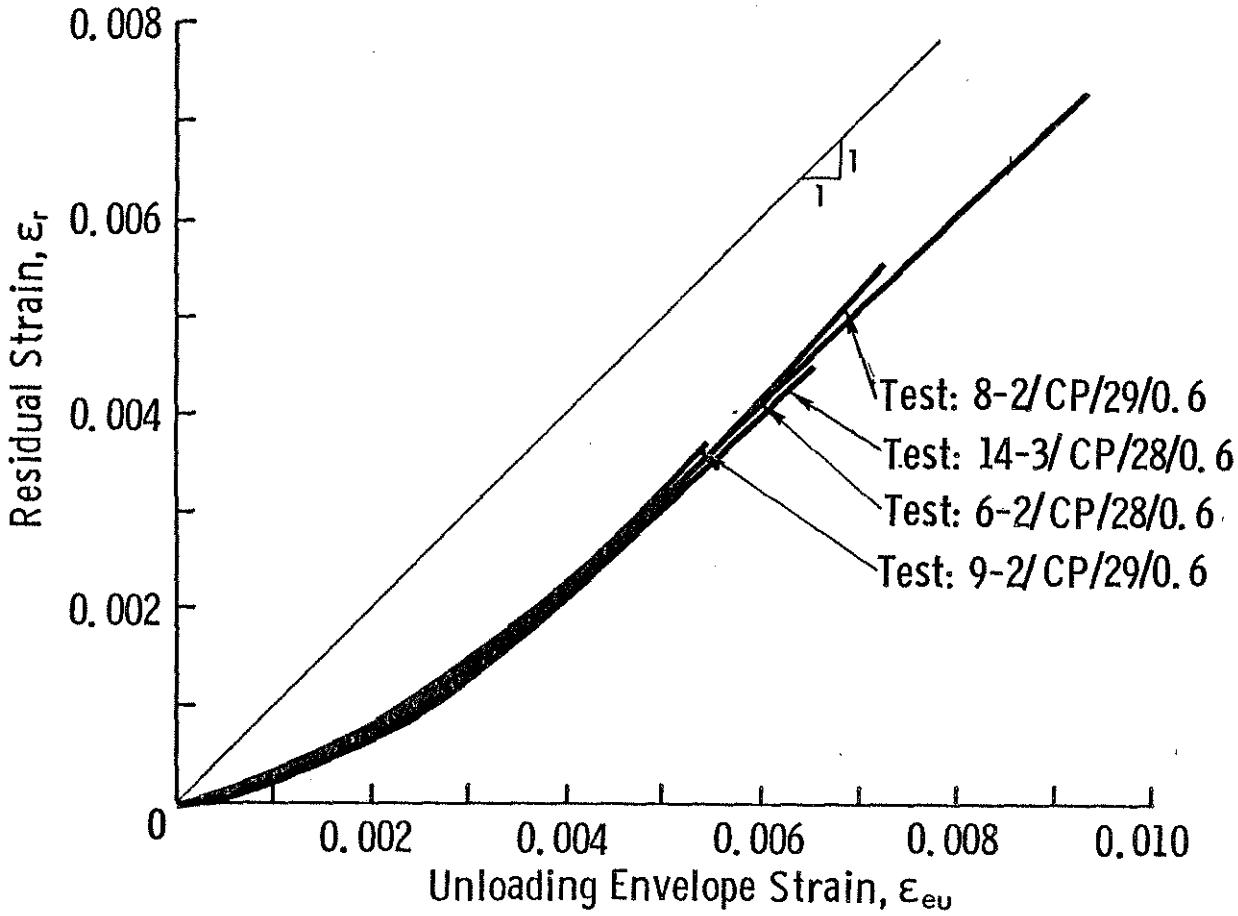

Fig. 3.6 Residual Strain versus Unloading Strain for Cycles to Common Points (First Cycle)

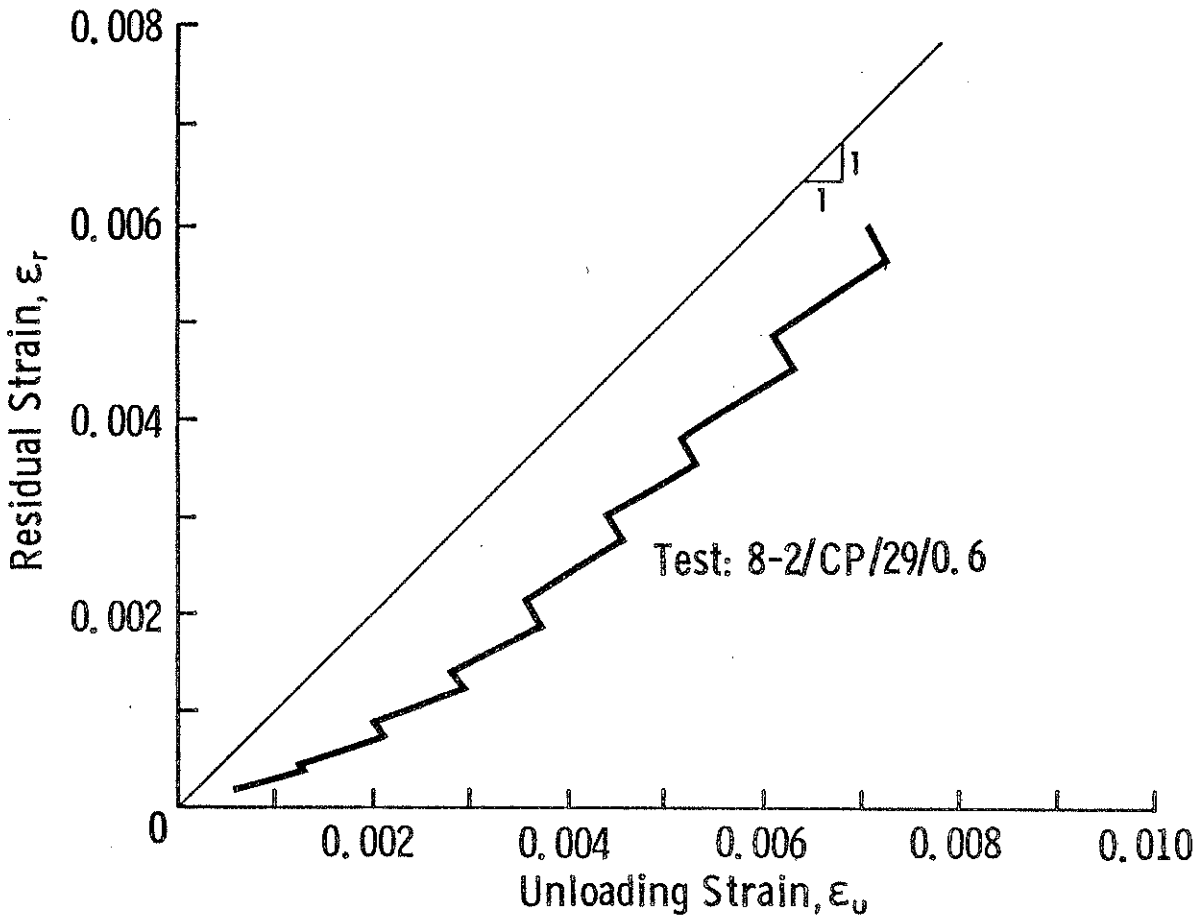

Fig. 3.7 Residual Strain versus Unloading Strain for Cycles to Common Points

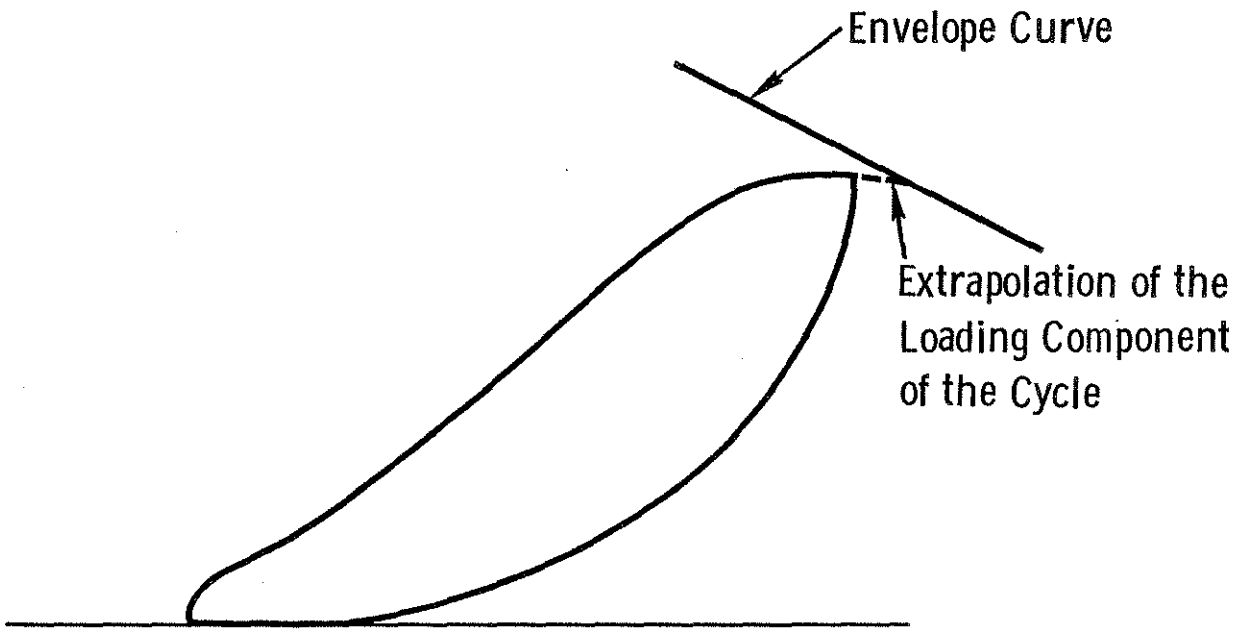

Fig. 3.8 Extrapolation of the Reloading Portion of a Cycle to Obtain the Reloading Envelope Strain

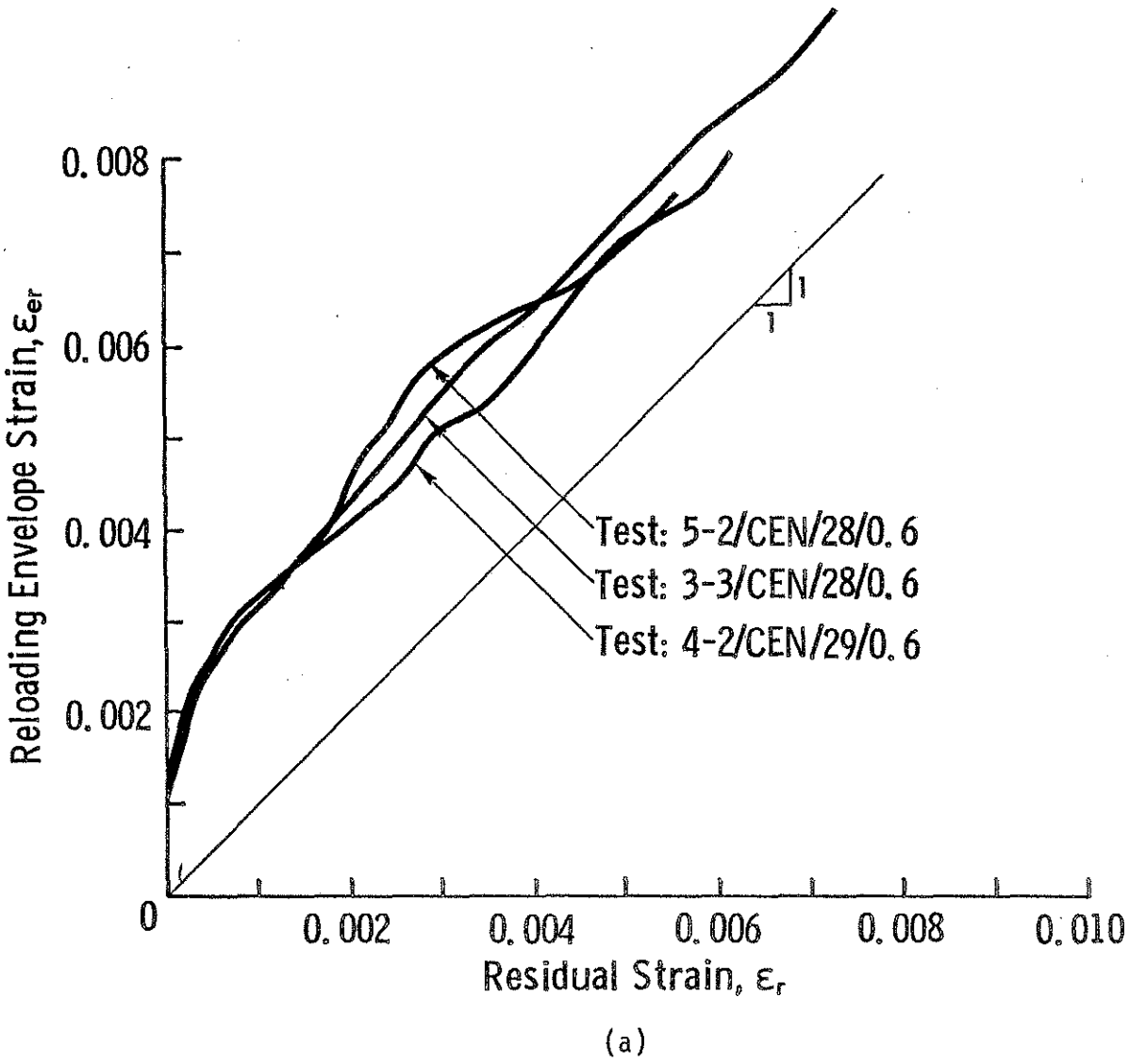

(a)

Fig. 3.9 Residual Strain versus Reloading Envelope Strain for Cycles to the Envelope

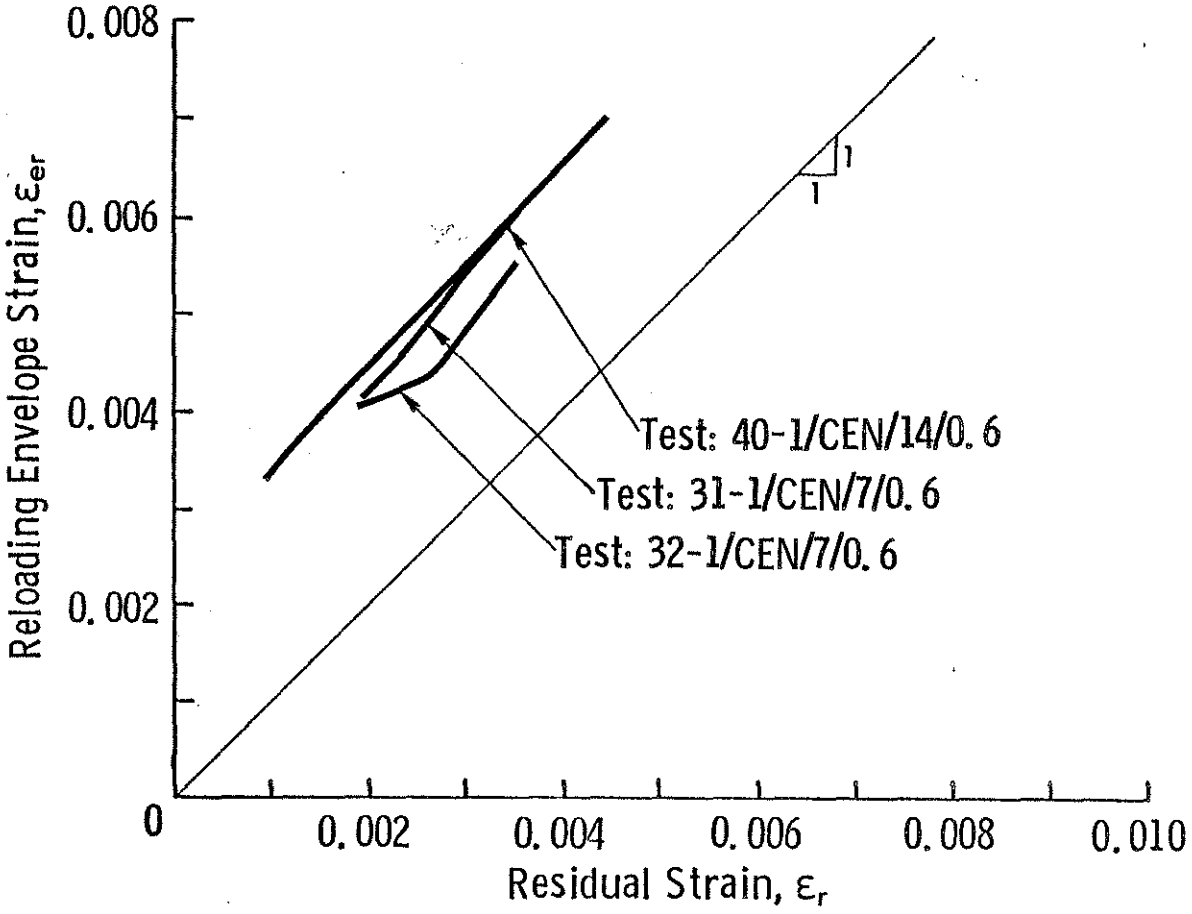

(b)

Fig. 3.9 Residual Strain versus Reloading Envelope Strain for Cycles to the Envelope (cont'd)

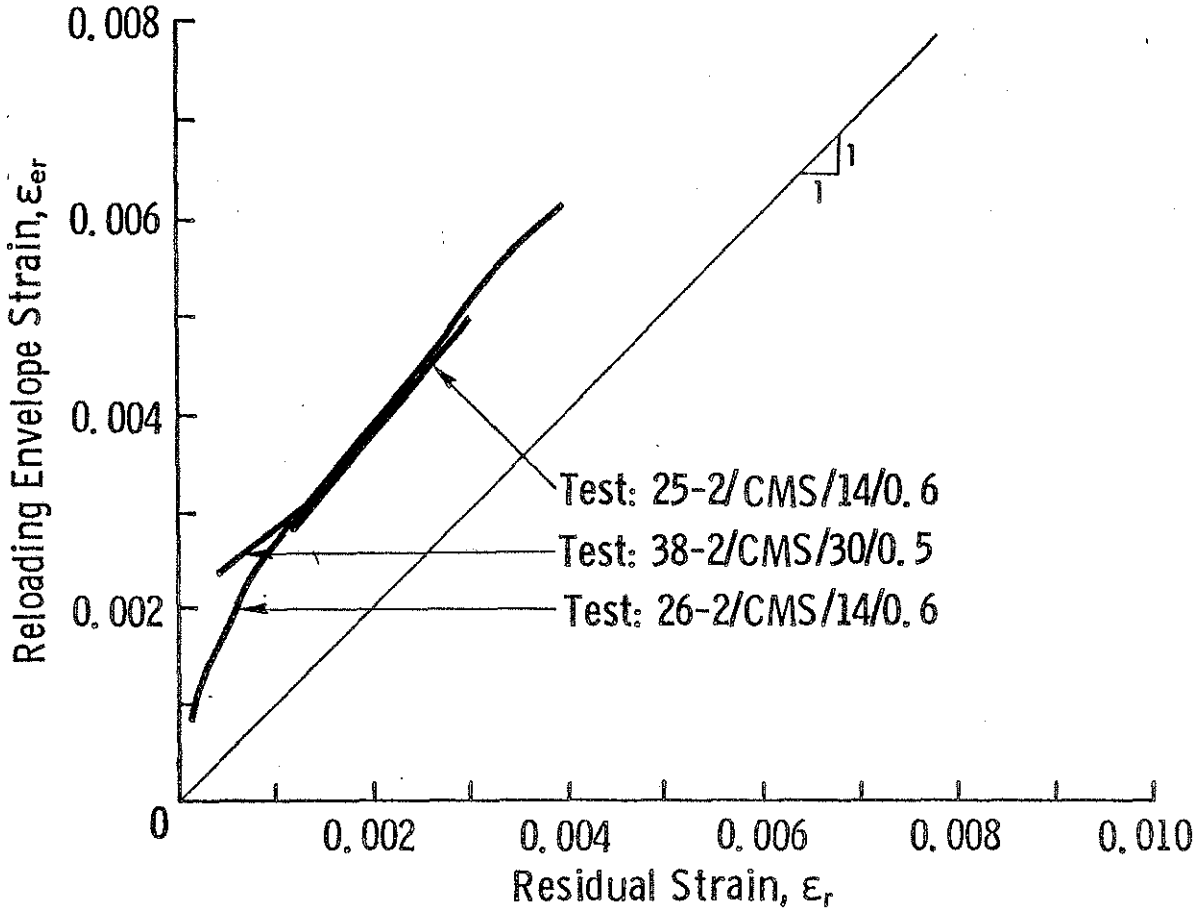

Fig. 3.10 Residual Strain versus Reloading Envelope Strain for Cycles to a Constant Maximum Strain

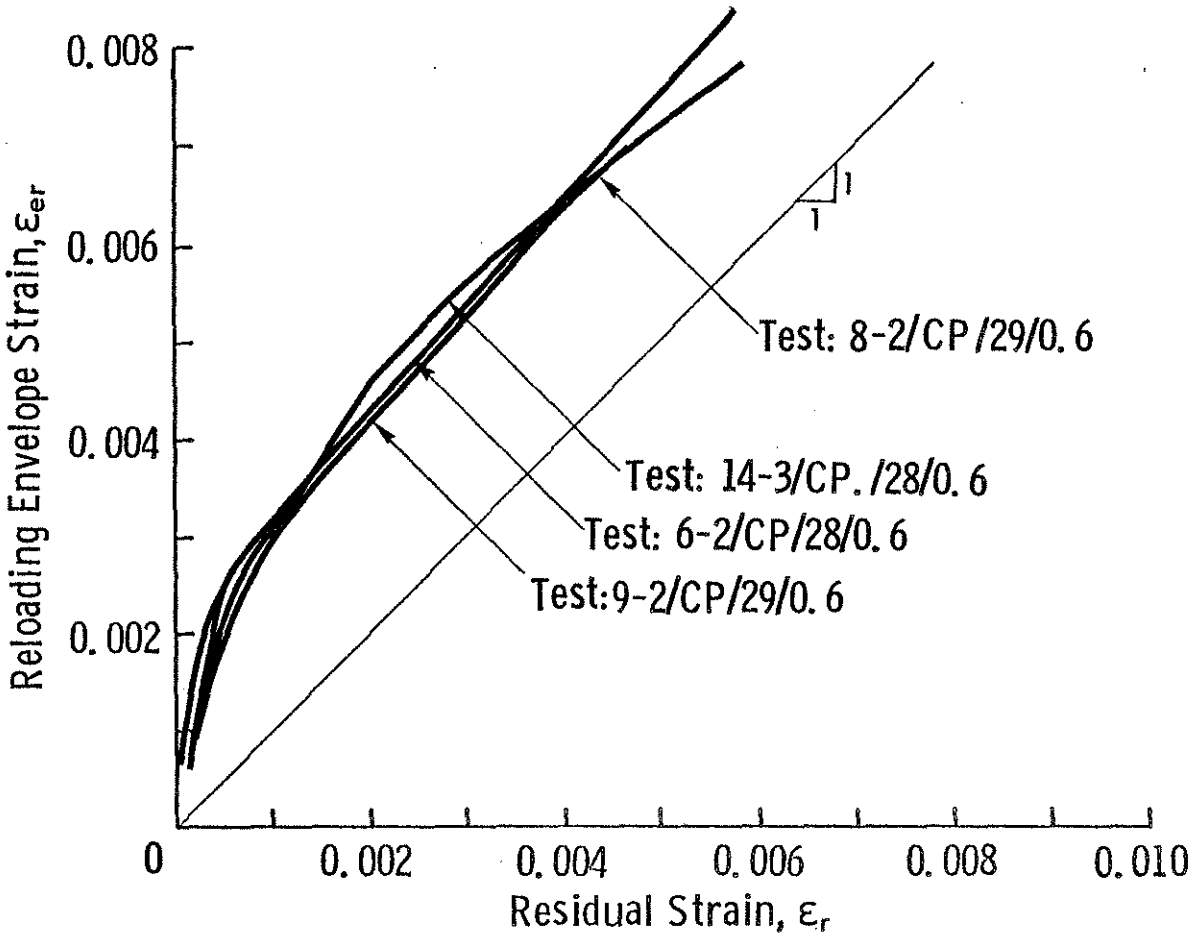

Fig. 3.11 Residual Strain versus Reloading Envelope Strain for Cycles to Common Points

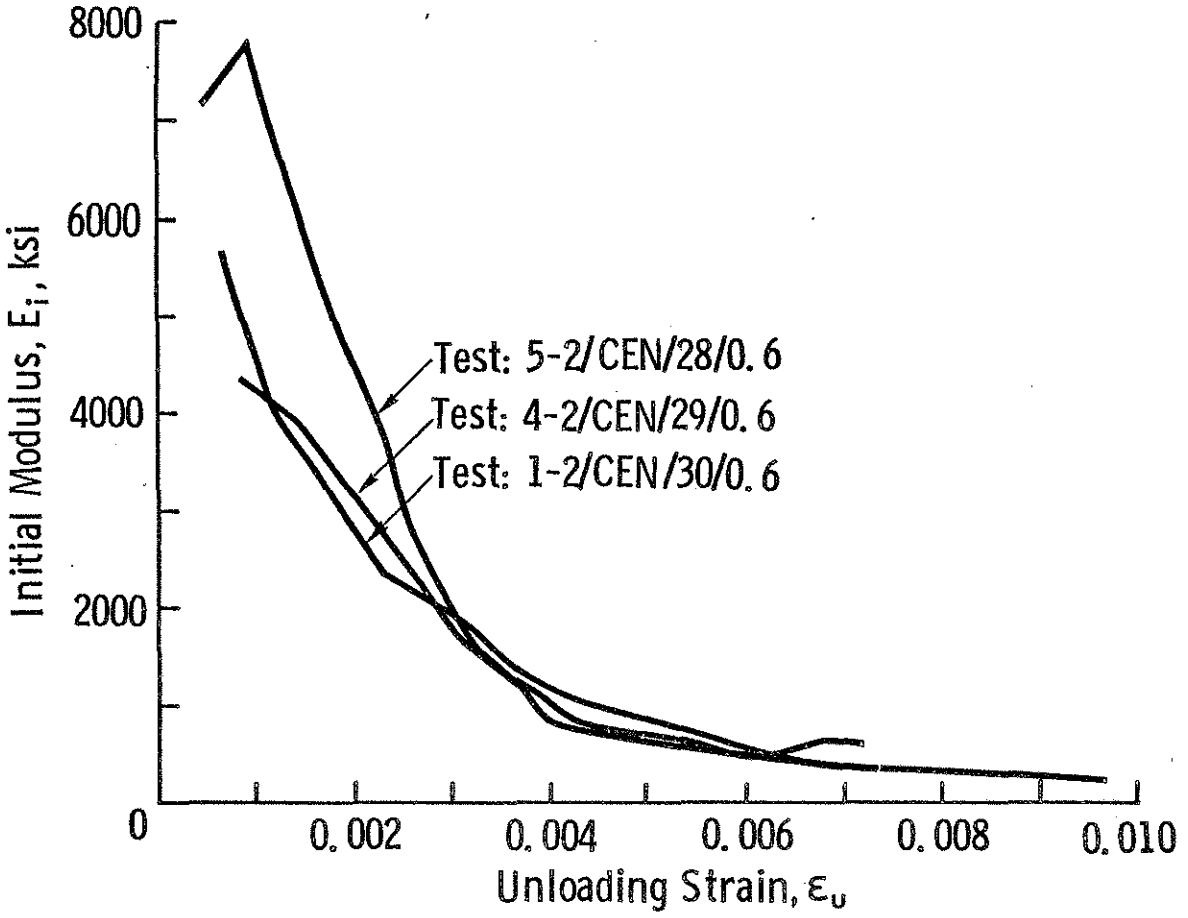

Fig. 3.12 Initial Modulus of Elasticity versus Unloading Envelope Strain for Cycles to the Envelope

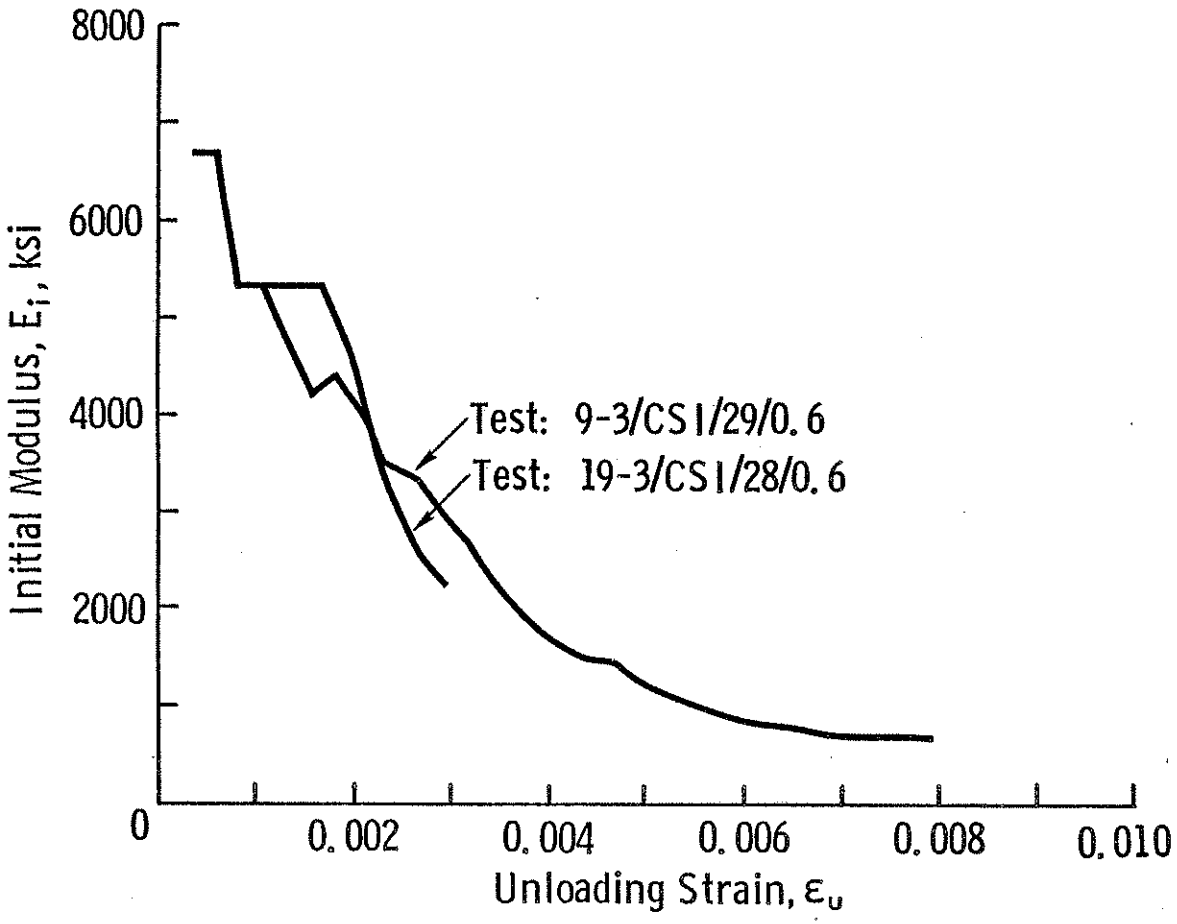

Fig. 3.13 Initial Modulus of Elasticity versus Unloading Strain for Cycles with a Constant Strain Increment

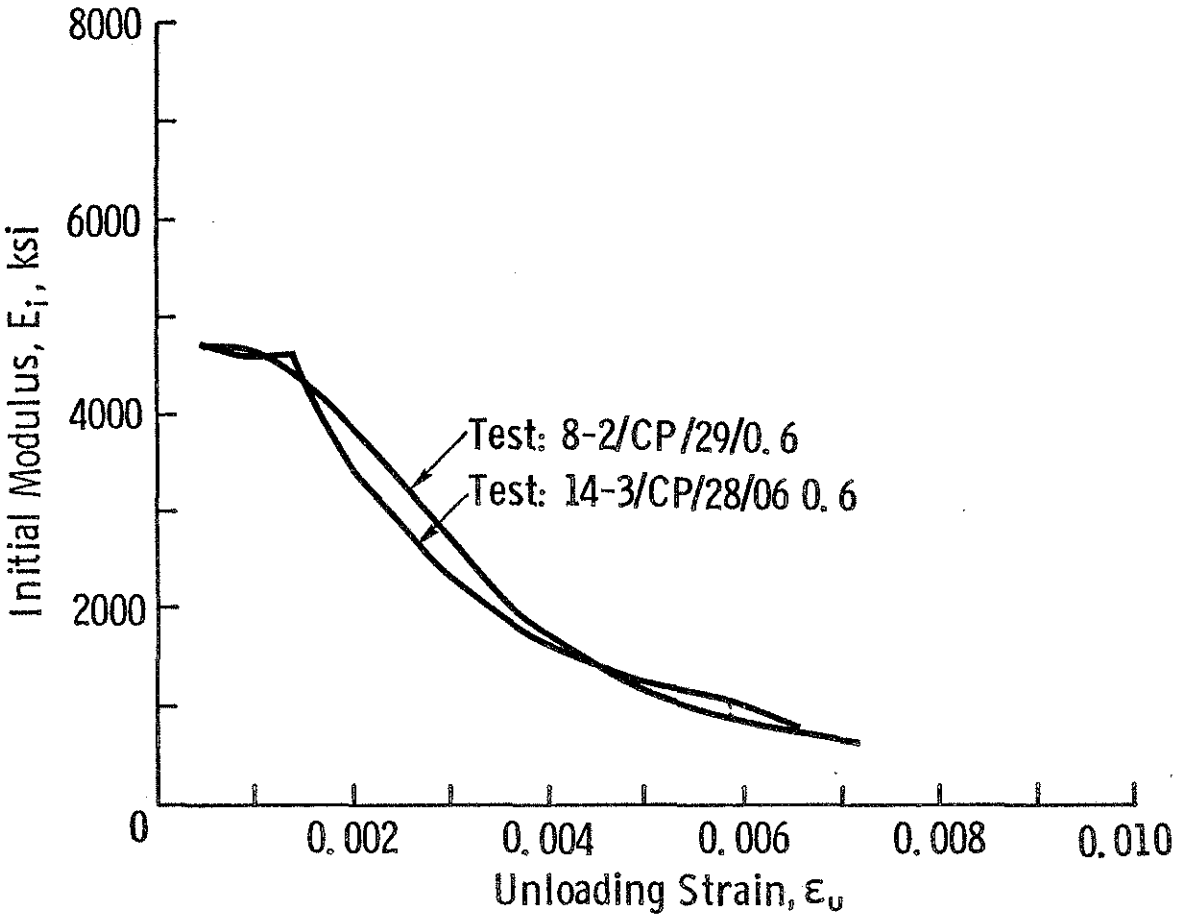

Fig. 3.14 Initial Modulus of Elasticity versus Unloading Envelope Strain for Cycles to Common Points

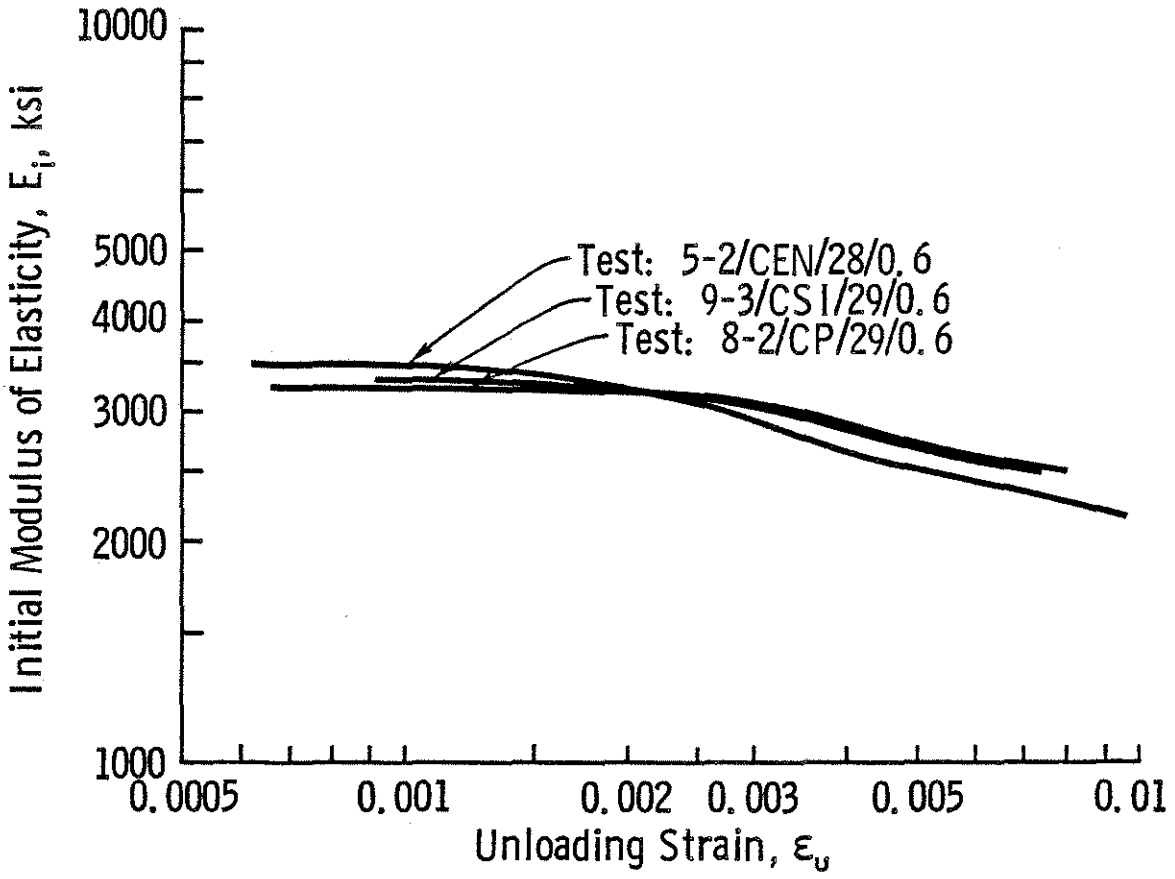

Fig. 3.15 Log-log Plot of Initial Modulus of Elasticity versus Unloading Strain for a Number of Loading Regimes

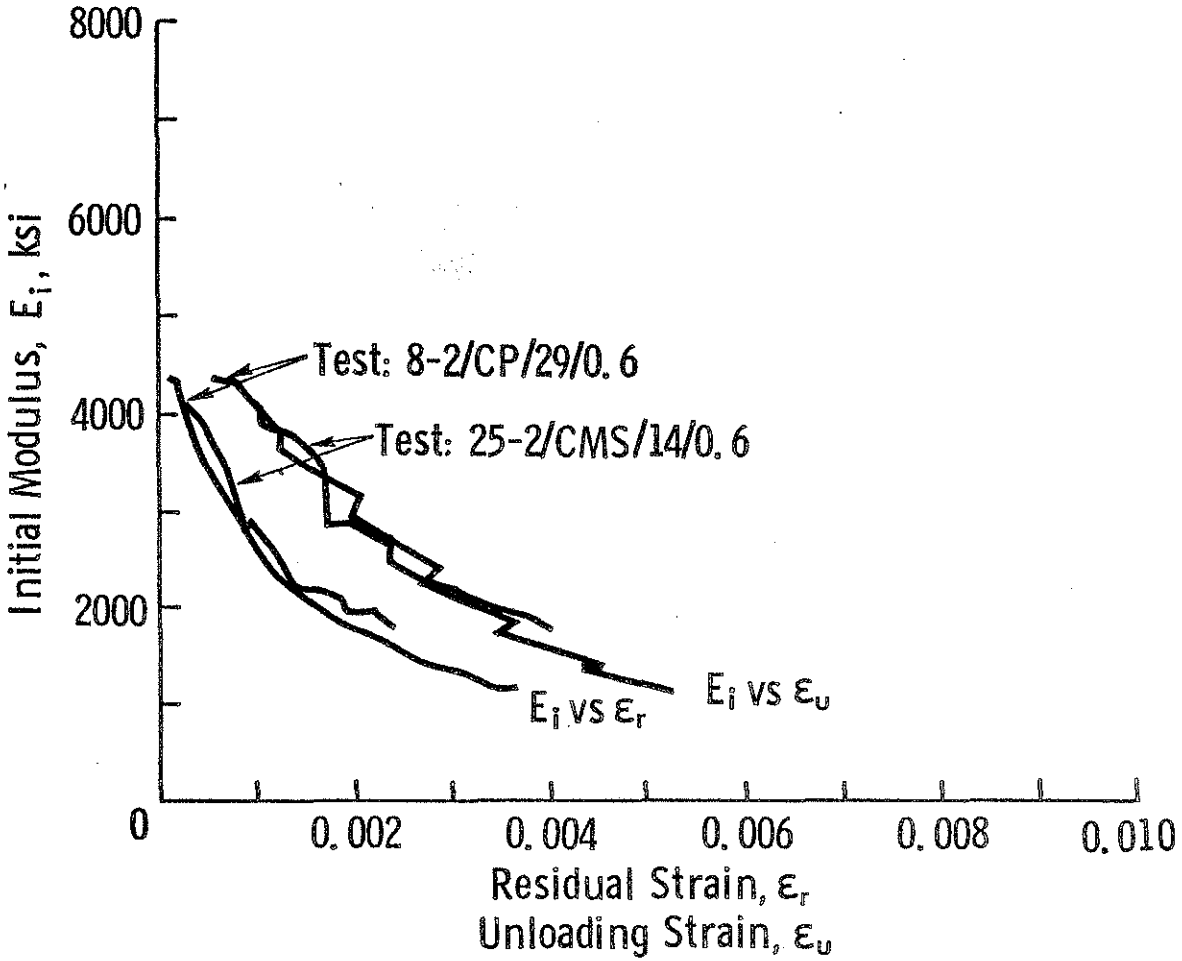

Fig. 3.16 Initial Modulus of Elasticity versus Unloading Strain and Residual Strain for Cycles to a Constant Maximum Strain and Cycles to Common Points

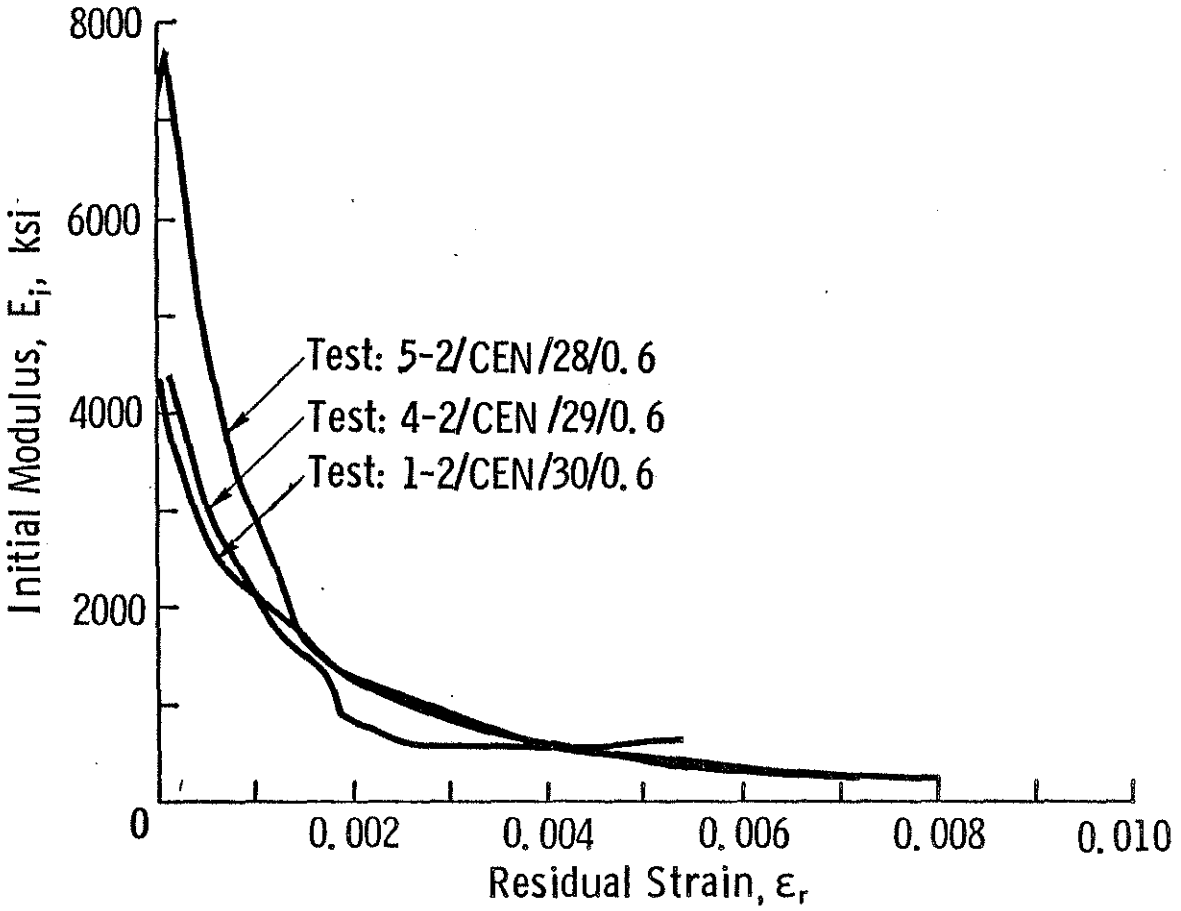

Fig. 3.17 Initial Modulus of Elasticity versus Residual Strain for Cycles to the Envelope

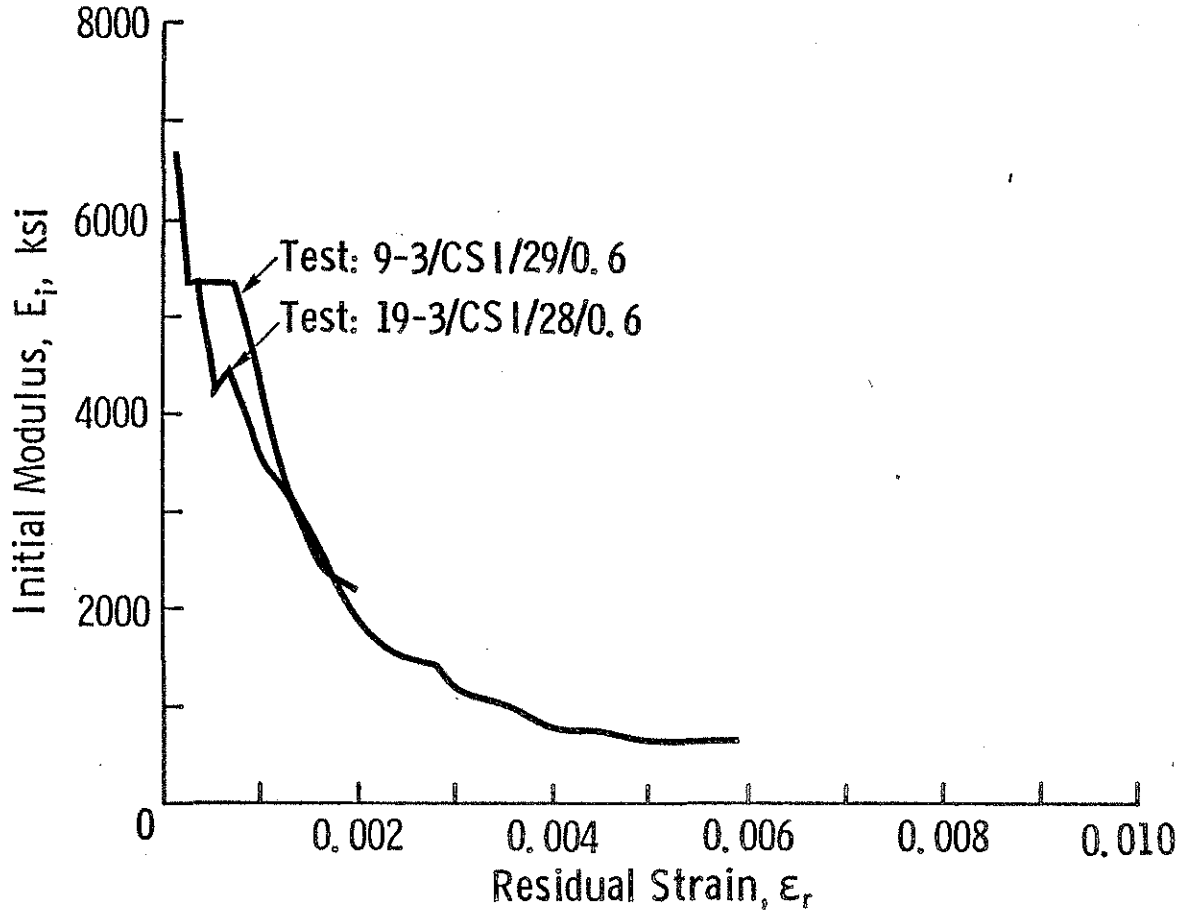

Fig. 3.18 Initial Modulus of Elasticity versus Residual Strain for Cycles with a Constant Strain Increment

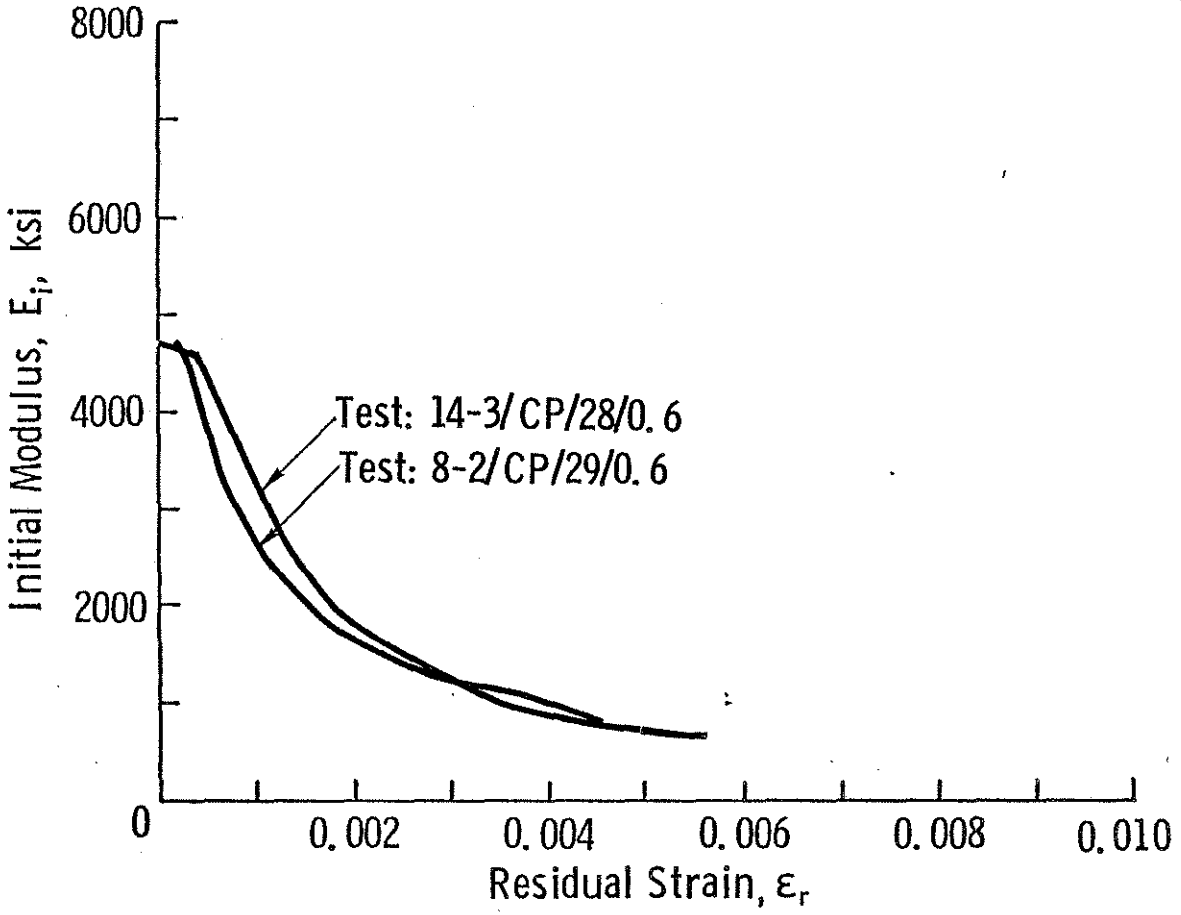

Fig. 3.19 Initial Modulus of Elasticity versus Residual Strain for Cycles to Common Points

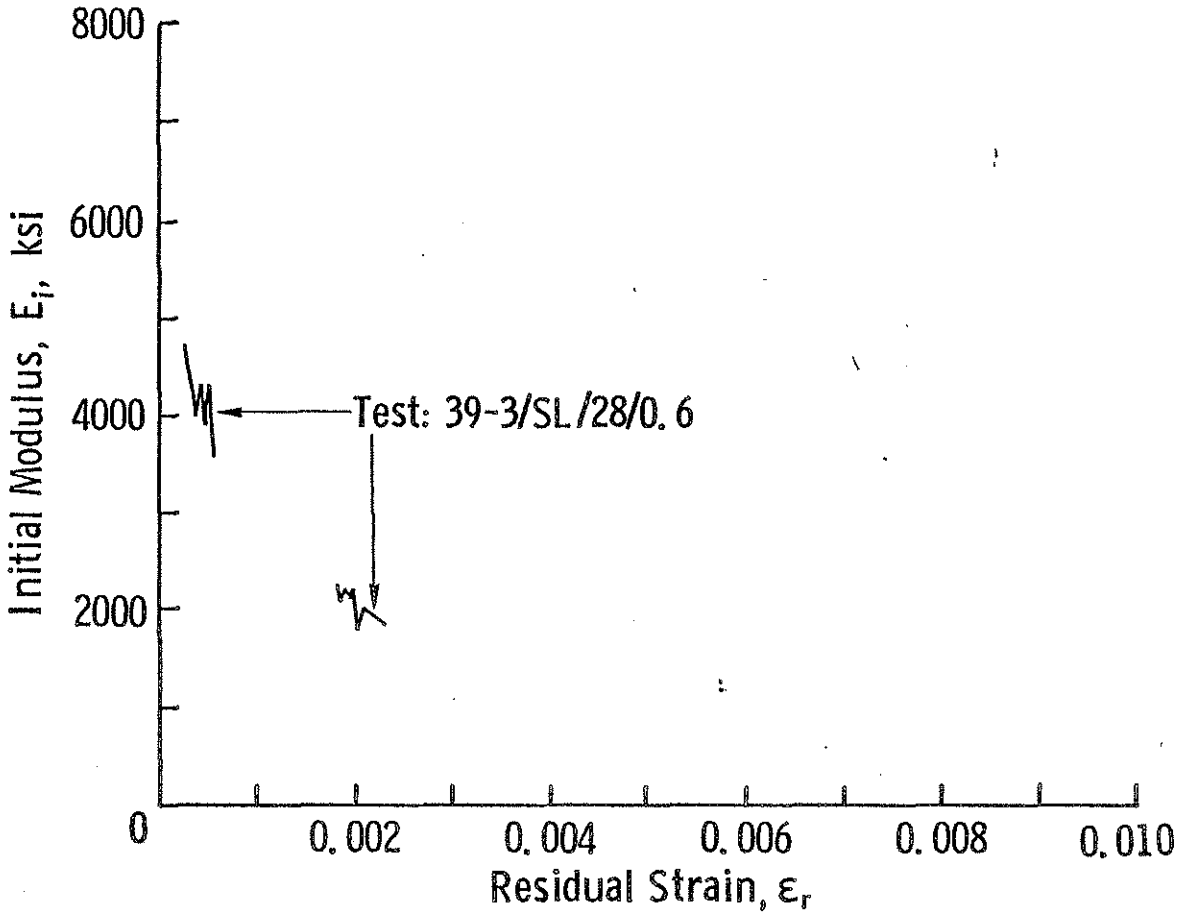

Fig. 3.20 Initial Modulus of Elasticity versus Residual Strain for Cycles between Fixed Stresses

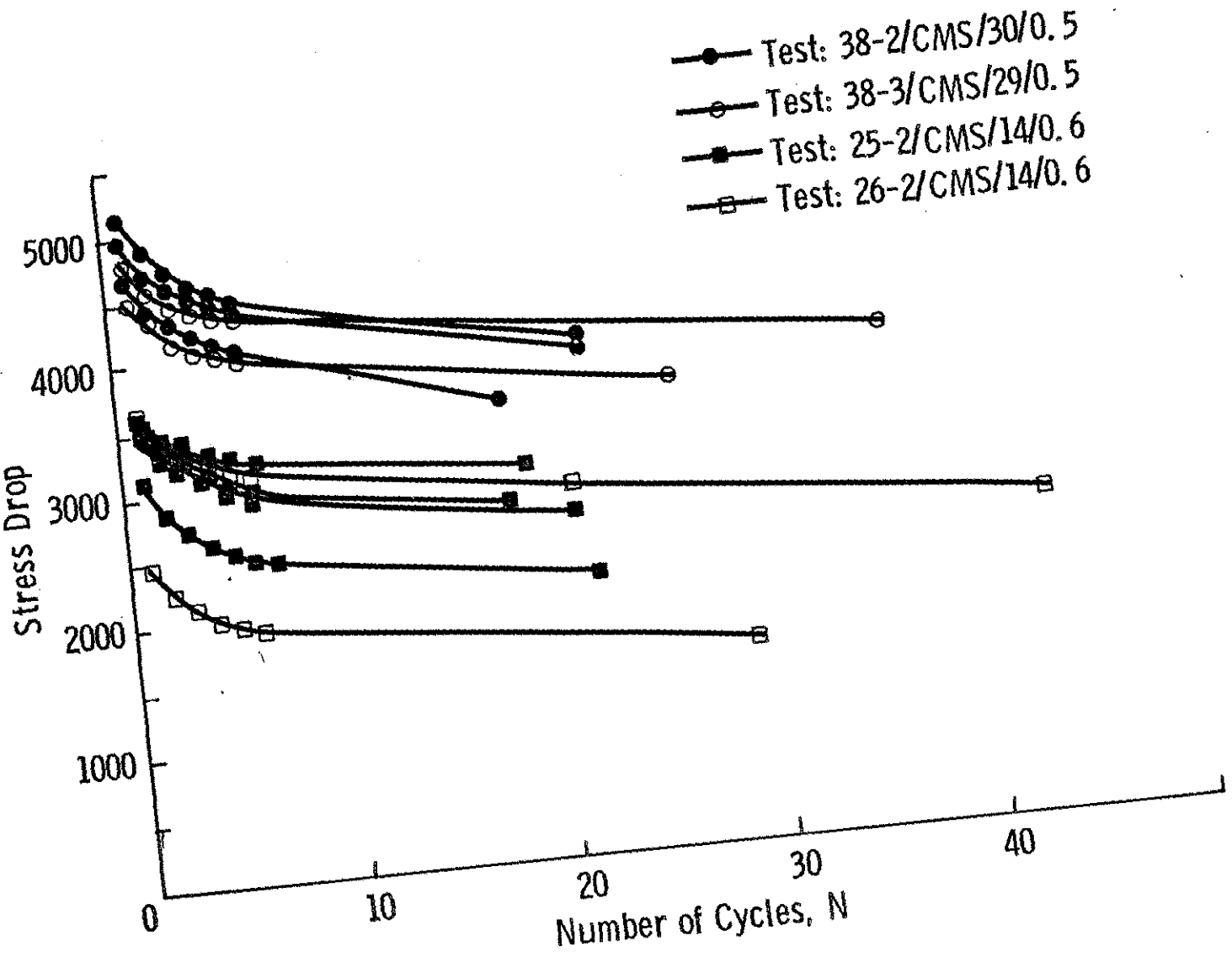

Fig. 3.21 Stress Drop versus Number of Cycles for Cycles to a Constant Maximum Strain

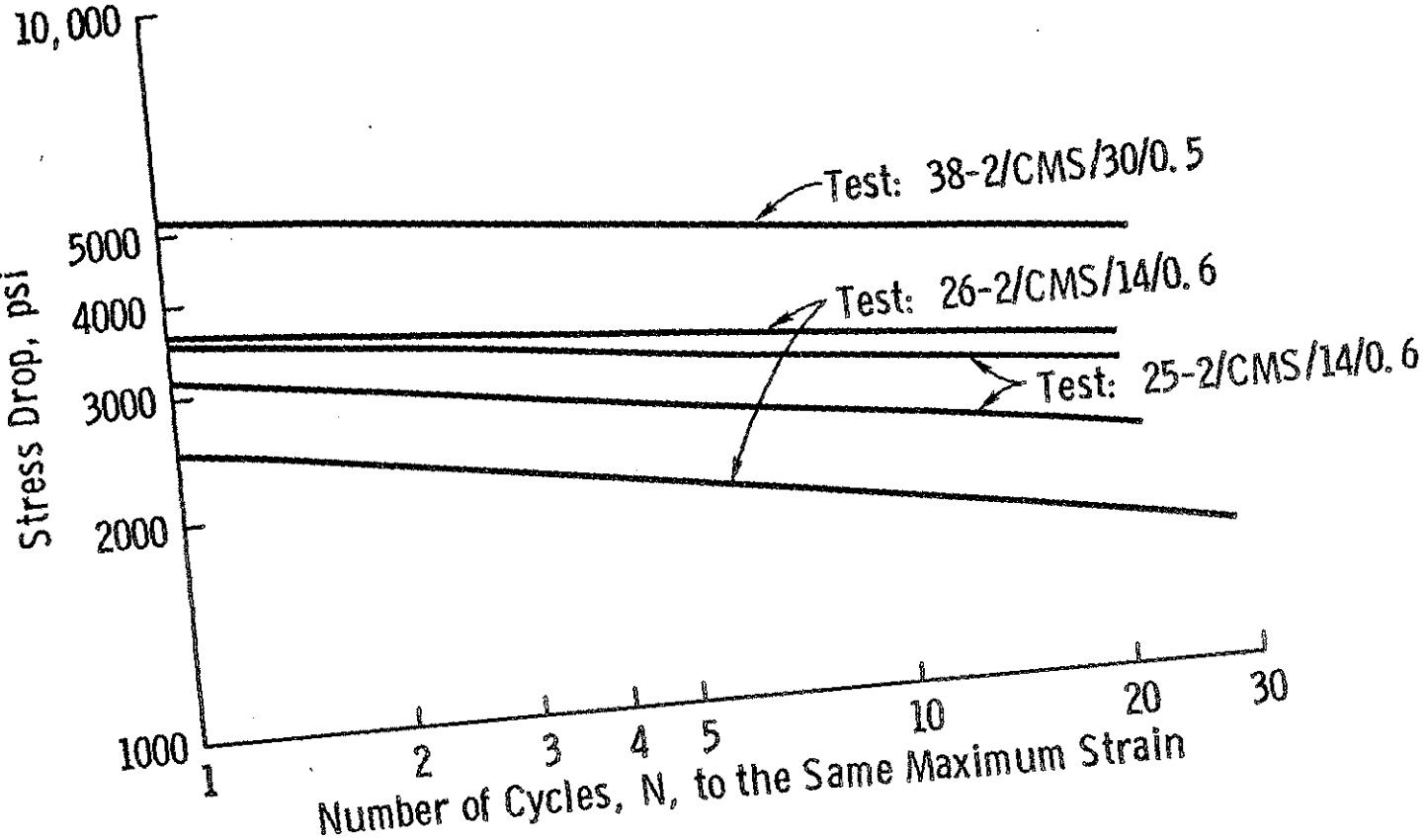

Fig. 3.22 Log-log Plot of Stress Drop versus Number of Cycles for Cycles to a Constant Maximum Strain

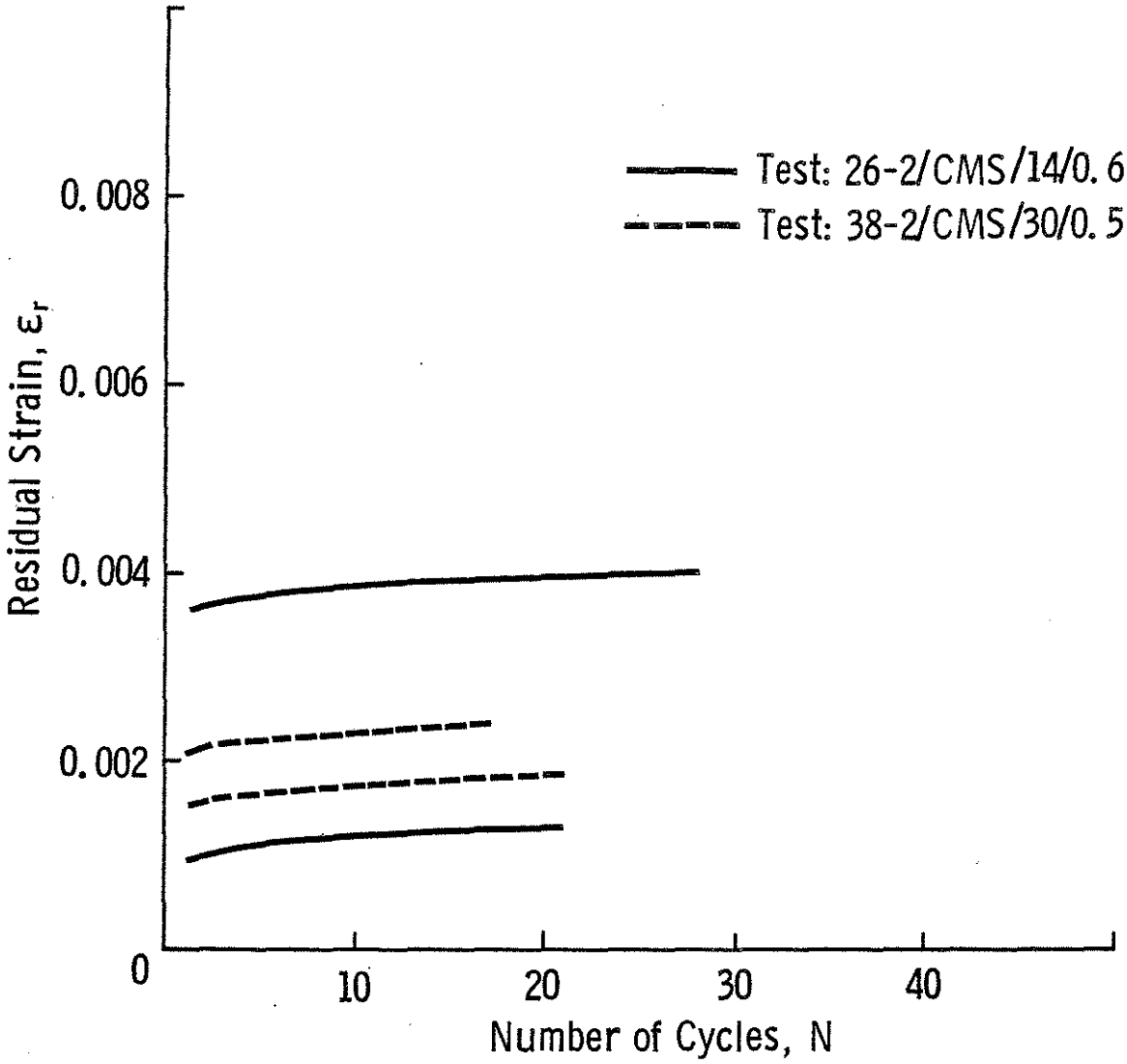

Fig. 3.23 Residual Strain versus Number of Cycles for Cycles to a Constant Maximum Strain

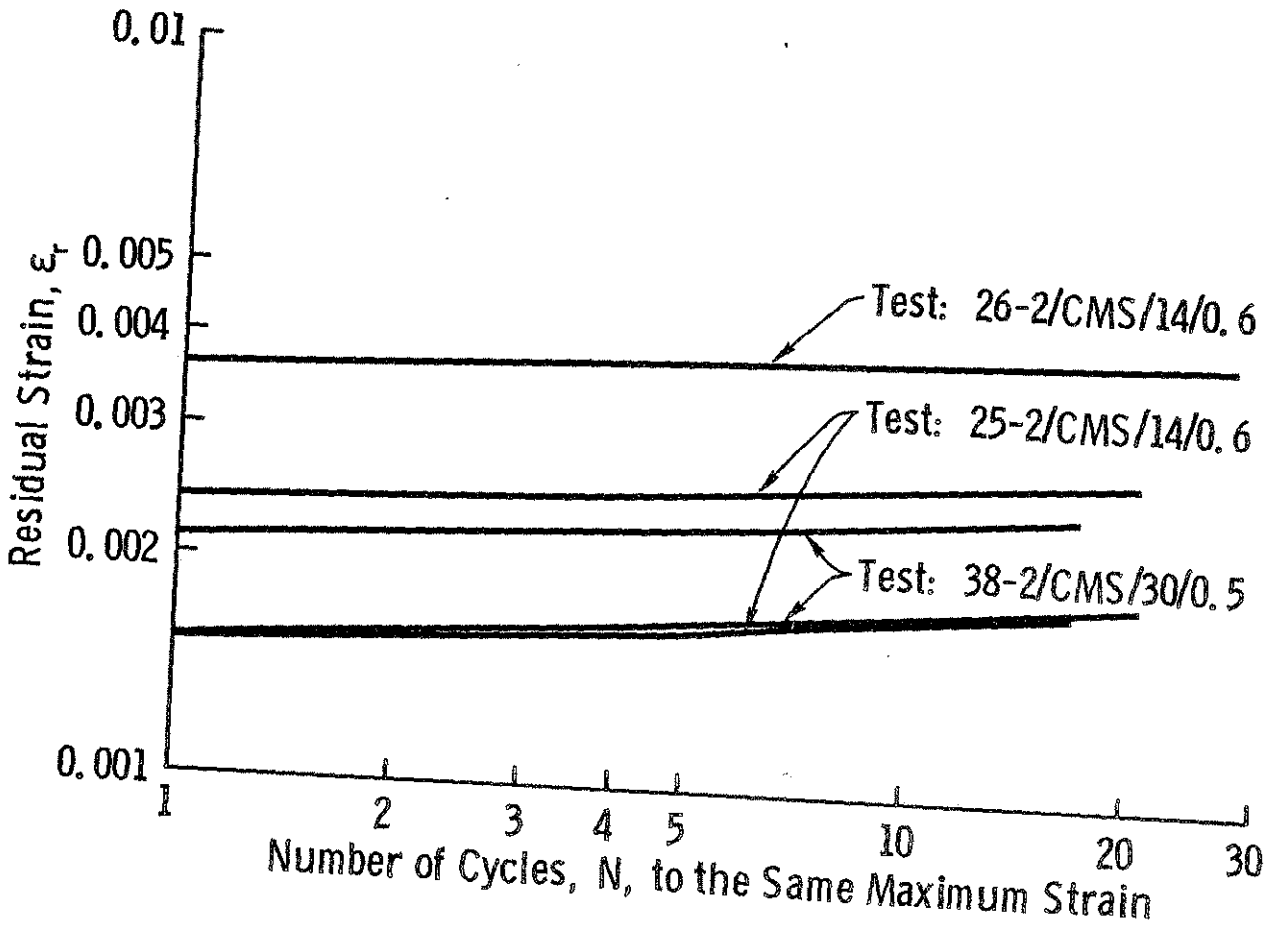

Fig. 3.24 Log-log Plot of Residual Strain versus Number of Cycles for Cycles to a Constant Maximum Strain

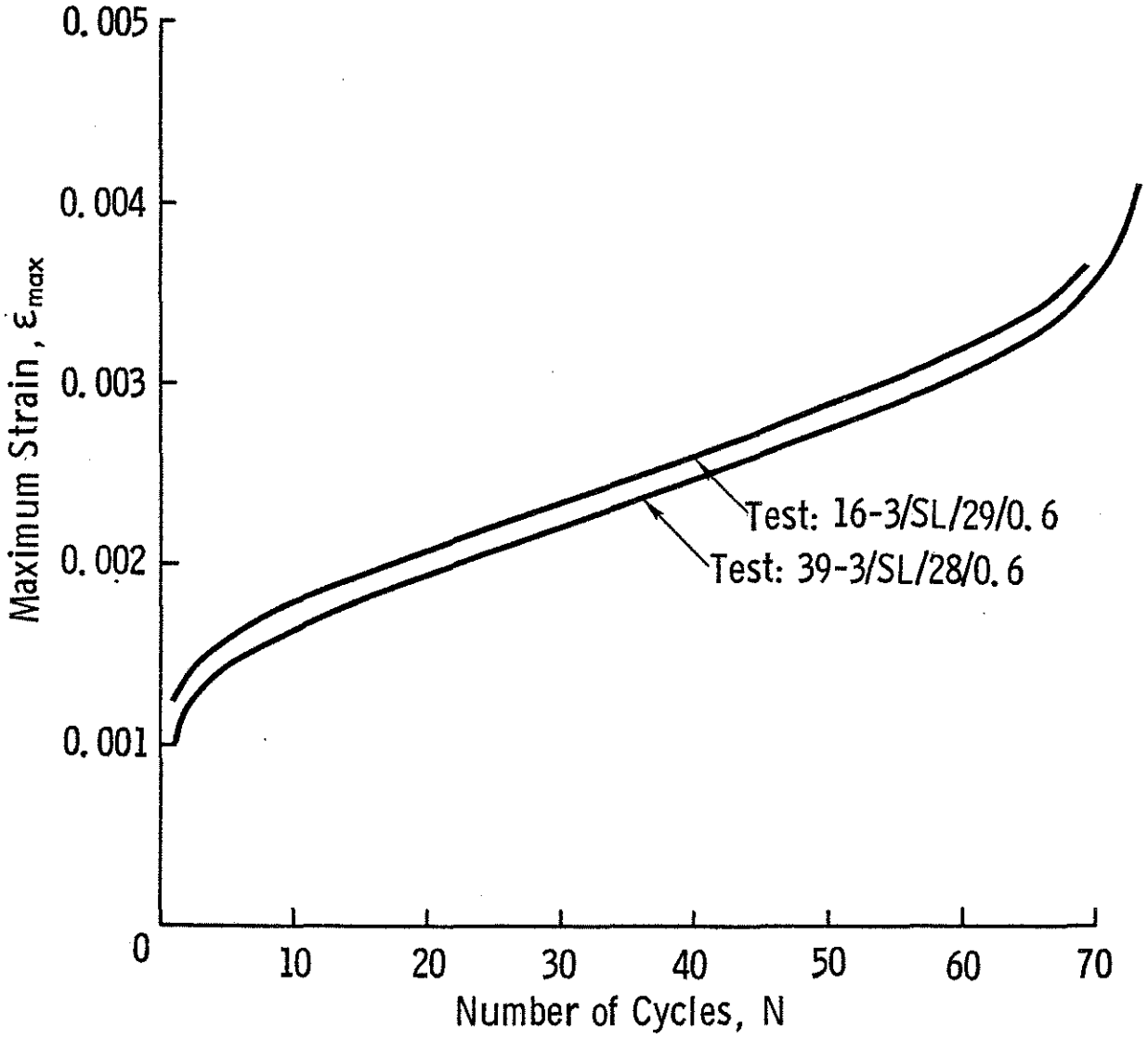

Fig. 3.25 Maximum Strain versus Number of Cycles for Cycles between Fixed Stresses

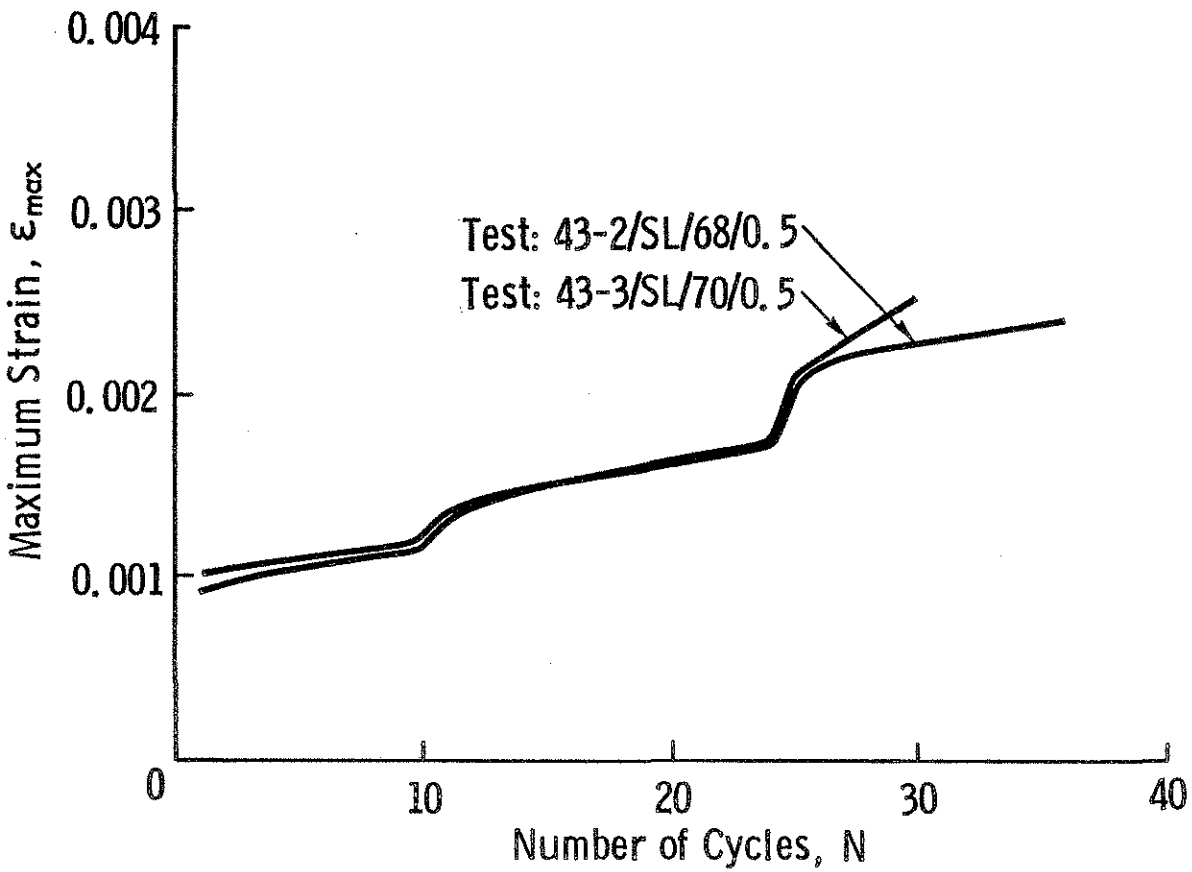

Fig. 3.26 Effect of Maximum and Minimum Stress on Maximum Strain versus Number of Cycles

Increase in Maximum Strain, $\Delta\varepsilon_u = 0.0005$
Increase in the Residual Strain, $\Delta\varepsilon_r = 0.0007$
Loading Component of Strain Range, $\Delta\varepsilon^r_l = 0.0023$
Unloading Component of Strain Range, $\Delta\varepsilon^r_u = 0.0015$
Strain Range, $\Delta\varepsilon^r = \Delta\varepsilon^r_l + \Delta\varepsilon^r_u = 0.0038$

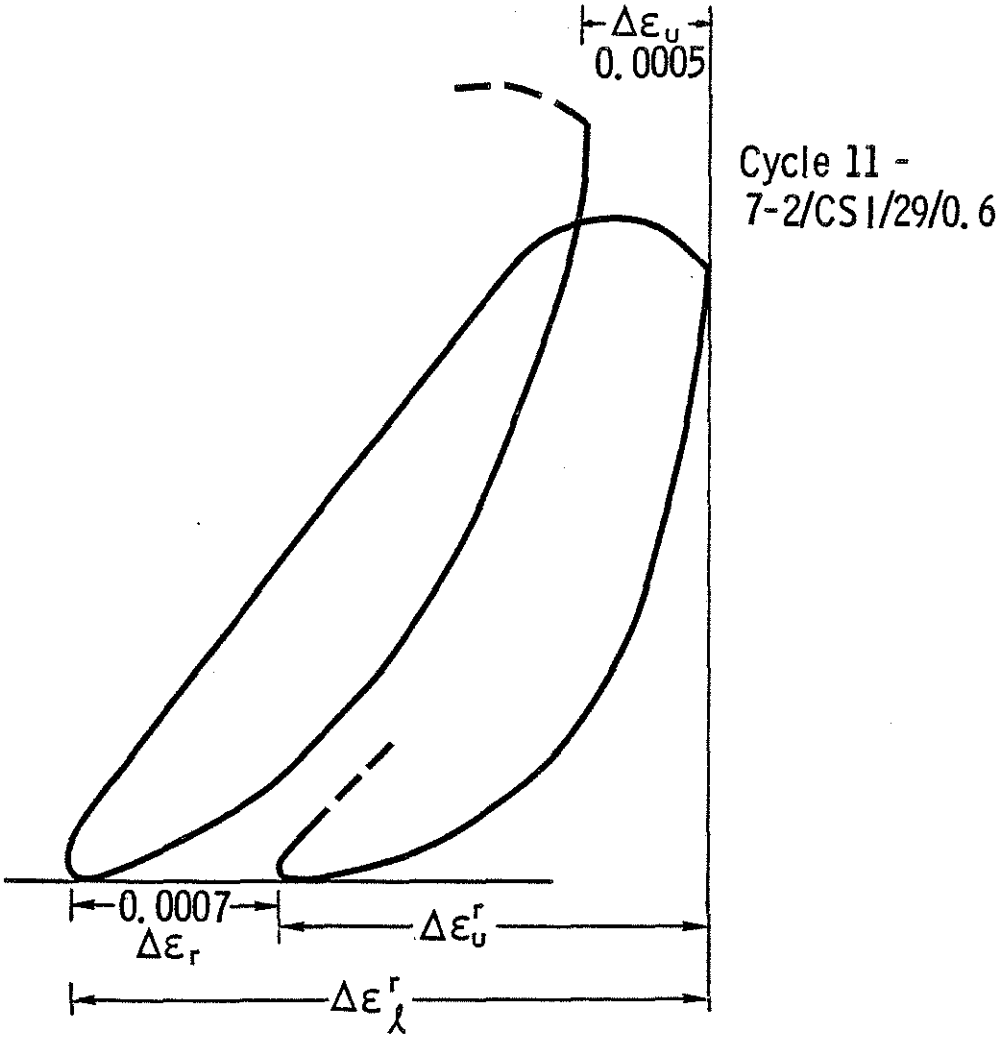

Fig. 3.27 Illustration of the Effect of Range of Strain in Controlling the Degradation of Mortar During Cyclic Loading

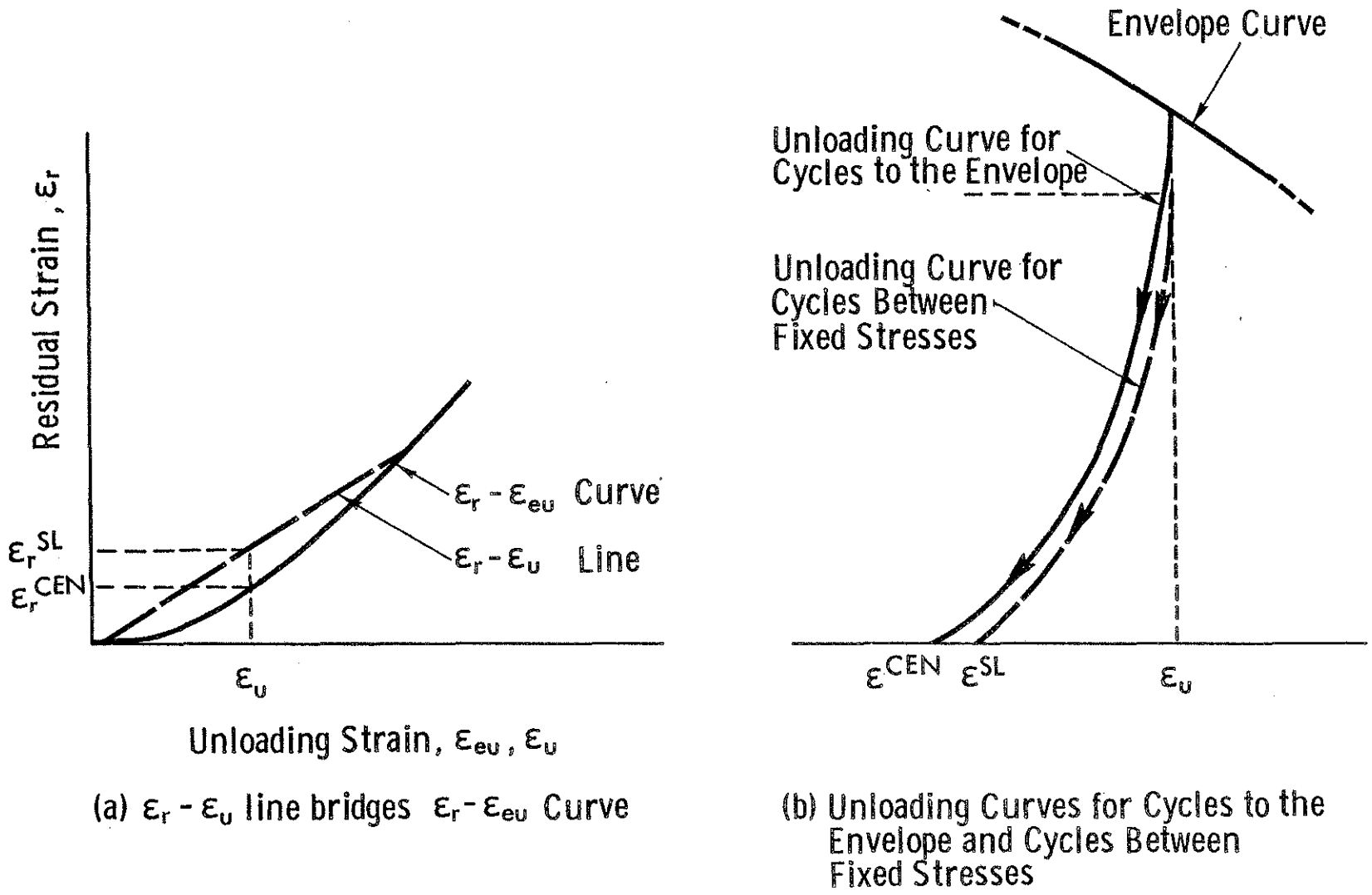

Fig. 3.28 Hypothetical Example Demonstrating that Residual Strain is Larger for Cycles between Fixed Stresses than for Cycles to the Envelope when Unloading from the Same Strain

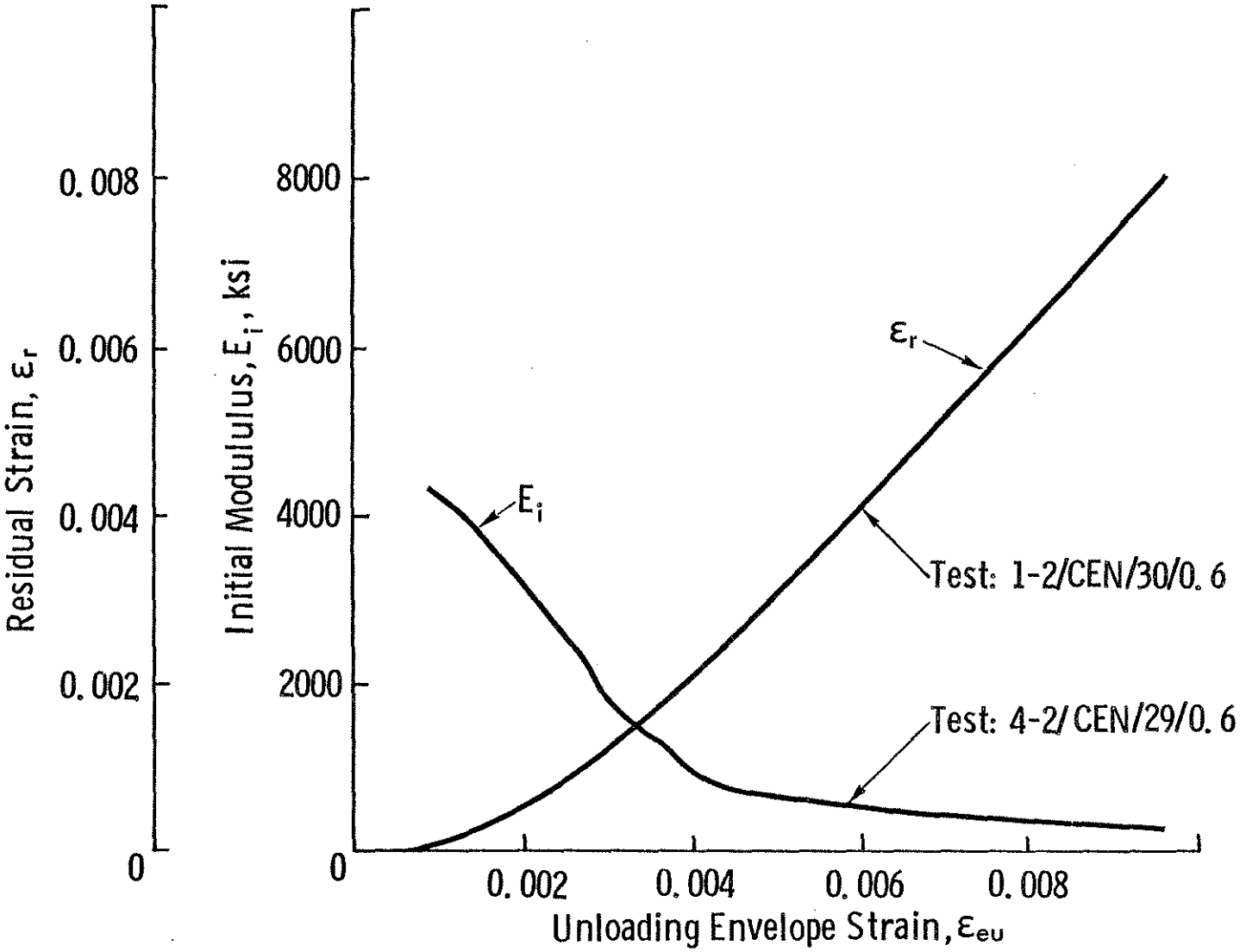

Fig. 3.29 Initial Modulus of Elasticity and Residual Strain versus Increasing Unloading Strain for Cycles to the Envelope

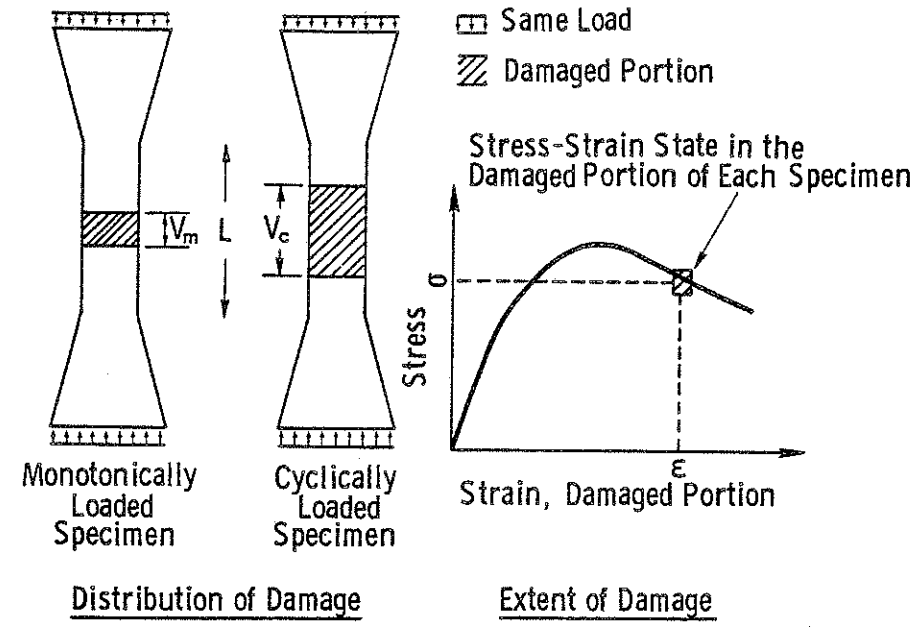

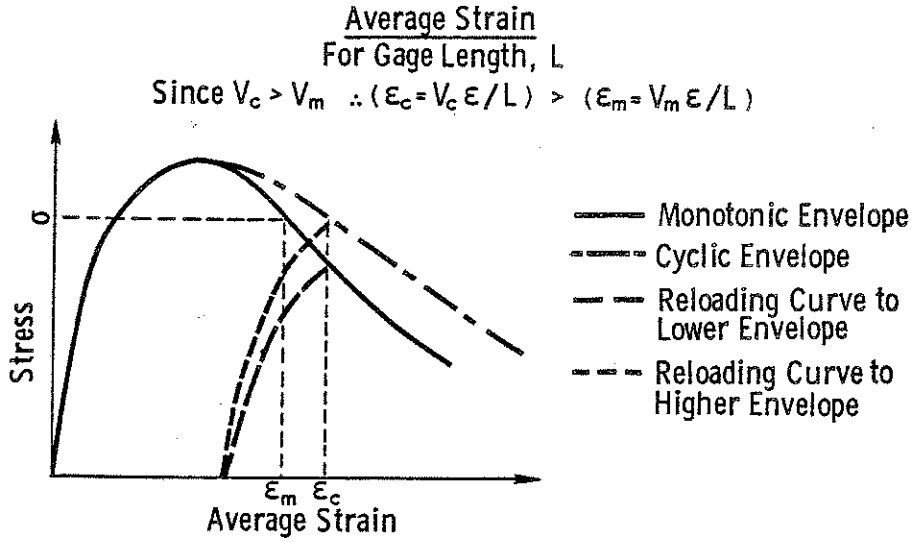

Fig. 3.30 Hypothetical Example Demonstrating the Dependence of the Shape of the Stress-Strain Envelope Upon the Distribution of Damage

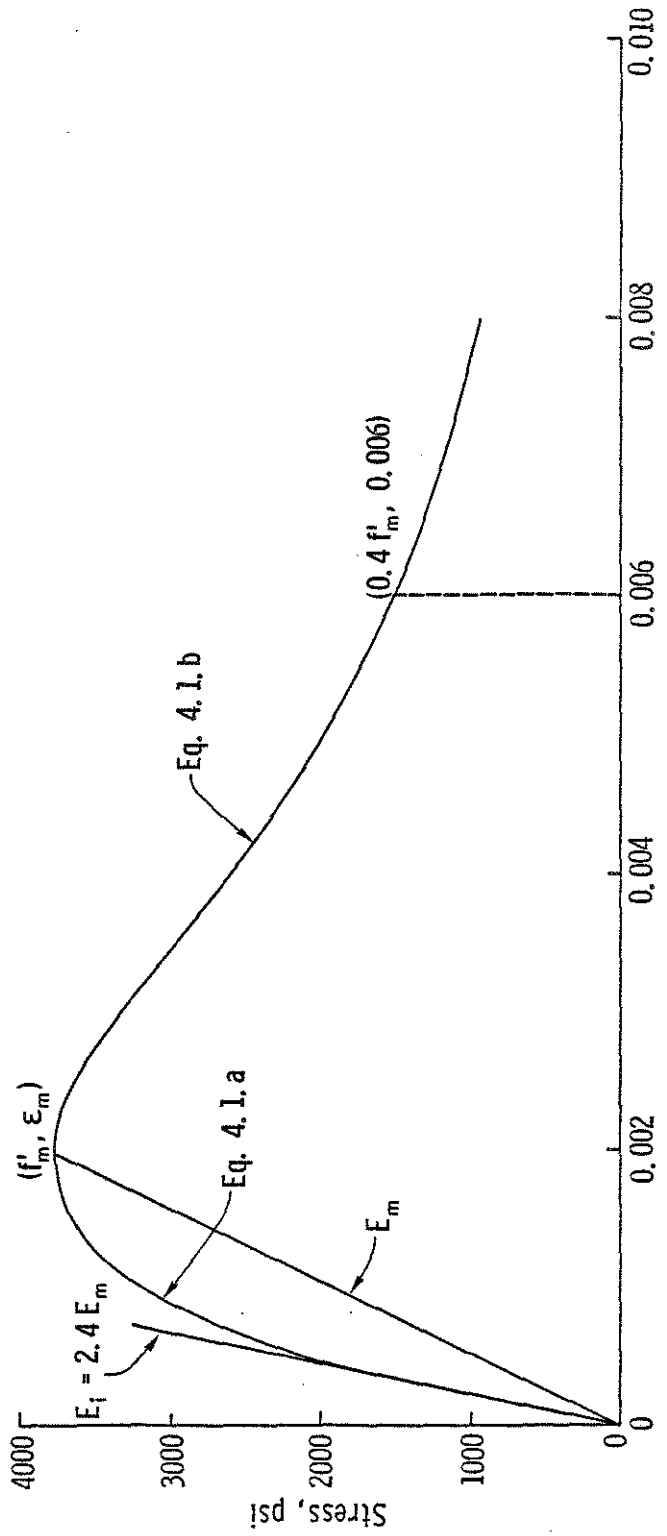

Fig. 4.1 Analytical Stress-Strain Envelope

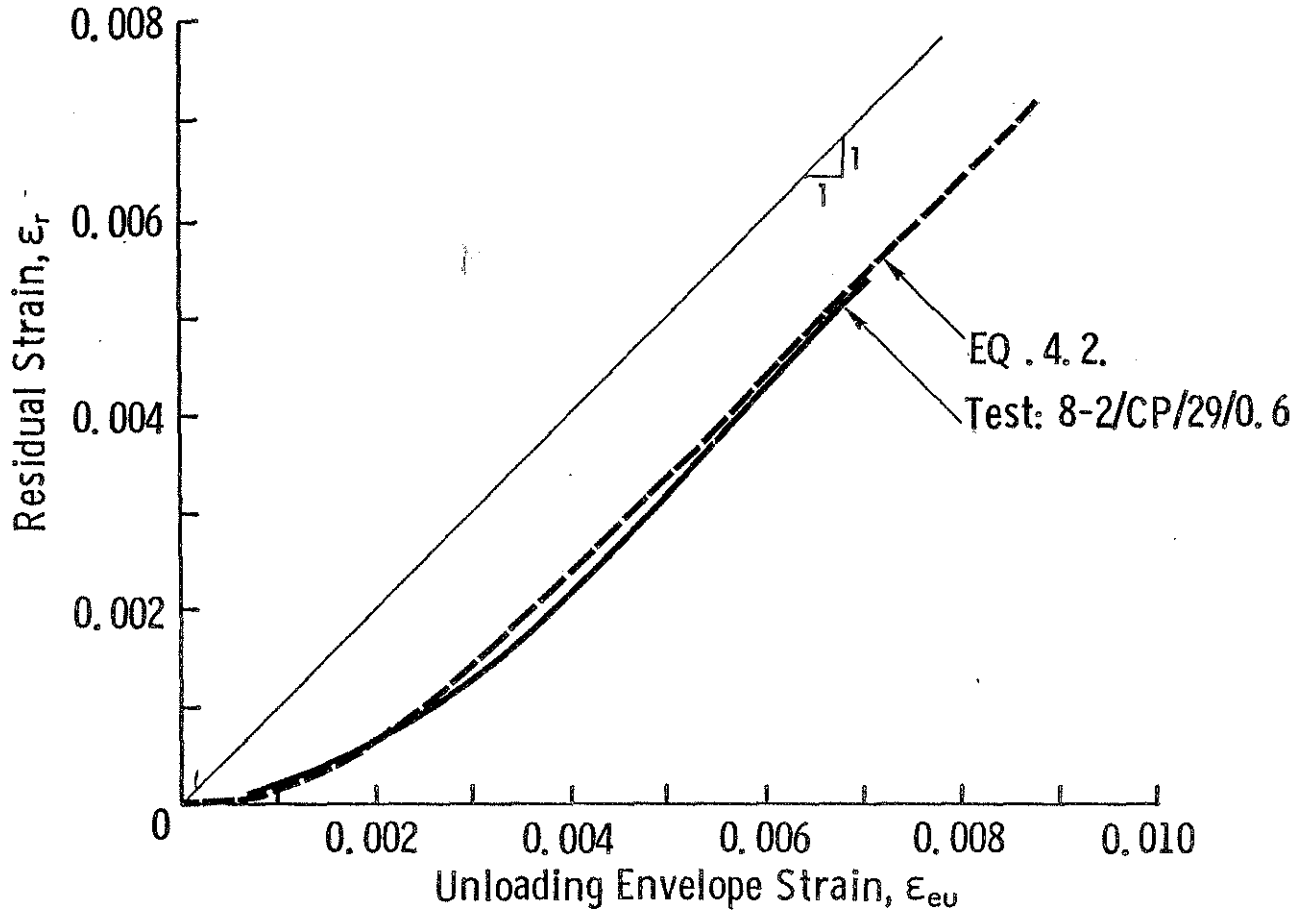

Fig. 4.2 Analytical Residual Strain versus Unloading Envelope Strain Relation Compared with Test Results

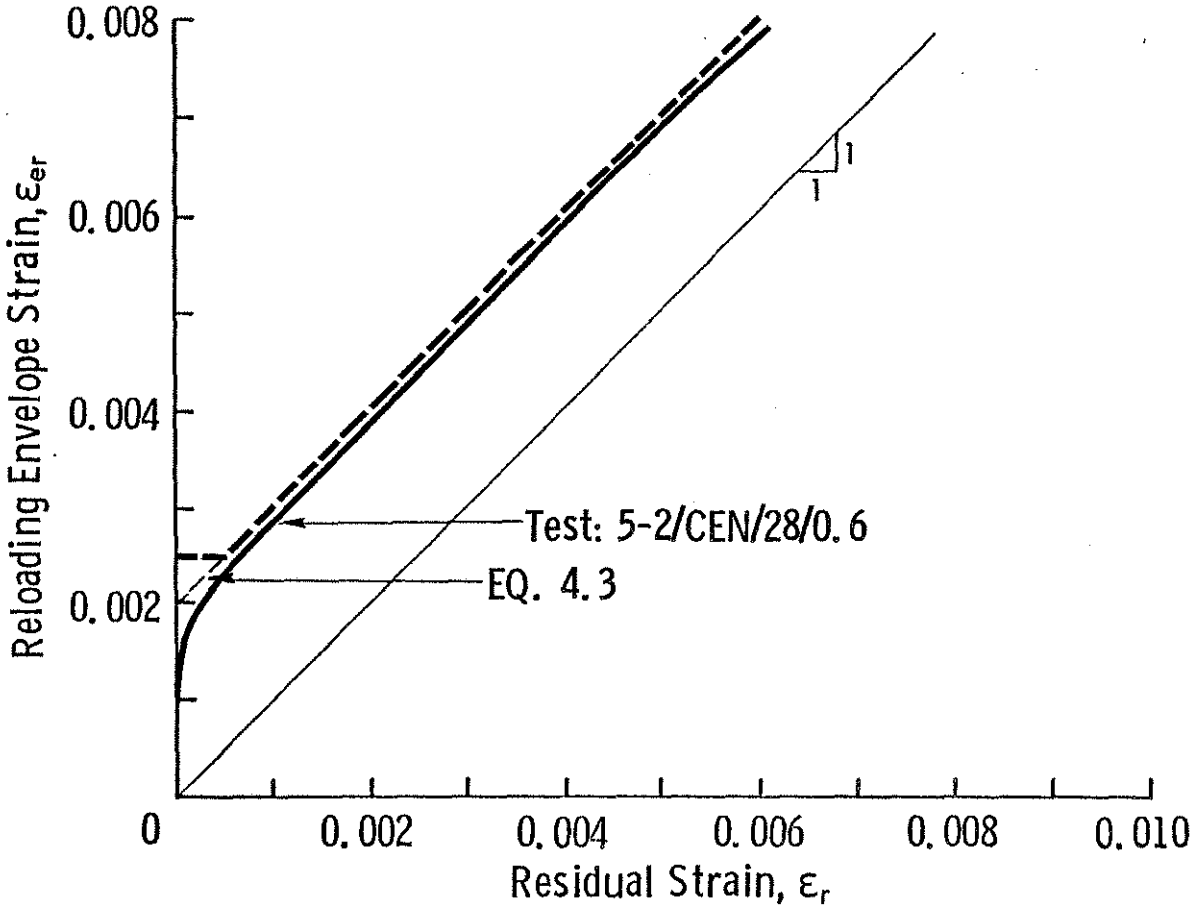

Fig. 4.3 Analytical Residual Strain versus Reloading Envelope Strain Relation Compared with Test Results

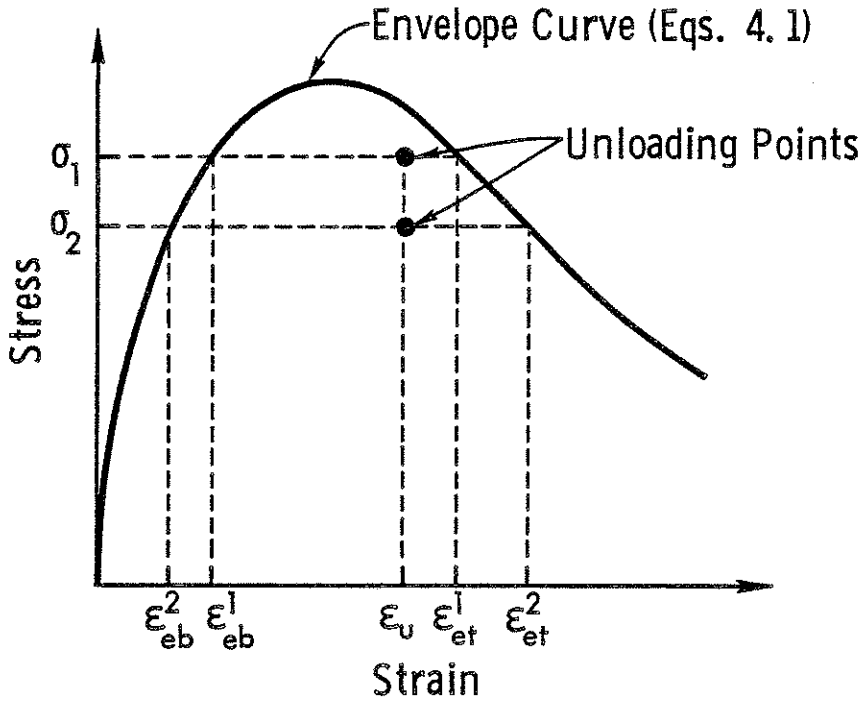

(a) Envelope Strain Intercepts

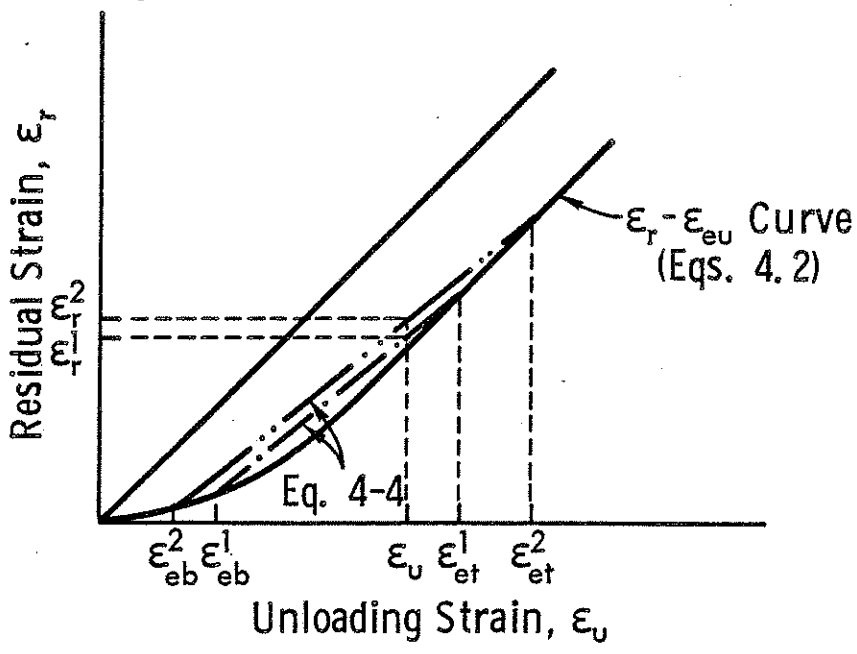

(b) ε_r Determined by the Straight Line (ε_r-ε_u) Bridging ε_r-ε_{eu} Curve at the Envelope Strain Intercepts

Fig. 4.4 Obtaining the Analytical ε_r-ε_u Line

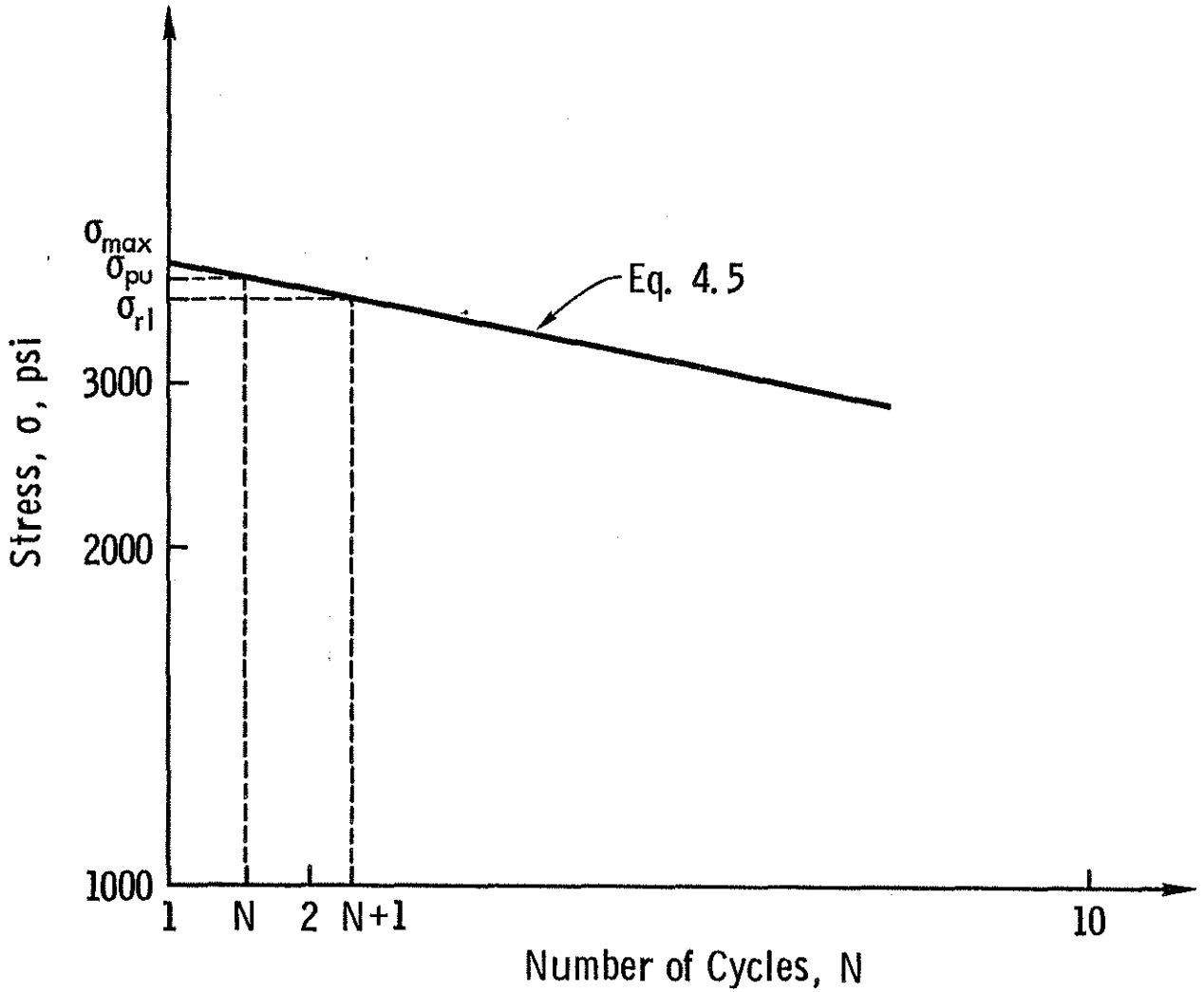

Fig. 4.5 Obtaining the Reloading Stress at the Previous Unloading Strain

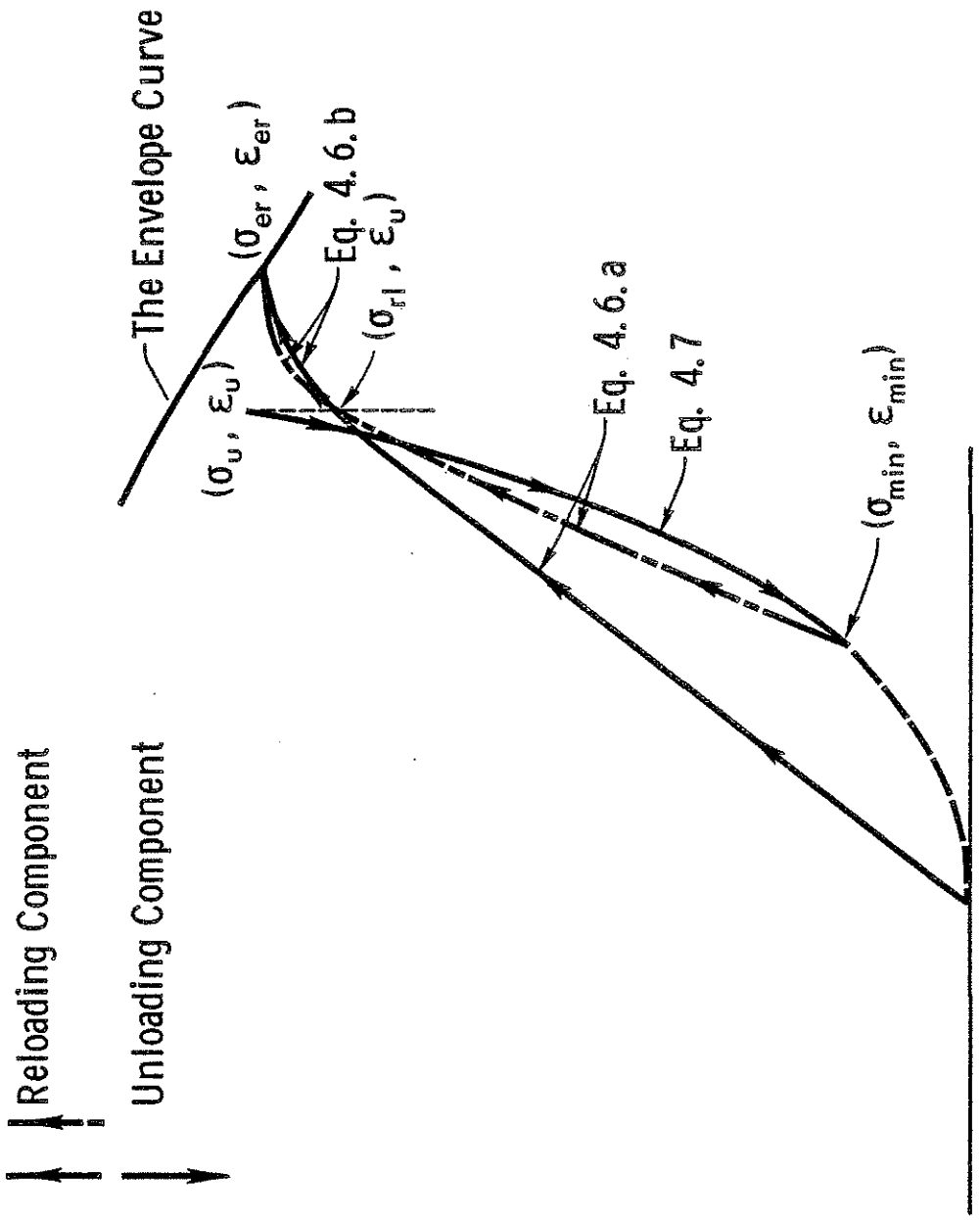

Fig. 4.6 The Reloading Component of a Cycle

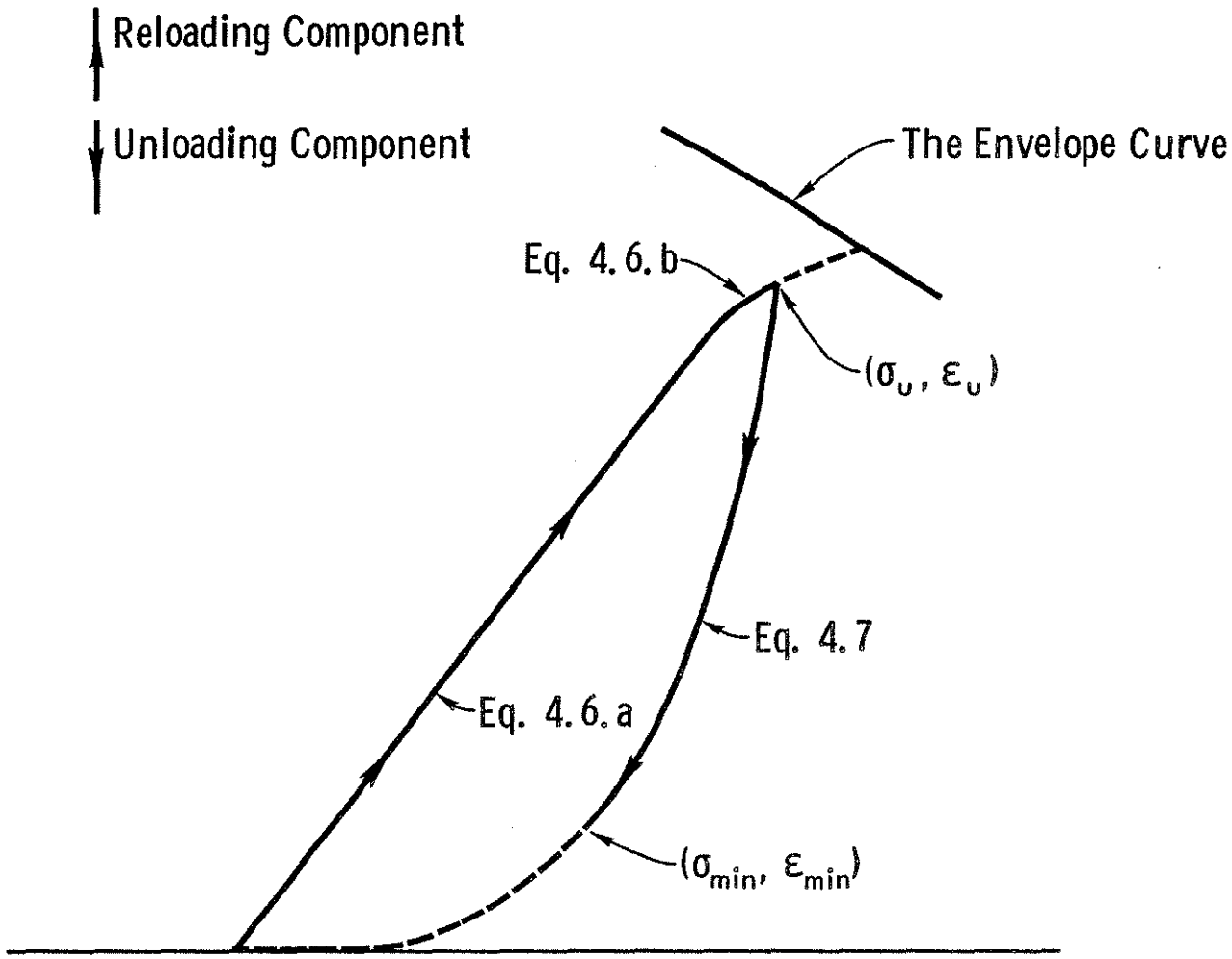

Fig. 4.7 The Unloading Component of a Cycle

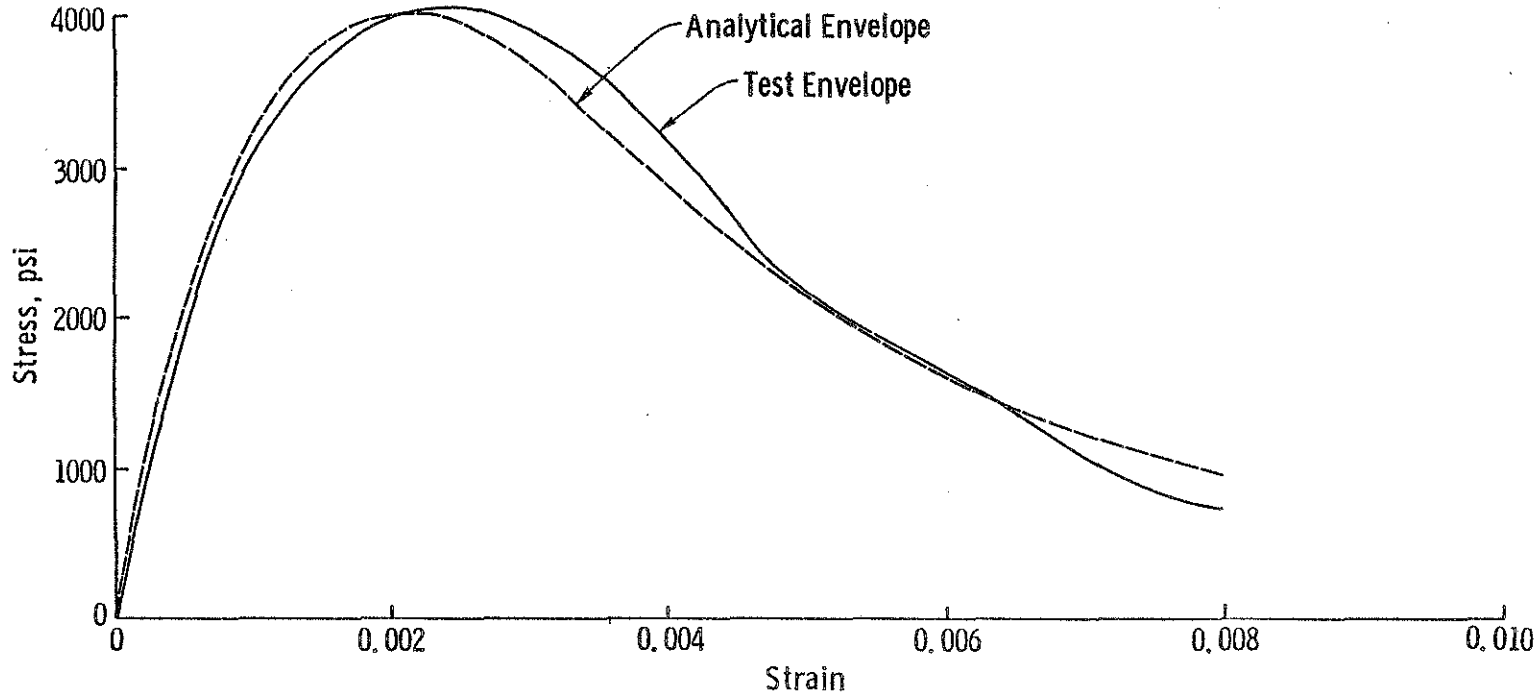

Fig. 4.8 Comparison of Experimental and Analytical Cyclic Envelopes for Test 8-2/CP/29/0.6

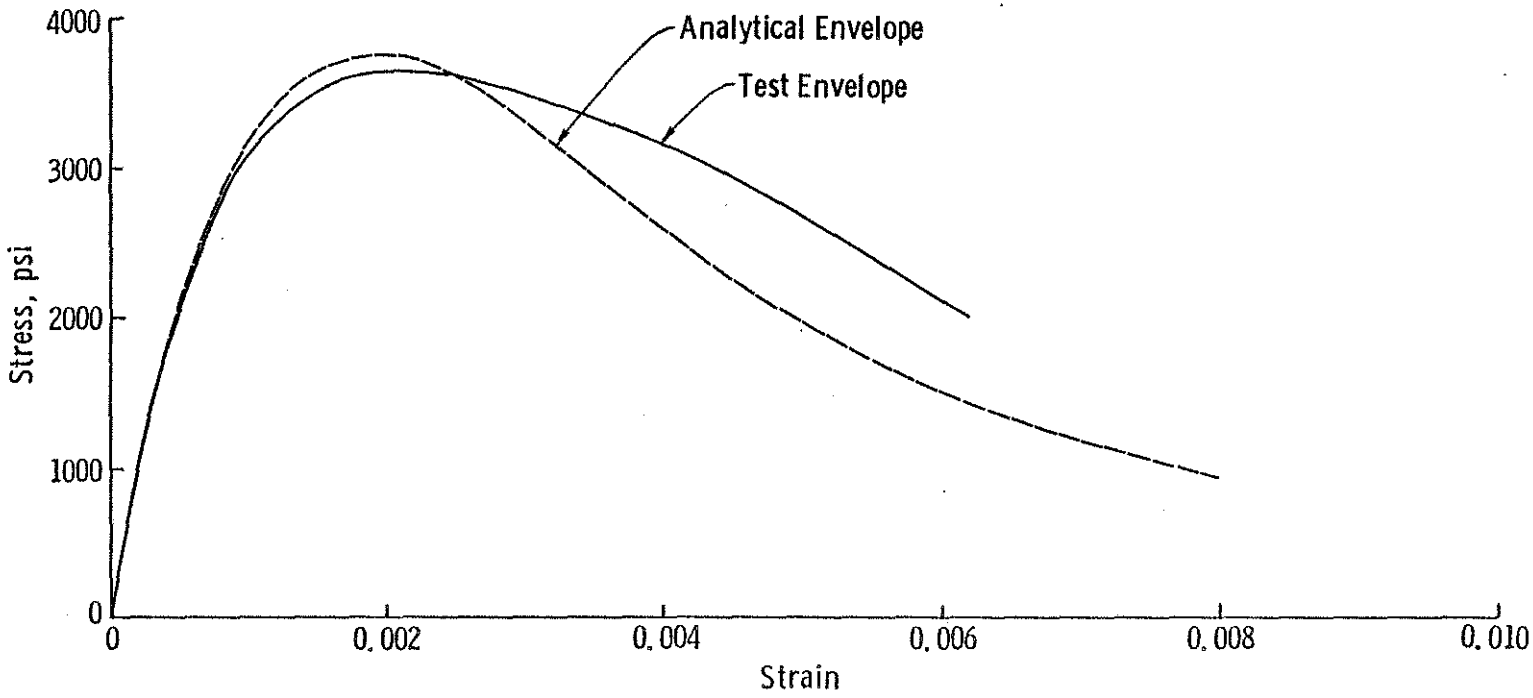

Fig. 4.9 Comparison of Experimental and Analytical Cyclic Envelopes for Test 26-2/CMS/14/0.6

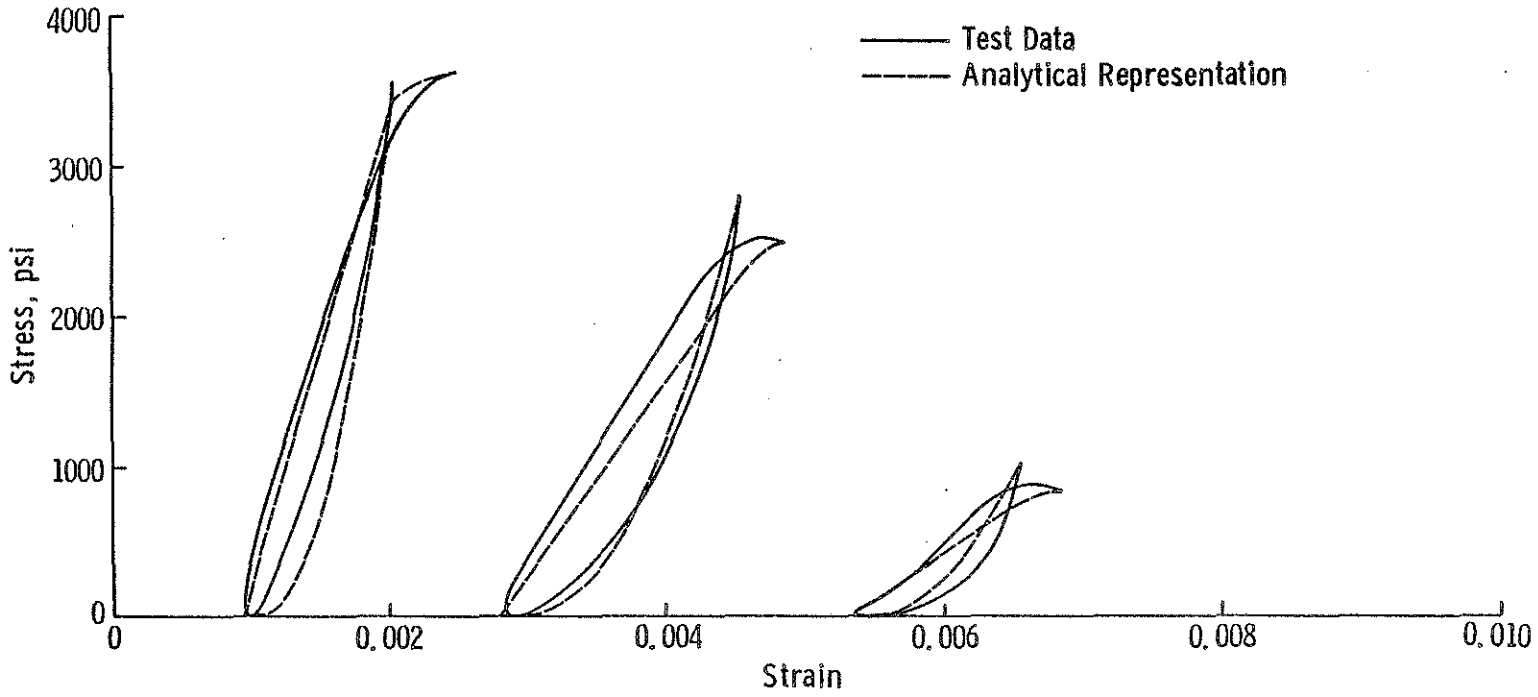

Fig. 4.10 Comparison of the Shapes of Individual Experimental and Analytical Cyclic Curves

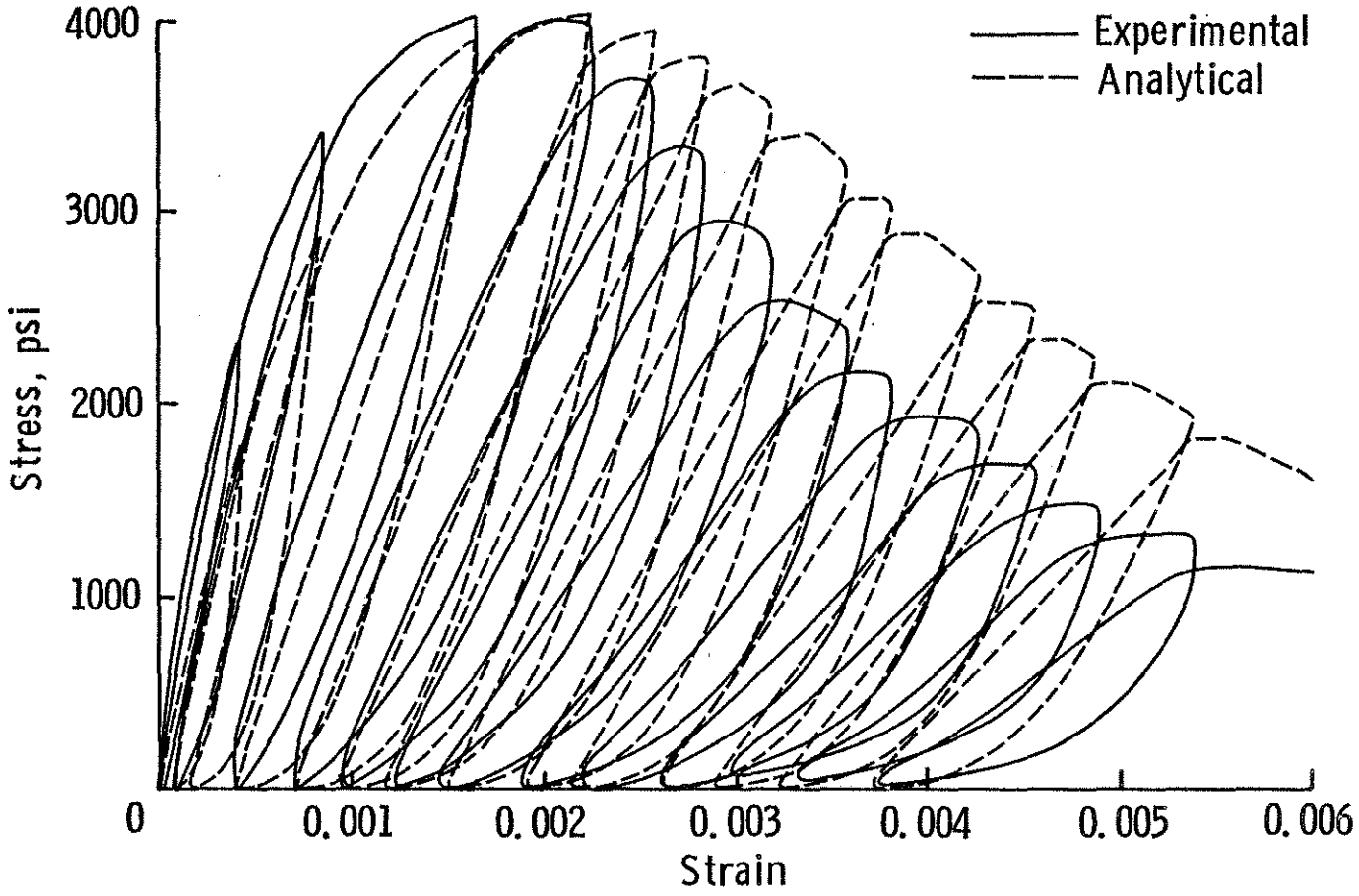

Fig. 4.11 Comparison of Experimental and Analytical Behavior of Mortar for Cycles to the Envelope for Test 4-2/CEN/29/0.6

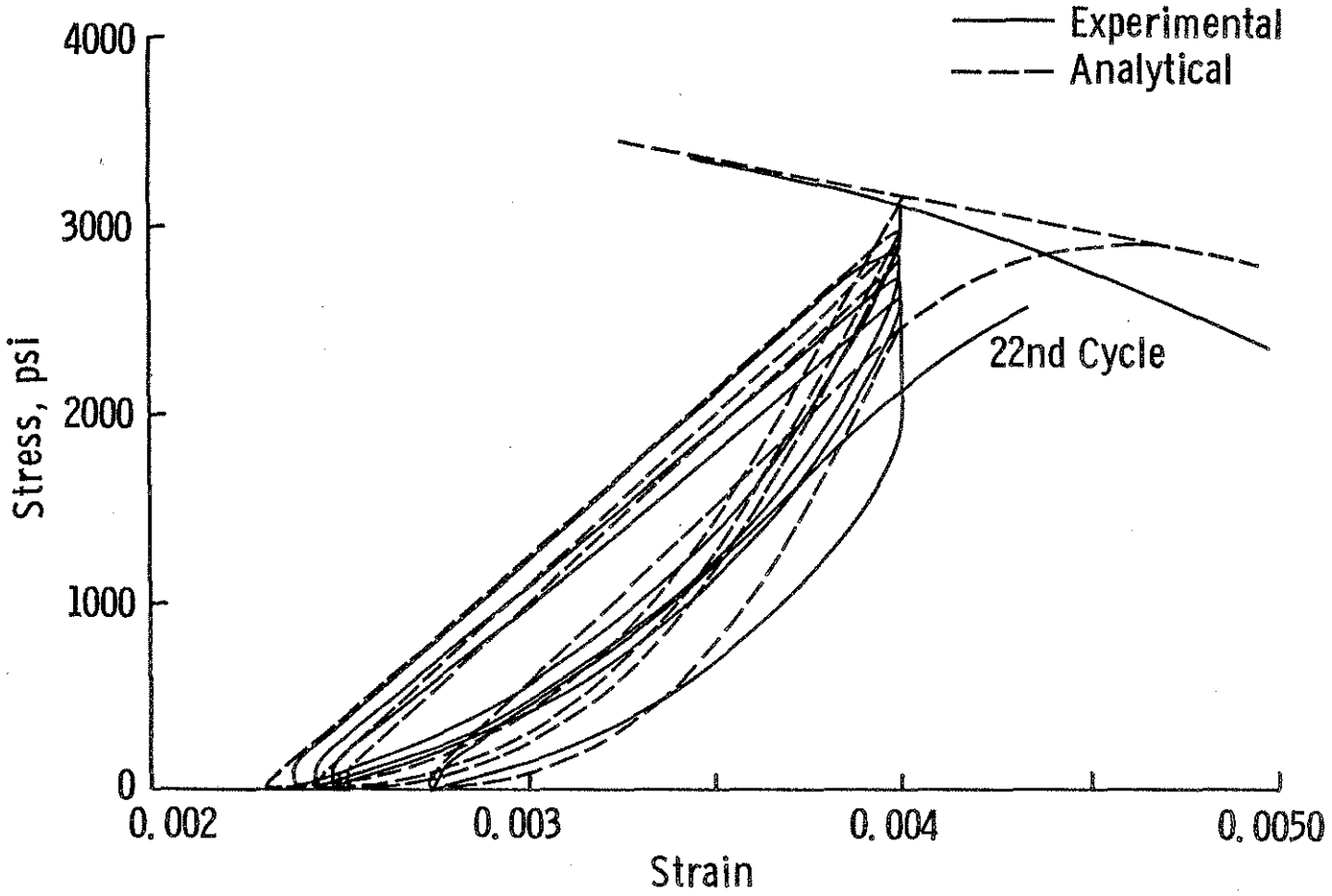

Fig. 4.12 Comparison of Experimental and Analytical Behavior of Mortar for Cycles to 0.0042 Strain for Test 25-2/CMS/14/0.6

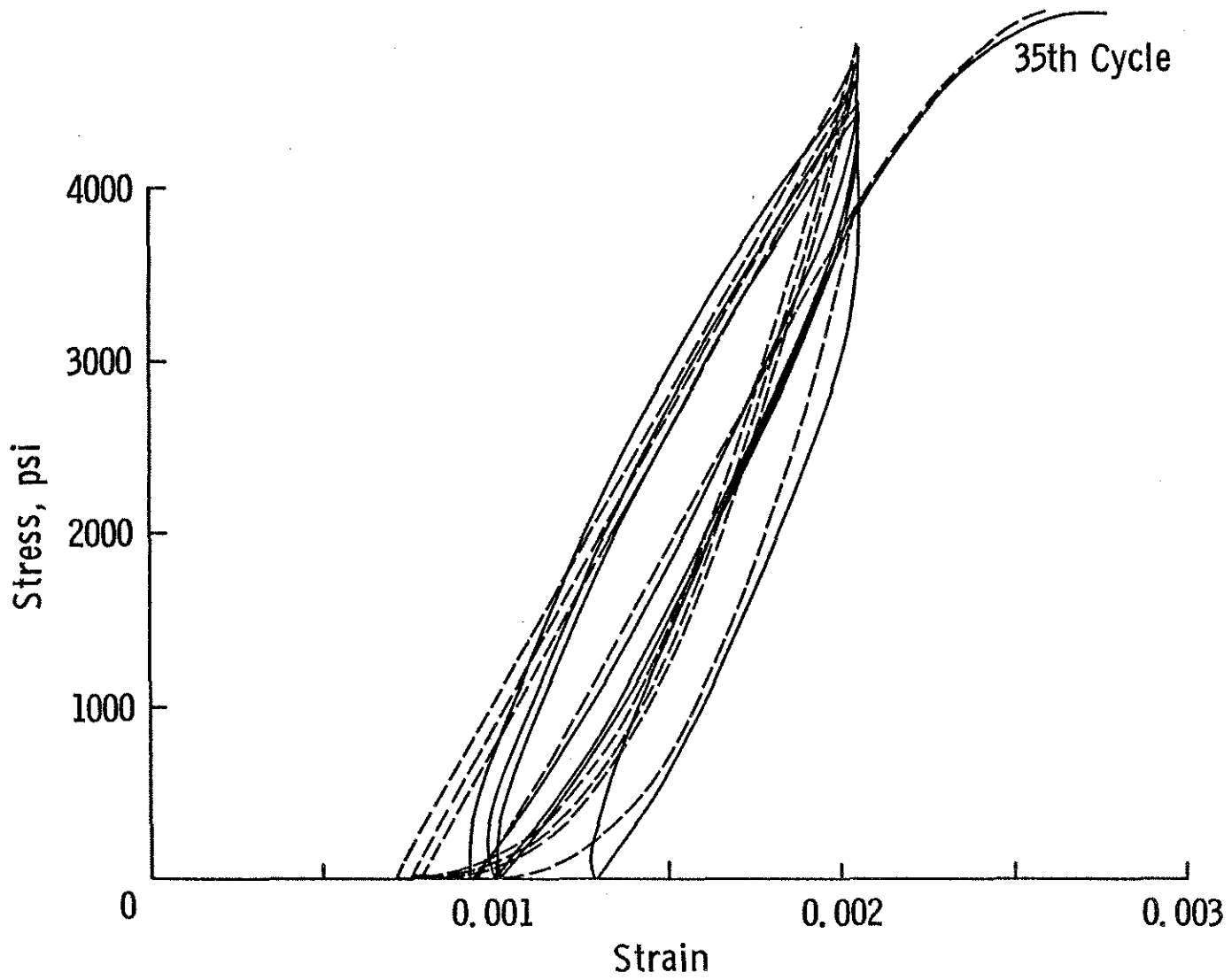

Fig. 4.13 Comparison of Experimental and Analytical Behavior of Mortar for Cycles to 0.0024 Strain for Test 38-3/CMS/29/0.5

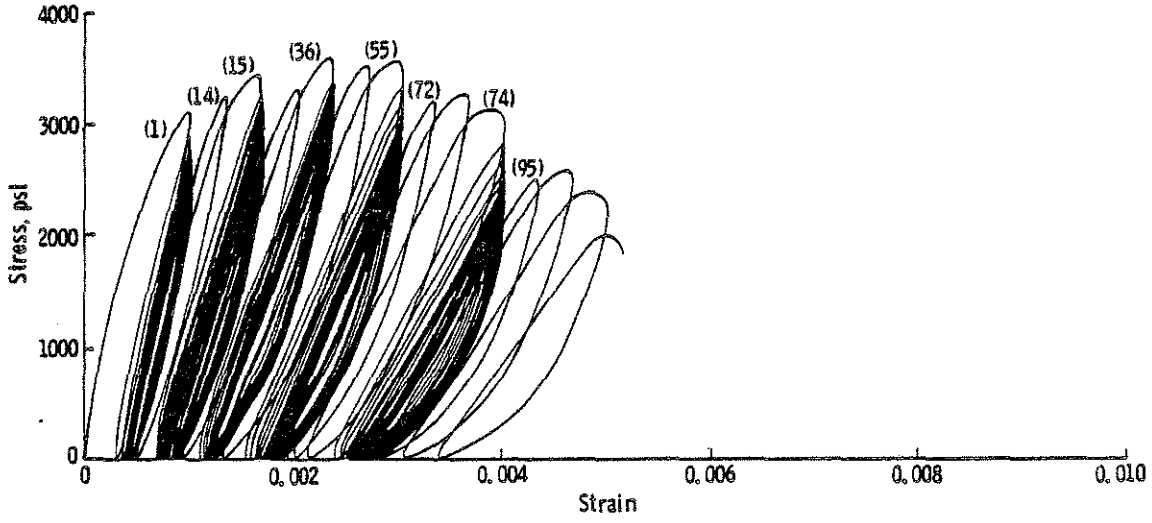

(a) Experimental Results

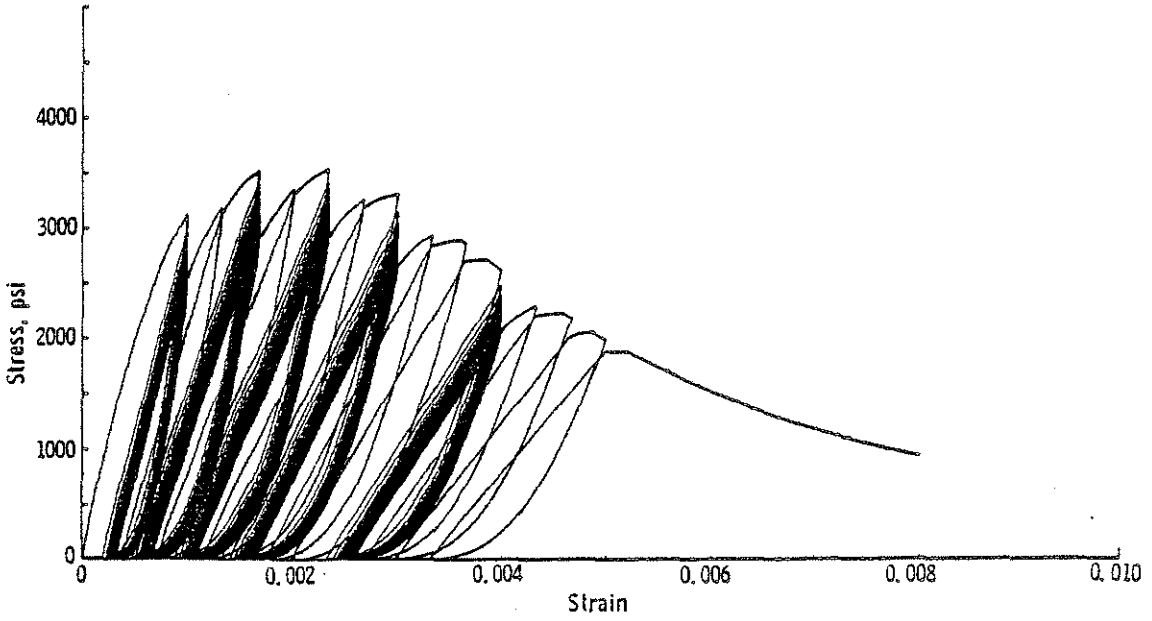

(b) Analytical Results

Fig. 4.14 Comparison of Experimental and Analytical Behavior of Mortar for Cycles to a Constant Maximum Strain

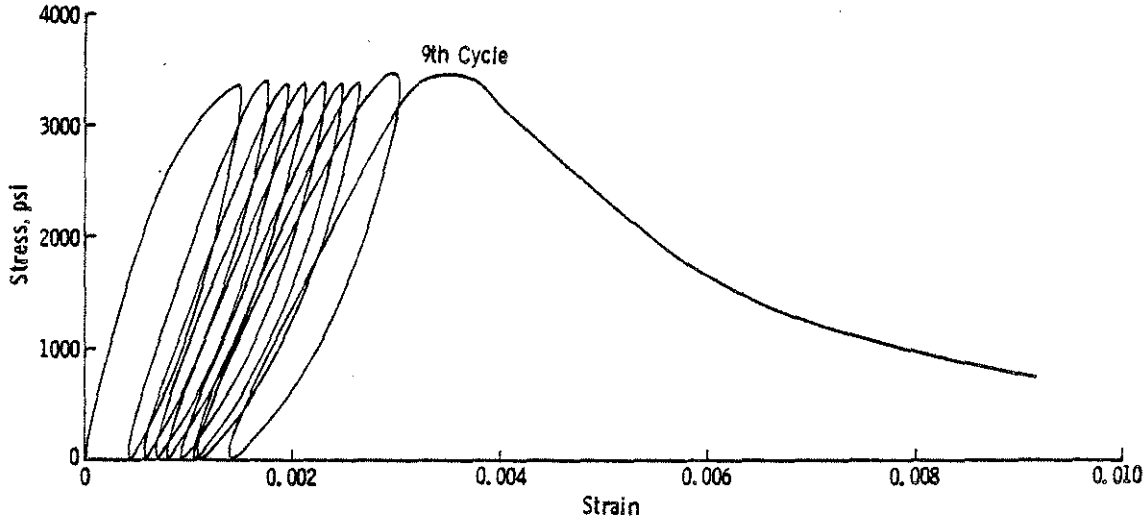

(a) Experimental Results

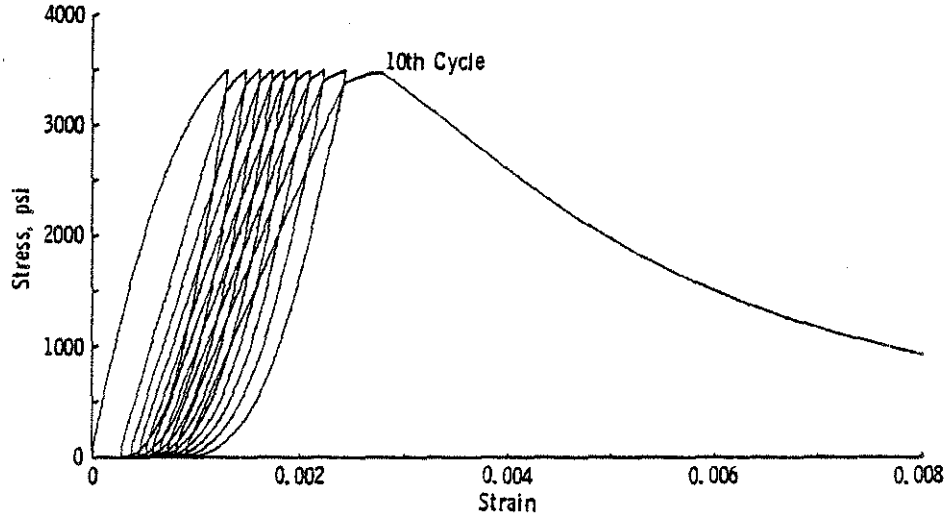

(b) Analytical Results

Fig. 4.15 Comparison of Experimental and Analytical Behavior of Mortar for Cycles between Fixed Stresses with Zero Minimum Stress for Test 41-2/SL/15/0.6

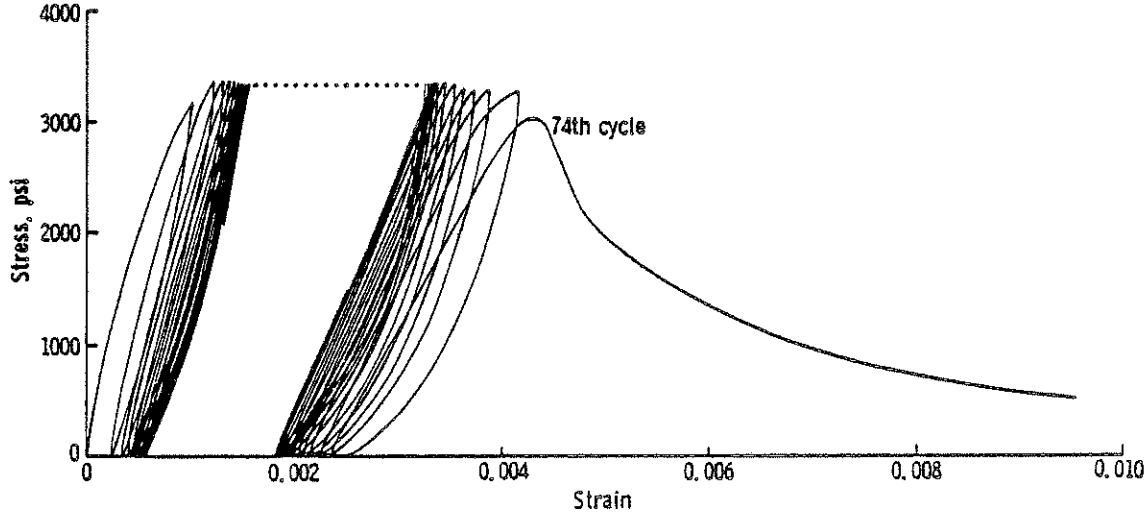

(a) Experimental Results

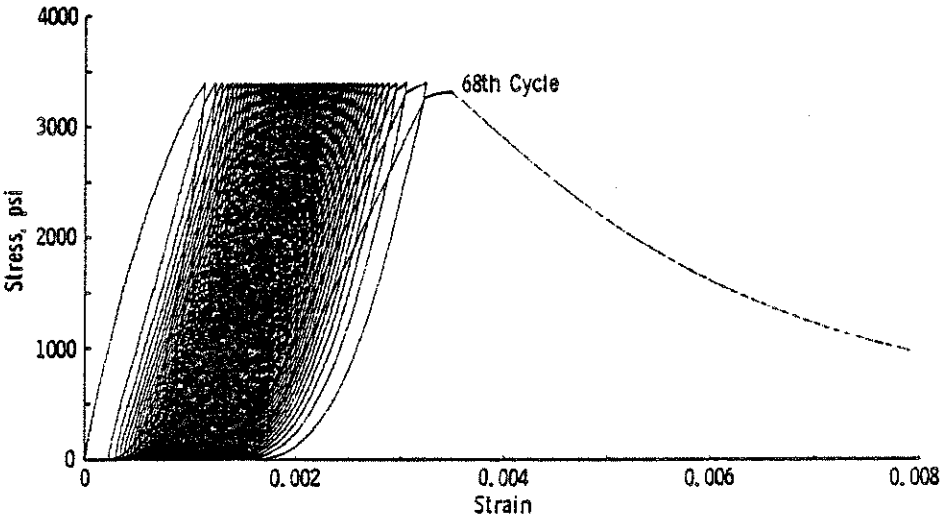

(b) Analytical Results

Fig. 4.16 Comparison of Experimental and Analytical Behavior of Mortar for Cycles Between Fixed Stresses with Zero Minimum Stress for Test 39-3/SL/28/0.6

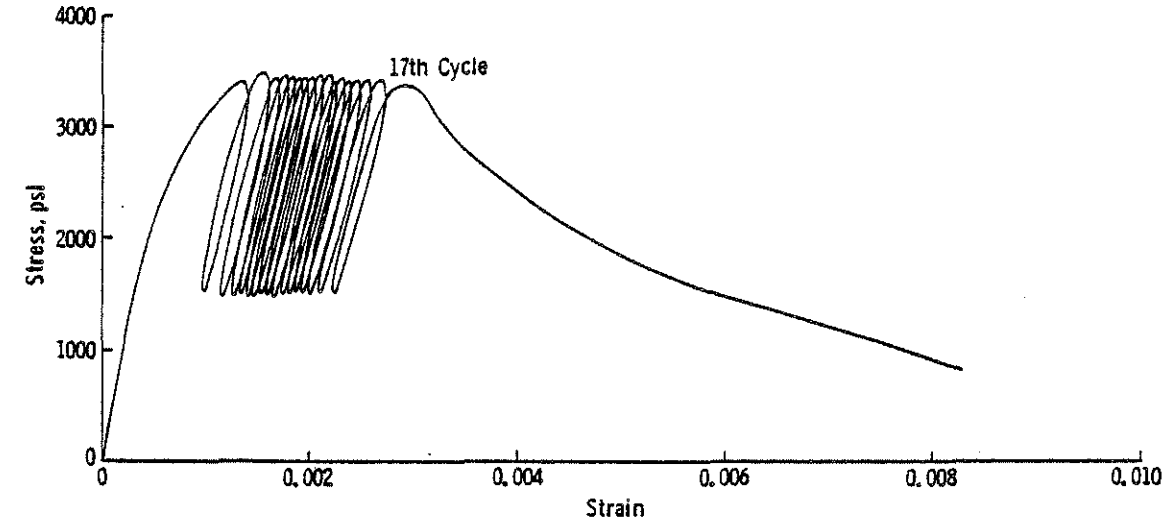

(a) Experimental Results

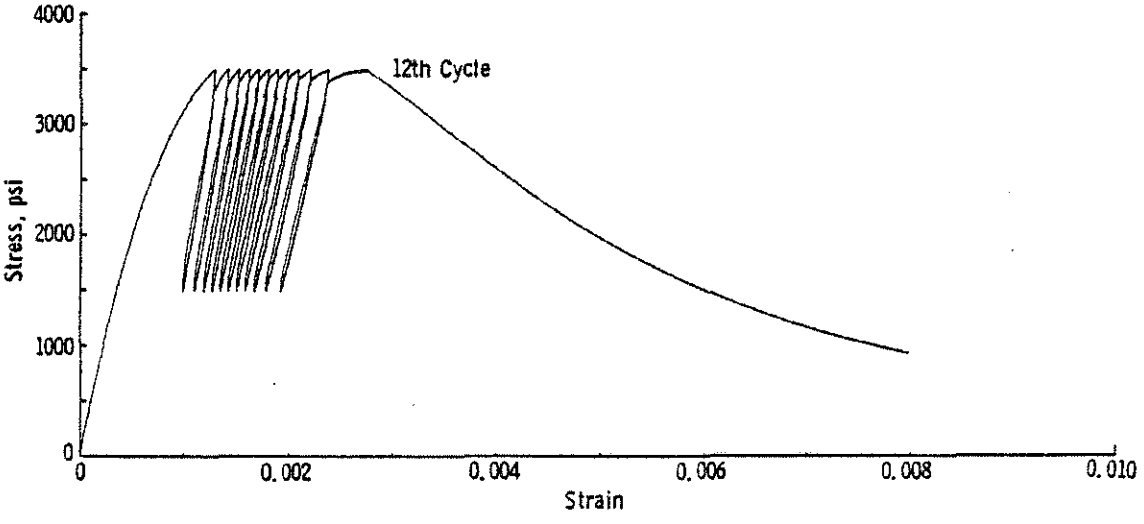

(b) Analytical Results

Fib. 4.17 Comparison of Experimental and Analytical Behavior of Mortar for Cycles Between Fixed Stresses with Non-zero Minimum Stress for Test 41-1/SL/15/0.6

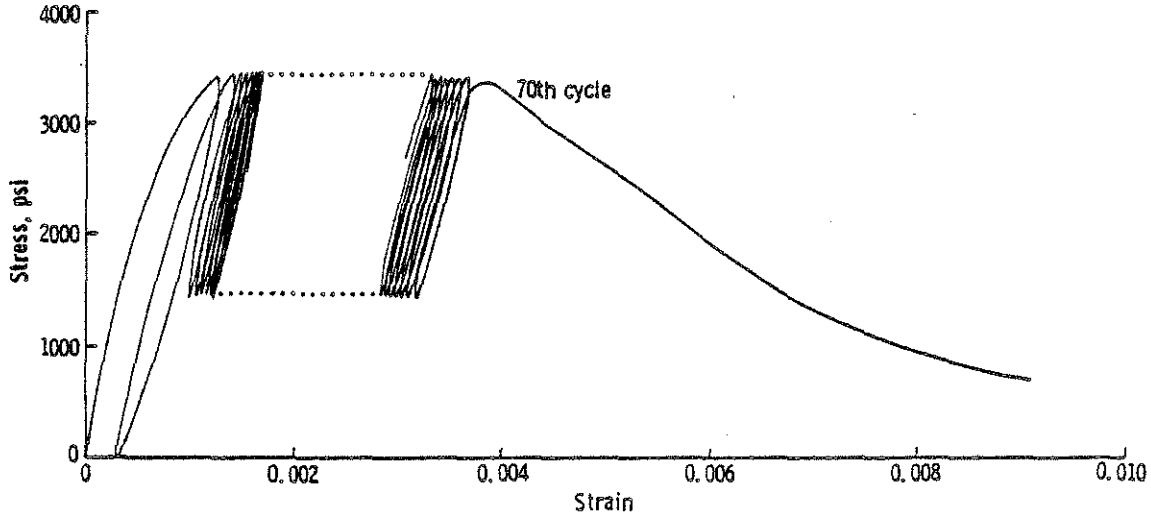

(a) Experimental Results

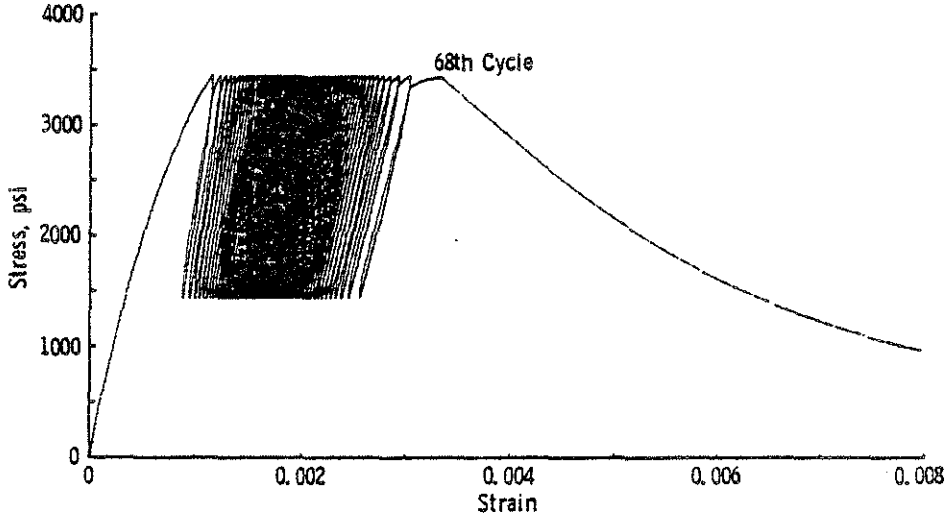

(b) Analytical Results

Fig. 4.18 Comparison of Experimental and Analytical Behavior of Mortar for Cycles between Fixed Stresses with Non-zero Minimum Stress for Test 16-3/SL/29/0.6

APPENDIX A

KEY TO SPECIMEN IDENTIFICATION

The specimens are identified as follows:

Identification: i-j/XXX/N/R

where

i = batch number

j = specimen number, in batch i

XXX = type of load regime

N = age in days

R = water-cement ratio

Types of load regimes, XXX

M = monotonic loading

MS = slow monotonic loading

CEN = cycles to the envelope

CSI = cycles with constant strain increment

SL = cycles between fixed stresses

SL* = cycles between fixed stresses followed by monotonic loading

CMS = cycles to a constant maximum strain

CP = cycles between common points

Example: 6-2/M/28/0.6

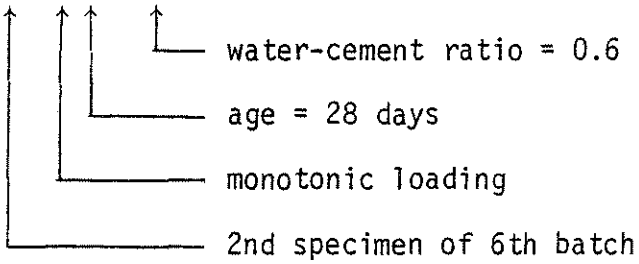

APPENDIX B

NOTATION

E_i = initial modulus of elasticity

E_m = secant modulus of elasticity at the peak of the stress-strain curve

f'_c = short-term compressive strength of concrete

f'_m = stress at the peak of the stress-strain envelope for mortar

N = number of cycles

W/C = water-cement ratio

$\Delta\varepsilon^r$ = range of strain traversed during a single cycle of load

$\Delta\varepsilon_r$ = residual strain increment between two successive cycles of load

$\Delta\varepsilon_u$ = maximum strain increment between two successive cycles of load

ε = strain

ε_{eb} = strain on the ascending branch of the envelope, corresponding to the stress prior to unloading

ε_{er} = envelope strain upon reloading

ε_{et} = strain on the descending branch of the envelope, corresponding to the stress prior to unloading

ε_{eu} = envelope strain prior to unloading or unloading envelope strain

ε_m = strain at the peak of the stress-strain envelope for mortar

ε_{max} = maximum strain (corresponds to maximum stress)

ε_{min} = minimum strain (corresponds to minimum stress)

ε_{pu} = strain prior to unloading in the previous cycle

ε_r = residual or permanent strain

ε_{rb} = residual strain obtained after unloading from the envelope strain, ε_{eb}

ε_{rt} = residual strain obtained after unloading from the envelope strain, ε_{et}

ε_u = strain prior to unloading or unloading strain; the corresponding stress is less than the stress at the envelope

σ = stress

σ_{max} = maximum stress

σ_{min} = minimum stress

σ_{pu} = stress prior to unloading in the previous cycle

σ_r = stress upon reloading to ε_{pu}

$\sigma_{2\varepsilon_m}$ = stress at twice the strain at the peak of the envelope

$\sigma_{3\varepsilon_m}$ = stress at three times the strain at the peak of the envelope